

State of Understanding of Nafion

Kenneth A. Mauritz* and Robert B. Moore*

Department of Polymer Science, The University of Southern Mississippi, 118 College Drive #10076, Hattiesburg, Mississippi 39406-0001

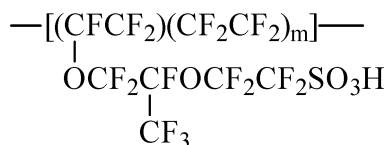
Received July 19, 2004

Contents

1. Introduction	4535
2. Morphological Characterization Using X-rays and Neutrons	4538
2.1. Early Studies of Nafion Morphology	4538
2.2. Scattering from PFSI Solutions and Recast Films	4543
2.3. Evaluation of Nafion Morphology through Studies of Oriented Membranes	4545
2.4. Current Models for the Morphology of Nafion	4548
2.5. The State of Understanding from X-ray and Neutron Investigations	4554
3. Microscopy Studies	4555
4. The Nature of Water, Other Solvents, and Ions in Nafion	4559
5. Mechanical Properties	4575
6. Molecular Simulation of Structure and Properties	4576
7. Conclusions	4581
8. Acknowledgment	4582
9. Literature References	4582

1. Introduction

Nafion ionomers were developed and are produced by the E. I. DuPont Company. These materials are generated by copolymerization of a perfluorinated vinyl ether comonomer with tetrafluoroethylene (TFE), resulting in the chemical structure given below.



Equivalent weight (EW) is the number of grams of dry Nafion per mole of sulfonic acid groups when the material is in the acid form. This is an average EW in the sense that the comonomer sequence distribution (that is usually unknown to the investigator and largely unreported) gives a distribution in m in this formula. EW can be ascertained by acid–base titration, by analysis of atomic sulfur, and by FT-IR spectroscopy. The relationship between EW and m is $\text{EW} = 100m + 446$ so that, for example, the side chains are separated by around 14 CF_2 units in a membrane of 1100 EW.

Common at the time of this writing are Nafion 117 films. The designation “117” refers to a film having 1100 EW and a nominal thickness of 0.007 in., although 115 and 112 films have also been available. Early-reported studies involved 1200 EW samples as well as special experimental varieties, some being rather thin. The equivalent weight is related to the property more often seen in the field of conventional ion exchange resins, namely the ion exchange capacity (IEC), by the equation $\text{IEC} = 1000/\text{EW}$.

The mention of the molecular weight of high equivalent weight ($\text{EW} > 1000 \text{ g}\cdot\text{mol}^{-1}$) Nafion is almost absent in the literature, although the range 10^5 – 10^6 Da has been mentioned. As this polymer does not form true solutions, the common methods of light scattering and gel permeation chromatography cannot be used to determine molecular weight as well as the size and shape of isolated, truly dissolved molecules. Studies of the structure of this polymer in solvent (albeit not a true solution) will be mentioned in the scattering section of this review. It should be noted that Curtin et al. performed size exclusion chromatography determinations of the molecular weight distribution in Nafion aqueous dispersions after they were heated to high temperatures (230, 250, and 270 °C).¹ Before heating, there was a high molecular weight shoulder on a bimodal distribution, due to molecular aggregates, but this shoulder disappeared upon heating, which indicated that the aggregates were disrupted. The peaks for the monomodal distribution for the heated samples were all located at molecular weights slightly higher than $10^5 \text{ g}\cdot\text{mol}^{-1}$. Also, light scattering experiments revealed that the radius of gyration had a linear dependence on the molar mass of the aggregates, which suggests that the particles are in the form of rods or ribbons, or at least some elongated structure.

Nafion ionomers are usually derived from the thermoplastic $-\text{SO}_2\text{F}$ precursor form that can be extruded into sheets of required thickness. Strong interactions between the ionic groups are an obstacle to melt processing. This precursor does not possess the clustered morphology that will be of great concern in this article but does possess Teflon-like crystallinity which persists when the sulfonyl fluoride form is converted to, for example, the K^+ form by reacting it with KOH in water and DMSO. Thereafter, the $-\text{SO}_3\text{H}$ form is achieved by soaking the film in a sufficiently concentrated aqueous acid solution. Extrusion of the sulfonyl fluoride precursor can cause microstructural orientation in the machine direction,

* Address correspondence to either author. Phone: 601-266-5595/4480. Fax: 601-266-5635. E-mail: Kenneth.Mauritz@usm.edu; RBMoore@usm.edu.



Dr. Kenneth A. Mauritz has been a Professor in the School of Polymers and High Performance Materials at the University of Southern Mississippi since 1984. He received a Ph.D. in Macromolecular Science at Case Western Reserve University in 1975. After a postdoctoral assignment at Case Western Reserve, he joined Diamond Shamrock Corporation as a Research Chemist in 1976. There, he began his long and continuous involvement with Nafion materials, mainly in the area of the molecular structure–property characterization and modeling as related to membrane performance optimization in chlor-alkali electrochemical cells for the production of chlorine and caustic. Later, at the University of Southern Mississippi, he produced some of the first inorganic/Nafion nanocomposite materials based on membrane–in situ sol–gel processes for inorganic alkoxides. Mauritz has collaborated with the coauthor of this review, R. B. Moore, in a number of projects involving Nafion materials. He has contributed numerous papers, reviews, and presentations on the topic of Nafion. He has coedited and contributed to the book *Ionomers: Synthesis, Structure, Properties and Applications* and was cochairperson of the 2003 Gordon Research Conference on Ion Containing Polymers. Other research interests include self-assembled, nanostructured organic–inorganic materials via domain-targeted inorganic syntheses in phase separated ionomers, microscopy, spectroscopy, dielectric relaxation/electrical impedance analysis, and the thermal, dynamic mechanical, and diffusion properties of polymers.

and this can be seen in the small-angle X-ray scattering peak that is attributed to the clustered morphology. Moreover, this orientation can affect the swelling and electrical conductance properties (anisotropy) of the ionomer form.

The earliest concerted effort in the research and development of Nafion perfluorosulfonate ionomers was directed toward their use as a permselective membrane separator in electrochemical cells used in the large scale industrial production of NaOH, KOH, and Cl₂. In short, the membrane in this application, in addition to keeping Cl₂ and H₂ gases separated, prevents the unfavorable back migration of hydrated OH[−] ions from the catholyte (concentrated aqueous NaOH or KOH) chamber, while allowing for the transport of hydrated Na⁺ ions from the anolyte chamber in which is aqueous NaCl.

Early experimental versions of Nafion within the context of chlor-alkali cells² consisted of SO₂F precursor forms that were first reacted on only one side with ethylenediamine (EDA) before the conversion of the remainder of the membrane to the sulfonate form took place. The result was a well-defined stratum of sulfonamide cross-links, that were formed upon heating after reaction, that served to reduce swelling at the catholyte interface, which, in turn, reduced OH[−] back migration.^{3–6} However, these EDA-modified membranes proved inadequate in chlor-alkali cells due to the chemical degradation of these cross-links



Dr. Robert B. Moore is currently a Professor in the School of Polymers and High Performance Materials at the University of Southern Mississippi. He received his Ph.D. in Analytical Chemistry from Texas A&M University in 1988 under the direction of Professor Charles R. Martin. His graduate research was focused on the chemical and morphological investigations of perfluorosulfonate ionomers. He then joined the group of Professor Adi Eisenberg at McGill University as a postdoctoral fellow and continued his work on the morphological characteristics of random ionomers using small-angle X-ray scattering methods. In 1991, he joined the faculty in the Department of Polymer Science at the University of Southern Mississippi. His research interests include structure–property relationships in ion-containing polymers, random ionomers, semicrystalline ionomers, ionomer membranes, and blends. A key consideration in this work, which has spanned from 1983 to the present, has involved the link between ionic aggregation and crystallization in semicrystalline ionomers, specifically Nafion. He has presented numerous papers and invited lectures on the topic of morphological manipulations of Nafion through the development of novel processing procedures and blends. He is currently an officer in the Division of Polymer Chemistry of the American Chemical Society and is the cochair of the 2005 Gordon Research Conference on Ion Containing Polymers.

in the harsh chemical environment. The membranes currently used in this application are of a sulfonate/carboxylate bilayer variety.

A lesser number of papers have appeared regarding the carboxylate version of Nafion, and the works of Yeager et al.,^{7,8} Seko et al.,⁹ and Perusich et al.¹⁰ are of special note. Nafion-like carboxylate materials have also been reported.¹¹ These similar materials will not be discussed here, as the exclusive emphasis is on the stronger-acid sulfonated versions because this critical review is within a collection of articles in which perfluorinated ionomers are considered within the context of fuel cells.

The DuPont Nafion materials, both sulfonate and carboxylate varieties, are not entirely unique, as similar perfluorinated ionomers have been developed by others such as the Asahi Chemical Company (commercial name: Aciplex) and the Asahi Glass Company (commercial name: Flemion). The comonomer chemical structures of and further information on these materials are given in the recent review article by Doyle and Rajendran.¹² Now commercially unavailable, but once considered a viable alternative, the Dow Chemical Company developed a somewhat similar perfluorinated ionomer that resembled the sulfonate form of Nafion except that the side chain of the former is shorter and contains one ether oxygen, rather than two ether oxygens, that is, $-\text{O}-\text{CF}_2-\text{CF}_2-\text{SO}_3\text{H}$.^{13,14}

The greatest interest in Nafion in recent years derives from its consideration as a proton conducting

membrane in fuel cells. It is clear that the tuning of these materials for optimum performance requires a detailed knowledge of chemical microstructure and nanoscale morphology. In particular, proton conductivity, water management, relative affinity of methanol and water in direct methanol fuel cells, hydration stability at high temperatures, electro-osmotic drag, and mechanical, thermal, and oxidative stability are important properties that must be controlled in the rational design of these membranes. This is a challenge for Nafion materials in which the possible chemical variations are rather limited. And, of course, all of these objectives must be achieved while maintaining low cost for this perfluorinated ionomer in the vast consumer market as well as in military applications. While a number of alternate polymer membranes, including nonfluorinated types, have been developed, Nafion is still considered the benchmark material against which most results are compared.

With respect to the morphological characterization of Nafion, it is important to note that the wealth of information gathered over the years using a variety of scattering methods is inherently indirect and often limited by the necessity of employing rather simple morphological models that involve specific assumptions of structure. While mentioned frequently throughout this review, the cluster-network model of Gierke et al. deserves special mention (from a historical perspective) as a "starting point" in an introduction to this now-vast topic. This model has endured for many years as a conceptual basis for rationalizing the properties of Nafion membranes, especially ion and water transport and ion permselectivity.^{15–17} It is presumed, based on small-angle X-ray scattering (SAXS) studies and several assumptions, that there are ~ 40 Å -in-diameter clusters of sulfonate-ended perfluoroalkyl ether groups that are organized as inverted micelles and arranged on a lattice. These micelles are connected by proposed pores or channels that are ~ 10 Å in size. These $-\text{SO}_3^-$ -coated channels were invoked to account for intercluster ion hopping of positive charge species but rejection of negative ions, such as OH^- , as in the case of chlor-alkali membrane cells.

A few things should be appreciated concerning this historical model. First, it was based on the limited structure–property information that was available at the time, namely the existence of a single SAXS peak and the behavior of this peak with water swelling as well as the observed selective permeation of Na^+ over OH^- ions in membrane chlor-alkali cells. Wide-angle X-ray diffraction (WAXD) investigations determined limited poly(tetrafluoroethylene) (PTFE)-like crystallinity associated with the perfluorocarbon backbone, although this structural detail was not factored into the Gierke model. In the sense that it does not assemble the phase separated morphology from basic chemical structure as, say, driven by a free energy minimization that incorporates molecular interactions as in a molecular simulation procedure, the model cannot be considered to be predictive but is calibrated to experimental data.

In the years following the introduction of the model of Gierke et al., more extensive structure–property studies have been conducted and, in many reports, alternate morphologies have been proposed. Through the use of state-of-the-art scattering methods, our understanding of the morphology of Nafion is evolving to include a more definitive picture of the nature of ionic aggregation in this polymer. It is a goal of this article to examine these studies, point out the salient features, and identify the elements that are in common.

Also, among the earliest concepts that were set forth regarding microstructure are those of Yeager and Steck, who proposed a three-phase model that was significantly different from that of Gierke et al. based on their studies of the diffusion of various ions.¹⁸ As compared with the model of Gierke et al., the clusters do not have a strict geometrical definition (spherical inverted micelles connected by cylindrical pores) and their geometrical distribution has a lower degree of order. Most importantly, there are transitional interphases between hydrophilic and hydrophilic regions, a concept that is becoming increasingly accepted.

It must be emphasized that this article is not meant to be a listing of the very large number of publications dealing with Nafion. To be sure, the literature since the late 1970s, when the main thrust for the development of these materials was membrane chlor-alkali cell technology improvement and, to a lesser degree, water electrolyzers, has proliferated. It was estimated (DuPont library), based on a coarse literature search that was performed a few years prior to this writing, that there were approximately 33 000 papers, patents, and so forth dealing with Nafion, and the number is growing. In part, to limit the scope of this review, the focus is on selected studies that have addressed the most fundamental aspects of the structure and properties of this polymer. Given this limited goal, the important issues of thermal and electrochemical stability, electro-osmotic drag, methanol crossover, gas permeation, and catalyst incorporation have been omitted, although numerous reports on these topics are found throughout the literature.

Chemical degradation in a fuel cell environment is also an important issue that must be addressed and so will be mentioned briefly here. It is thought that generated peroxide radicals attack polymer end groups having H-containing terminal bonds ($-\text{CF}_2\text{COOH}$) that are formed during processing. H_2O_2 , formed by reactions between oxygen and hydrogen, then decomposes, giving $\cdot\text{OH}$ or $\cdot\text{OOH}$ radicals that attack the H-containing terminal bonds, and this initiates chemical decomposition. Membranes become thinner, and fluoride ions are detected in product water. The reader is directed toward the article by Curtin et al., for the details of this mechanism and characterization of the degradation process.¹

Other reviews of the literature on Nafion and similar perfluorinated ionomers have appeared over the years. The early book (1982) by Eisenberg and Yeager, *Perfluorinated Ionomer Membranes*, remains

a useful series of monographs dealing with early work in the area.¹⁹ Later (1996), Heitner-Wirguin assembled a comprehensive review that contains topics not included in the document presented here.²⁰ Most recent is the compilation of Doyle and Rajendran entitled *Perfluorinated Membranes* that contains an excellent history of the evolution of this material that begins with the discovery of PTFE by Plunkett in 1938.¹²

Also, discussions of a number of applications of Nafion are not included in this document and are, at most, mentioned within the context of a particular study of fundamental properties. A number of these systems are simply proposed rather than in actual commercial applications. Membranes in fuel cells, electrochemical energy storage systems, chlor-alkali cells, water electrolyzers, Donnan dialysis cells, electrochromic devices, and sensors, including ion selective electrodes, and the use of these membranes as a strong acid catalyst can be found in the above-mentioned reviews.

It should be mentioned that, because the microstructure and properties of this ionomer are known to be quite sensitive to history and the details of preparation of samples for analysis, an effort has been made in this article, where possible, to delineate these important parameters in each described study so that the results of different investigations can be meaningfully compared.

Finally, the scope of the discussed literature is not confined to recent contributions but extends back to the 1970s because a number of excellent studies have not been repeated since then and often do not appear on Internet search engines.

2. Morphological Characterization Using X-rays and Neutrons

Over the last 30 years, a wealth of morphological information from numerous scattering and diffraction studies of Nafion has been obtained and reported in an attempt to precisely define the molecular/supramolecular organization of perfluorinated ionomers in a variety of physical states. However, while the quality and quantity of data from state-of-the-art instrumentation, facilities, and methods has increased, a universally accepted morphological model for the solid-state structure of Nafion has yet to be defined. The source of the ongoing debate over the morphology of Nafion stems from the fact that this unique ionomer has a random chemical structure that is capable of organizing in the complex formation of ionic and crystalline domains with a significant distribution in dimensions over a wide range of length scales. Moreover, quantitative morphological information is limited by the fact that Nafion yields only a single, broad scattering maximum attributed to characteristic dimensions within the ionic domains and the diffraction reflections of the PTFE-like crystallites are broad and relatively weak due to low degrees of crystallinity.

Unfortunately, the small-angle scattering techniques used in the investigations of Nafion morphology generally probe but a small region of reciprocal space and Fourier inversion methods of analyzing the

data are of limited use. Thus, the investigator is forced to compare the experimentally determined scattered profiles with that predicted by necessarily simple models that must be *assumed* for the structure. To further complicate matters, very low angle scattering information characteristic of long-range dimensions is convoluted by overlapping signals associated with the spatial distribution of crystallites (i.e., a weak maximum or shoulder often attributed to the long spacing between crystallites) and long-range heterogeneities in electron density associated with the disordered distribution of ionic domains (i.e., a small-angle upturn in intensity commonly observed with ionomers). This morphological complexity precludes the general application of simple two-phase models and thus further limits the useful angular range for precise model comparisons.

In considering the complicating factors associated with extracting detailed morphological information from scattering and diffraction data for Nafion, it is not surprising that a number of morphological models, constituting significantly different structural features, have been proposed and are still the focus of considerable debate. Since the vast majority of the applications of Nafion involve the hydrated or solvent swollen state and current processing methods for membrane formation often involve solvent casting, considerable attention has been devoted to the influence of swelling solvents (specifically water) on the characteristic morphological features of perfluorosulfonate ionomers (PFSIs). As noted above, scattering and diffraction studies of these polymers generally yield limited information; however, many groups have demonstrated success in evaluating the influence of solvent swelling on the scattering profiles for comparison and validation of morphological models. Furthermore, recent detailed studies of the morphological continuum from the dry state through the swollen "gel" state to the "dissolved" (or suspended) state, and *visa versa*, have begun to address important questions related to the organization of ionic and crystalline domains and the impact of solvent-casting on the morphology of perfluorosulfonate ionomers. In this section of the review, the prominent morphological studies of Nafion in a variety of physical states will be reviewed with a historical perspective, including a comparative evaluation of the latest state of the debate over the key morphological models.

2.1. Early Studies of Nafion Morphology

During the 1970s and early 1980s, general concepts and morphological details associated with ionic aggregation in the class of lightly ionized polymers, referred to as ionomers, were actively debated in the literature.^{21,22} The fundamental information from these studies, based in large part on small-angle X-ray scattering (SAXS) studies of dry, polyethylene²³ and polystyrene-based ionomers,^{24,25} formed the foundation for the morphological characterization of Nafion.²⁶ By the late 1970s, experimental evidence for ionic aggregation in Nafion from small-angle scattering data was emerging,²⁷⁻³⁰ and this new information subsequently led to extensions of the prevailing models for the structure of ionomers

to the interpretation of ionic domain morphology in the perfluorosulfonate ionomer systems.

Using SAXS and wide-angle X-ray diffraction (WAXD), Gierke and co-workers^{16,17,31,32} examined and compared the morphological features of Nafion, having a range of equivalent weights, in the unhydrolyzed sulfonyl fluoride precursor form, the hydrolyzed sulfonic acid form, and the neutralized metal sulfonate form. For the unhydrolyzed precursor, a low angle SAXS maximum near $0.5^\circ 2\theta$ and a diffraction peak at $18^\circ 2\theta$ (superimposed on a broad amorphous halo from 10 to $20^\circ 2\theta$) were observed for samples having equivalent weights (EW, the grams of polymer per equivalent of sulfonate groups) ranging from 1100 to 1800 g/equiv. Since these scattering and diffraction peaks were found to increase in intensity with equivalent weight (i.e., with an increase in the statistical length of crystallizable PTFE chain segments between side chains) and were also found to disappear at temperatures near the melting point of PTFE, these features were attributed to crystalline organization within the fluorocarbon matrix. With the hydrolyzed form of Nafion, an additional scattering peak was observed at $\sim 1.6^\circ 2\theta$, corresponding to a Bragg spacing of 3–5 nm, characteristic of a system containing ionic clusters within a semicrystalline matrix. It is important to note here that the term “ionic clusters” (used conventionally in the perfluorosulfonate ionomer literature) generally refers to nano-phase separated, hydrated ionic aggregates, and this term differs from the current definition used for other dry ionomers (e.g., sulfonated polystyrene) to designate regions of closely spaced ionic multiplets.³³

In contrast to the SAXS and WAXD behavior observed for the crystalline features, the ionomer peak was shown to increase in intensity and shift to lower angles with a decrease in equivalent weight. Furthermore, for a given equivalent weight, this peak was found to shift to lower angles and increase in intensity with increasing water content. Based on these findings, and considering the three most prevalent models for the morphology of ionomers at the time, including a model of spherical clusters on a paracrystalline lattice, a core–shell model, and a lamellar model, Gierke and co-workers concluded that the water-swollen morphology of Nafion was best described by a model of ionic clusters that were approximately spherical in shape with an inverted micellar structure.^{17,31} In consideration of the high ionic permselectivity and the requirement of a percolation pathway for ionic transport in Nafion membranes, the spherical ionic clusters were further proposed to be interconnected by narrow channels, constituting a morphology referred to as the cluster-network model,¹⁶ shown in Figure 1.

Based on this new model for the morphology of Nafion, the dimensional variations of the scattering entities with water content were used in simple space-filling calculations to estimate the cluster diameter, the number of sulfonate sites per cluster, and the number of water molecules per cluster.^{16,17} The results of these model calculations showed that, for a given equivalent weight, the cluster diameter,

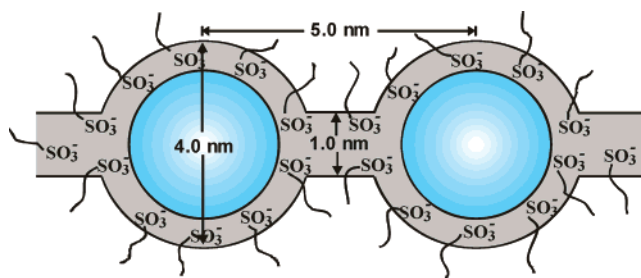


Figure 1. Cluster-network model for the morphology of hydrated Nafion. (Adapted with permission from ref 16. Copyright 1983 Elsevier.)

the exchange sites per cluster, and the number of water molecules per exchange site increased linearly with water content. While the linear relationships were not addressed in this study, the growth of clusters with increasing water content was proposed to occur by a combination of expansion in cluster size and a redistribution of the sulfonate sites to yield fewer clusters in the fully hydrated material.¹⁷ Although this original, yet phenomenological, cluster-network model has received significant acceptance in the literature and has served as the foundation for numerous studies of morphology–property relationships of Nafion, it has also been vigorously debated with respect to alternative morphologies that are also quantitatively consistent with a wide range of scattering results. Specifically, current studies focused on the morphological and dimensional changes that occur with variations in solvent swelling have raised critical questions related to the shape and spatial distribution of the ionic clusters within the semicrystalline matrix of Nafion.

Roche and co-workers used SAXS and small-angle neutron scattering (SANS) to study the morphology of 1200 EW Nafion membranes in the acid and neutralized forms with a range of water contents.^{34,35} In the as-received state, Nafion was found to have three contrast regions (i.e., a three-phase system) in the angular range probed by SAXS and SANS consisting of a crystalline phase, ionic clusters, and an inhomogeneous matrix phase. By quenching the Na^+ form ionomer from 330°C , the sample was rendered amorphous, as confirmed by WAXD, and the low angle scattering maximum, corresponding to a Bragg spacing of ~ 18 nm, was found to disappear. From these results, the 18 nm peak, also observed by Gierke,¹⁷ was attributed to interference between crystalline structures. In considering the lamellar periodicity (i.e., the long spacing) of ~ 100 nm observed in PTFE, the fact that copolymerization is known to decrease the lamellar thickness, and the average spacing of about 1.5 nm between side chains in 1200 EW Nafion, it was concluded either that a nonrandom distribution of side chains exists in some portion of the material or that the side groups were somehow included in the crystalline structure.³⁴

Using contrast matching methods of SANS,³⁵ Nafion was swollen with various mixtures of H_2O and D_2O in order to highlight the scattering features of the water swollen ionic domains. Furthermore, quenched samples were used in these studies to eliminate the scattering features attributed to the crystalline do-

mains. Roche et al. found that these quenched samples exhibited just the ionomer peak at $q \approx 1.2 \text{ nm}^{-1}$ (q is the scattering vector equal to $(4\pi/\lambda) \sin \theta$, where λ is the wavelength of the scattered radiation and θ is half the scattering angle, 2θ) and a low angle upturn in intensity at $q < 0.5 \text{ nm}^{-1}$. In agreement with the behavior expected from a simple, two-phase system (i.e., a hydrophobic phase and a hydrophilic phase), the normalized scattering intensities of the water swollen membranes were found to vary linearly with relative fractions of D_2O in H_2O . This observation indicated that both the zeroth-order scattering at low q -values and the ionomer peak arise from the same scattering length density differences and could be attributed to the same morphological features (i.e., clusters).³⁵ To account for the larger dimensions associated with the zeroth-order scattering, an inhomogeneous distribution of clusters within the fluorocarbon matrix was proposed. Moreover, these results demonstrated that the zeroth-order scattering could not be attributed to impurities, as previously proposed for other ionomer systems.³⁵

In agreement with the work of Gierke et al.,¹⁷ Roche and co-workers found that the intensity of the ionomer peak increased and the position of the scattering maximum shifted to lower angles with increasing water content.³⁴ A Porod analysis of the SAXS data over a wide range of scattering angles also indicated that the majority of water molecules in the swollen ionomer were phase separated with sharp phase boundaries. Despite the close agreement in scattering results between both groups, Roche et al. argued that an interparticle scattering concept associated with Gierke's cluster-network model was unlikely due to the lack of evidence for a required potential giving rise to ordering of a paracrystalline lattice.³⁴ As an alternative, the origin of the ionomer peak was attributed to an intraparticle scattering model for which the scattering maximum corresponded to characteristic distances between structural elements inside the ionic particles.^{34,35} While this intraparticle scattering model was consistent with the morphology proposed for other ionomers, a detailed quantitative analysis in support of this model was not provided.

Fujimura et al. reported the results of detailed SAXS and WAXD experiments in a series of two papers focused on defining the morphological origins of the two scattering maxima³⁶ and evaluating various scattering models for the origin of the ionomer peak.³⁷ Samples characterized in this work included Nafion with a range of equivalent weights (1100 EW through 1500 EW) in the acid, Na^+ , and Cs^+ forms. To further investigate the effect of ionic interactions on the morphology of Nafion,^{17,34} the sulfonate groups of these materials were also chemically derivatized to yield carboxylated and nonionic, sulfonyl chloride analogues to Nafion. In agreement with the previous scattering studies of Nafion, two scattering maxima at $s \approx 0.07$ and 0.3 nm^{-1} (the scattering vector s is defined as $s = (2 \sin \theta)/\lambda$) were observed and attributed to morphological features associated with crystalline and ionic domains, respectively.

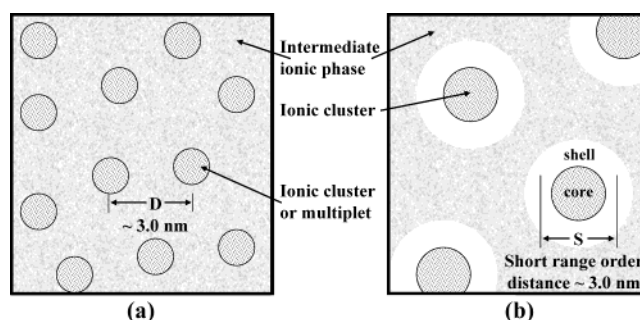


Figure 2. Two morphological models used to describe the origin of the ionic SAXS maximum observed for Nafion: (a) the modified hard-sphere model depicting interparticle scattering and (b) the depleted-zone core-shell model depicting intraparticle scattering. (Adapted with permission from ref 36. Copyright 1981 American Chemical Society.)

In the analysis of the low angle scattering maximum at $s \approx 0.07 \text{ nm}^{-1}$, Fujimura et al. found that the intensity was greatest for the carboxylated and nonionic forms of Nafion, relative to the regular sulfonated ionomer.³⁶ In agreement with the work of Gierke¹⁷ et al., this low angle maximum also increased in intensity with increasing equivalent weight. Similarly, a detailed analysis of the crystallinity in these materials by WAXD indicated that 1100 EW Nafion was 23% and 18–14% crystalline in the nonionic and carboxylated forms, respectively, while it was 12–3% crystalline in the sulfonated forms. With varying equivalent weight from 1100 EW to 1500 EW, the degree of crystallinity increased from 12% to 22%.³⁶ Based on the quantitative correlation of this SAXS and WAXD information and on the behavior observed with uniaxial deformation, the origin of the low angle scattering maximum at $s \approx 0.07 \text{ nm}^{-1}$ was attributed to an average spacing between crystalline lamellar platelets.³⁶

The effect of solvent swelling (with water) on the characteristic dimensions of the ionic clusters associated with the scattering maximum at $s \approx 0.3 \text{ nm}^{-1}$ was also evaluated for 1100 EW Nafion. With the cesium sulfonate form of the ionomer, ionic clusters were shown to exist in the dry state.³⁶ With increasing water content, the cluster dimensions deduced from the scattering maxima were shown to increase.³⁷ Furthermore, over a range of water contents, the microscopic degree of swelling, as determined by SAXS, was found to be much greater than the macroscopic degree of swelling.³⁷ A similar correlation of microscopic versus macroscopic dimensions was observed for Nafion subjected to varying degrees of uniaxial deformation.³⁷ Based on these observations, Fujimura et al. concluded that the scattering behavior of Nafion is best described by an intraparticle core-shell model (Figure 2b) similar to that proposed by MacKnight²³ and co-workers³⁸ rather than an interparticle, two-phase, hard sphere model proposed by Cooper et al.³⁹ (Figure 2a). In this particular core-shell model an ion-rich core is proposed to be surrounded by an ion-poor shell (i.e., a depleted zone)³⁷ that is composed mainly of perfluorocarbon chains. These core-shell particles are dispersed in a matrix of fluorocarbon chains containing nonclustered ions and multiplets, such that the

short-range order distance within the core-shell particle gives rise to the ionic scattering maximum.

While the nonaffine swelling behavior observed by Fujimura et al.³⁷ has been reproduced by many others in subsequent studies and has been the focus of significant debate over the years, it is important to note that the argument against the interparticle hard sphere model relies on the key assumptions that the clusters are uniformly distributed in space and that no redistribution of the ionic groups occurs during swelling. However, the cluster-network model proposed by Gierke¹⁷ clearly allows for cluster reorganization during swelling, and the low angle upturn in scattering intensity observed by Roche et al.³⁵ strongly suggests an inhomogeneous distribution of clusters. With the recognition of the importance of these considerations, Fujimura et al. attempted to quantitatively distinguish the two models by conducting a thorough analysis of the scattering data with the aid of computer simulation.³⁷ For both the core-shell model and the two-phase hard sphere model, quantitative expressions for the variations in the scattering profiles with water uptake were derived from standard scattering theories and fit to the experimental data. Unfortunately, however, this analysis was inconclusive, as both models adequately fit the experimental data and were found to yield similar effects on the variation of the profiles with water uptake and deformation. Moreover, the core-shell model does not give a clear view of long-range structure such as that which might be useful in understanding long-range properties such as molecular transport. In a more recent SAXS investigation, Miura and Yoshida⁴⁰ also supported the core-shell model but suggested (without quantitative support) that some degree of ionic redistribution with swelling in different solvents was possible due to differences in internal stresses within the cluster morphology. Nevertheless, later investigators would challenge this view in favor of the two-phase model.

The organization of crystalline domains in Nafion was further investigated by Starkweather using X-ray diffraction analysis of oriented fiber samples.⁴¹ The unit cell structure derived from the indexed diffraction patterns indicated that the crystallites in Nafion were packed in a hexagonal lattice with true three-dimensional character and cell dimensions roughly equivalent to those of PTFE. Furthermore, the positions of the principal 100, 101, and 002 reflections for the sulfonyl fluoride precursor were essentially unchanged as the polymer was hydrolyzed to the potassium sulfonate form. Peak width measurements, following the Scherrer approach, were used to estimate minimum values for the crystallite size. This analysis suggested that the crystallite size along the *c*-axis was 4.4 nm (or 34 carbon atoms along a planar zigzag conformation), which was noted to be significantly larger than the average of 15 CF₂ groups between side chains in the copolymer.

Based on the fiber diffraction data and the morphological constraints imposed by Geirke's cluster-network model,¹⁷ Starkweather developed a model for the crystalline structure of perfluorosulfonate ionomers.⁴¹ Given a 1 nm wall space between clusters,

this proposed model consisted of a bilayer of hexagonally packed planar zigzag chains with the side chains extending outward on both sides into the clusters. With the assumption that all comonomer units were incorporated in a head-to-tail configuration, this arrangement allowed for all side chains to be on the same side of the planar zigzag chains such that the crystallite thickness could exceed the average separation distance between side chains. While this model provides a simple illustration of the packing of small crystallites between clusters, it was, however, acknowledged to involve "a very efficient use of the polymer's components".⁴¹

One concern for this bilayer model arising from the diffraction data was noted to involve the width of the 100 reflection; the Scherrer analysis indicated that the size of the crystals normal to the chain axis was on the order of 3.9 nm rather than the proposed 1 nm bilayer thickness. In addition, a number of further considerations raise important questions as to the validity of this model. For example, given the recognition that Nafion contains a heterogeneous distribution of clusters³⁵ (i.e., long-range heterogeneities observed in the SAXS profiles at low angles), rather than a homogeneous network of clusters and channels in an ordered paracrystalline lattice,¹⁷ it is not necessary to impose the organization of crystals in the narrow space between nearest neighbor clusters. Furthermore, Nafion is a statistical copolymer that is likely to contain both short and long runs of TFE units between side chains. The longer runs could thus pack into small PTFE-like crystallites in regions somewhat removed from the ionic domains. These crystallites, while few in number, would provide the three-dimensional order required to yield the observed WAXD reflections and the high ΔH_f and T_m values similar to those for PTFE as reported by Starkweather.⁴¹ More recent studies, discussed below, provide strong evidence for this alternative organization of crystallites and clusters in Nafion.

In 1986, Kumar and Pineri published a report focused on the interpretation of small-angle X-ray and neutron scattering data for perfluorosulfonated ionomer membranes in order to elucidate the possible cluster morphology in PFSI membranes.⁴² This detailed study involving model calculations and comparisons of experimental scattering profiles to theoretical fits was placed in context with the morphological models of Nafion, to date. Since the paracrystalline lattice model (i.e., the basis for calculations from the Gierke cluster-network model)¹⁷ was found to be inadequate to explain the observed scattering and swelling data, and the depleted-zone core-shell model relied on questionable assumptions involving the applicability of Bragg's equation in estimating microscopic versus macroscopic swelling and the requirement of a constant number of clusters with swelling,^{36,37} an alternative model involving noninteracting hard spheres was chosen for this analysis. With this model, Kumar and Pineri found that the SAXS ionomer peak could be quantitatively attributed to the interference between clusters, assuming them to be noninteracting hard spheres.⁴² Furthermore, the increase in intensity at very low angles

was accounted for by considering a previously neglected intensity term for scattering from a dense group of particles and/or an intercluster potential arising from Coulombic interactions between clusters.

In contrast to Gierke's model,¹⁷ which predicted a large increase in the number of ions per cluster, with increasing water content, parameters from these model calculations⁴² showed a moderate increase in N_p at low water uptake and a significant decrease in N_p at higher water contents. This behavior was attributed to an increase in elastic forces on the chains that effectively forces some ions out of the existing clusters at high degrees of swelling, thus decreasing the N_p . Since the ions forced out of clusters with swelling are free to form other clusters, the average distance between clusters was argued to be an invalid measure of the microscopic swelling without some account for the change in the total number of clusters. For Nafion of different equivalent weights, Kumar and Pineri also found that the number of ionic sites per cluster, and thus the cluster radius, only moderately decreased with increasing equivalent weight.⁴² This observation, as confirmed by Manley et al.⁴³ in a later study using a similar model analysis, was noted to again show a distinct discrepancy with the results of Gierke, which indicated a sharp decrease in N_p with increasing equivalent weight.

The spatial distribution of clusters in water-swollen Nafion was investigated by Dreyfus and co-workers through SANS experiments.⁴⁴ The shape and intensity of the scattering profiles obtained from samples with water contents ranging from 6 to 26% (by volume) were fit to a local-order model that describes the distribution of spherical, hydrated clusters in a locally ordered structure with four first neighbors located at a well-defined distance embedded in a matrix of completely disordered (gaslike) clusters. Using a radial distribution function for this locally ordered (tetrahedral) structure and a form factor for homogeneous spheres, the following intensity function was derived

$$I(q) = \frac{I(0)}{S(0)} \left(\frac{3(\sin qR - qR \cos R)}{(qR)^3} \right)^2 \left(1 + z \frac{\sin qD}{qD} - z' \frac{3(\sin q\alpha D - q\alpha D \cos q\alpha D)}{(q\alpha D)^3} \right)$$

where $I(0)$ and $S(0)$ are the coherent scattering intensity and an interference term at $q = 0$, respectively; q is the scattering vector, R is the radius of the scattering particle, D is the distance between locally ordered particles, αD is the distance from the origin cluster beyond which a disordered distribution of clusters exists; and z and z' are the number of clusters in the locally ordered structure and the number of clusters in the volume corresponding to the correlation hole between 0 and αD , respectively. The a priori choice of a diamond-like structure led to the refinement of constant values of $\alpha = 1.122$, $z = 4$, and $z' = 4.39$.

With this local-order model,⁴⁴ only two adjustable parameters (D and R) were needed to obtain reason-

able fits over the q -range 0.2 – 2.6 nm^{-1} . Based on the excellent agreement between the theoretical and experimental SANS curves, the authors concluded that both the small-angle upturn and the ionomer peak may be attributed to the existence and spatial distribution of ionic clusters. Using the values of D and R from the model fits (e.g., $D = 3.4 \text{ nm}$ and $R = 1.7 \text{ nm}$ for the fully hydrated membrane), the specific surface area per charge site on the cluster was found to be relatively constant at 73 \AA^2 . In agreement with previous studies that suggested a redistribution of ions between clusters with swelling,¹⁷ the number of charge sites per cluster was calculated using space-filling arguments based on the D values and found to increase from ~ 25 to 45 with increasing hydration. Despite the excellent fits with this local-order model, however, the number of charge sites per cluster, directly calculated from the R values, was unrealistically large. In addition, the fundamental requirement of this model for an attractive potential between neighboring clusters in the formation of the local-order structure is consistent with the suggestion by Kumar and Pineri⁴² that the small-angle upturn could be attributed to such a potential; however, this plausible correlation was not addressed in this analysis.

Lee et al.⁴⁵ utilized a novel combination of small- and wide-angle neutron scattering methods to study local and long-range structure of water in Nafion 117 membranes. Since small-angle scattering methods suffer from an inherent inability to probe a sufficiently large region of reciprocal space, the results of small-angle (low q) and wide-angle (high q) scattering experiments were combined so that direct Fourier mathematical inversions (integral transforms) could be applied to data that were thereby expanded over q -space. Using this method, atom–atom radial distribution functions for the atom pairs associated with water (i.e., H–H and O–H) in the cluster domains of Nafion were calculated to provide real space information. It was stated that Nafion in the Ni^{2+} ion exchanged form was used so that the counterion radial distribution function could be derived, as well, although these results do not appear in the report.

It is important to describe the preparation of these samples, which were annealed at high temperature in dry nitrogen gas and then rapidly quenched in liquid nitrogen.⁴⁵ Because they were thereby rendered amorphous, there was no scattering due to the PTFE-like crystallinity that would complicate the data interpretation. Membranes were boiled in NiCl_2 solutions and then soaked in H_2O , D_2O , and $\text{H}_2\text{O}/\text{D}_2\text{O} = 50:50$ solutions. Due to the elimination of crystallinity from the melt-quench pretreatment, these samples were considerably hydrated at 41 vol %.

The following equation shows the relationship between the partial structure factors, $S_{\alpha\beta}(q)$, and the atom–atom correlation functions, $g_{\alpha\beta}(r)$, that refer to the distance, r , between atoms α and β :

$$S_{\alpha\beta}(q) = 4\pi\rho \int r^2 [g_{\alpha\beta}(r) - 1] \frac{\sin(qr)}{qr} dr$$

ρ is the macroscopic density. This equation was inverted to give $g_{\alpha\beta}(r)$ using the principle of maximum entropy. The total coherent structure factor is a linear combination of all of the partial structure factors where each term is multiplied by the product of the atomic fractions and coherent scattering lengths of the species α and β .

The intramolecular correlations of O–H at $r = 1.00$ Å and of H–H at $r = 1.56$ Å are identical, and the second peaks show small differences, perhaps arising from interactions between water molecules and sulfonate groups, although it would seem that water coordination around Ni^{2+} would have to be considered, as well. From this, the authors concluded that the structure of water in the clusters is essentially that of water in the bulk state.⁴² This would seem reasonable considering that the water uptake of these samples corresponded to an average of 21 H_2O molecules per $-\text{SO}_3^-$ group.

The H–H radial distribution appears in the function $r[g_{\text{HH}}(r) - 1]$ which was plotted versus distance r . The peak observed at low r was associated with the cluster radius. If the clusters are *assumed* to be spherical, this distribution is consistent with a cluster radius of 18.5 Å, which is similar to values based on scattering based estimates from other studies.^{17,42} At higher r , the function shows a mean periodicity of these structures (i.e., cluster center-to-center distance) of 70 Å. This would leave a rather large space between the “surfaces” of adjacent clusters of 33 Å, which seems rather large, especially when compared to that estimated in the model of Gierke et al.,¹⁷ which was only around 10 Å. The analysis ceased to be of an *ab initio* nature when the assumption of spherical clusters was made and the 33 Å space had to be accounted for. The authors explain that these data reflect a continuous network of water structure rather than an array of isolated hydrated clusters for two reasons. (1) 41 vol % of water is considerably above the percolation threshold, and a structure in which water is distributed in spheres of this size and having this center-to-center spacing can only accommodate 8 vol % of water. (2) Because the cluster center-to-center spacing is much larger than the cluster diameter, $g_{\text{HH}}(r)$ would be expected to drop to around zero at about $r = 40$ Å before approaching the asymptote of 1.00 at large r , which it does not. These and other arguments led the authors to invoke the presence of connective water structures and suggested a view consisting of rodlike aqueous regions that intersect at “nodes” (i.e., clusters).⁴⁵ It should be remembered that these data and the derived conclusions refer to the distribution of water—the sole scattering source in these experiments—throughout the Nafion structure and not to the direct structure of Nafion.

2.2. Scattering from PFSI Solutions and Recast Films

In the early 1980s, reports surfaced that detailed procedures for dissolving Nafion membranes in water/alcohol mixtures at elevated temperatures and pressures.^{46,47} Currently, Nafion solutions are available commercially, and these solutions are now used in

commercial processes to uniformly cast thin membranes for fuel cell applications. Since the properties and performance of Nafion membranes are directly related to their complex morphology, and the supermolecular organization of ionic and crystalline domains may be altered by the processing history, it is of great importance to understand the nature of these Nafion solutions and the subsequent evolution of morphological development during the casting process. With this fundamental knowledge, the means to enhance the transport properties and efficiencies of PFSI membranes by controlling and tailoring the morphology for specific applications may be realized.

With the availability of dissolution procedures for Nafion, Aldebert and co-workers used SANS to study the nature and structure of Nafion solutions in water and ethanol.⁴⁸ Similar to the case observed in the scattering results of Nafion membranes, the “solutions” were found to be heterogeneous, yielding a single scattering maximum attributed to interference between nanometer-scale scattering objects that were distributed throughout the total volume of the sample. Moreover, since the separation distance, d , varied systematically with the volume fraction of the ionomer, ϕ_v , the particles were suggested to exhibit electrostatic repulsion similar to that observed for a colloidal suspension of charged particles. Since the experimental plot of $\log d$ versus $\log \phi_v$ varied following the law $d \sim \phi_v^{-0.5}$, the solutions in both water and ethanol were assumed to consist of a dispersion of rodlike particles.^{48,49} In comparing the scattering results to dimensional parameters calculated from three different models (i.e., a three-dimensional fcc lattice, a two-dimensional hexagonal array of rods, and a cubic phase of rods), the authors found that the cubic phase model was most likely. Furthermore, the rodlike particles were suggested to have a compact cylinder structure with the solvent–polymer contact at the surface of the charged “micelle” as opposed to a more open coil model. The center of the rodlike particles was also proposed to contain crystallites of the PTFE backbone segments oriented along the rod axis.⁴⁹

From SAXS results, Rebrov and co-workers also found that Nafion solutions could be characterized as containing colloidal suspensions of anisotropic polymeric particles.⁵⁰ By manually extrapolating the experimental scattering curves to a state of infinite dilution in order to eliminate interparticle interference effects, the form of the scattering particles was suggested to most closely resemble that of flattened disklike particles. While this questionable practice of approximating the scattering profiles at infinite dilution raises concern as to the validity of the chosen form factor, the results are qualitatively consistent with the previous study of Aldebert et al.⁴⁸ in that Nafion “solutions” are not “true” solutions but contain relatively large colloidal aggregates of anisotropic structure with dimensions exceeding 15 nm.

More recently, Loppinet and co-workers have used both SAXS and SANS (with contrast variation methods) to characterize the morphology of dilute PFSI solutions having a volume fraction of polymer less

than 0.5%.^{51,52} The intensity profiles of these dilute solutions were found to decrease as $1/q$ at low q -values in a manner typical of rodlike particles. The scattering profiles in the low q -range were also found to satisfactorily fit the form factor of cylindrical particles having a radius of ~ 2.0 – 2.5 nm. For higher volume fraction solutions, the asymptotic behavior of the scattering profiles was also found to be consistent with that predicted for cylindrical particles. By studying the effect of various solvents, different counterions, and added salt, the formation of the colloidal particles was attributed to aggregation of the neutral part of the ionomer chains. In contrast to the behavior of low molecular weight surfactants, the rodlike shape of the polymeric particles did not show evidence of any phase transitions with changes in concentration, salt, temperature, or the nature of the solvent or counterions. Furthermore, the size of the cylindrical particles was shown to be related to the polymer–solvent interfacial energy. Using SANS contrast variation studies, the particles were found to be dense, indicating that the thickness of the polymer–solvent interface is negligible compared to the cross-sectional size. From the apparently high particle densities calculated from the constant neutron scattering length densities, the authors suggest that the rods contain a crystallinity index of approximately 50%. At relatively high volume fractions (i.e., 5–20%), the cylinders are proposed to be distributed in the solution with the existence of some local order. Space-filling analysis assuming a local order in a hexagonal array yields radius values consistent with the previous determinations.

Since Nafion films possess excellent chemical stability and a high affinity toward large organic cations, Nafion solutions have been widely used in the formation of polymer modified electrodes for a variety of electroanalytical investigations. For many of these applications, it has been assumed that the morphologies, physical properties, and chemical characteristics of the solution-cast PFSI films were identical to those of the as-received membranes. Moore and Martin, however, discovered that this simple assumption was inaccurate.^{53,54} For example, Nafion films cast from ethanol–water solutions at room temperature (i.e., the general method used to produce polymer-modified electrodes), referred to as recast films, were found to be “mud-cracked”, brittle, and soluble at room temperature in a variety of polar organic solvents. In contrast, the as-received Nafion membranes are flexible, tough, and insoluble in virtually all solvents at temperatures below ~ 200 °C. However, through the application of high boiling point solvents in the casting procedure, Moore and Martin demonstrated that the desirable properties of as-received Nafion could be reconstituted in solution-cast films and membranes, referred to as solution-processed films, if the casting temperature exceeded ~ 160 °C.⁵³ This observation suggested that the contrast in properties between the recast and solution-processed films was of a morphological origin and the resulting solid-state structure of the cast films was a function of the macromolecular organization of chains in solution during solvent evaporation.

Using WAXD and SAXS, Moore and Martin found that the as-received and solution-processed films were semicrystalline (having similar degrees of crystallinity), while the recast films were virtually amorphous.^{54,55} The SAXS profiles of the as-received and solution-processed films displayed a distinct ionomer peak at $q = 1.2$ nm⁻¹, attributed to the presence of ionic clusters, and a prominent low angle maximum at $q = 0.5$ nm⁻¹, attributed to the long spacing within well-organized crystalline domains. In contrast, the scattering profile of the recast material displayed only the ionomer peak at $q = 1.2$ nm⁻¹. While all samples possessed ionic clusters, regardless of processing history, the enhancement in crystallinity and physical properties of the solution-processed films was attributed to the ability of the ionomer chains to reorganize from the colloidal aggregate state in solution to a more entangled network in the solid film with added thermal energy and solvation from the high boiling point solvents at elevated casting temperatures. The presence of ionic clusters in the recast films was attributed to the aggregation of ions on the surface of the contacting micelle-like colloidal particles in the absence of solvent. Moreover, the high solubility and “mud-cracked” character of the recast material supported the conclusion that the colloidal morphology observed in solution remained intact in the recast state with little if any chain entanglement or coalescence between particles.

Gebel and co-workers used a similar high temperature casting procedure with high boiling point solvents to prepare reconstructed Nafion membranes.⁵⁶ WAXD and SAXS results from this study indicated that the morphology of the PFSI membranes reconstructed at room temperature (i.e., cast at room temperature with added high boiling point solvent) or at high temperature was different from that of the as-received membrane. In agreement with the results of Moore and Martin,^{53,54} the room temperature cast membranes were essentially noncrystalline, while the high temperature process reestablished significant crystallinity with long-range order.

The morphology of recast Nafion films, processed at room temperature in wet and dry environments, was studied by Scherer and co-workers using WAXD and SAXS.⁵⁷ In agreement with the previous studies, room temperature casting yielded little if any crystallinity in the resulting films.⁵⁴ The films cast under wet environments, however, yielded intense scattering maxima positioned at lower q -values relative to those of the films cast under dry conditions. Based on this behavior, the authors suggested that the number and size of the clusters increased with increasing relative humidity during the casting process. Since previous studies of the morphology of as-received films also show an increase in the intensity of the ionomer peak and a shift to lower q -values with increasing water content, the assertion that relative humidity during casting affects the cluster morphology seems inconclusive within the context of this limited study. Nevertheless, the results of this study and the above investigations strongly support the general suggestion that specific casting procedures may be developed to alter the crystalline and ionic

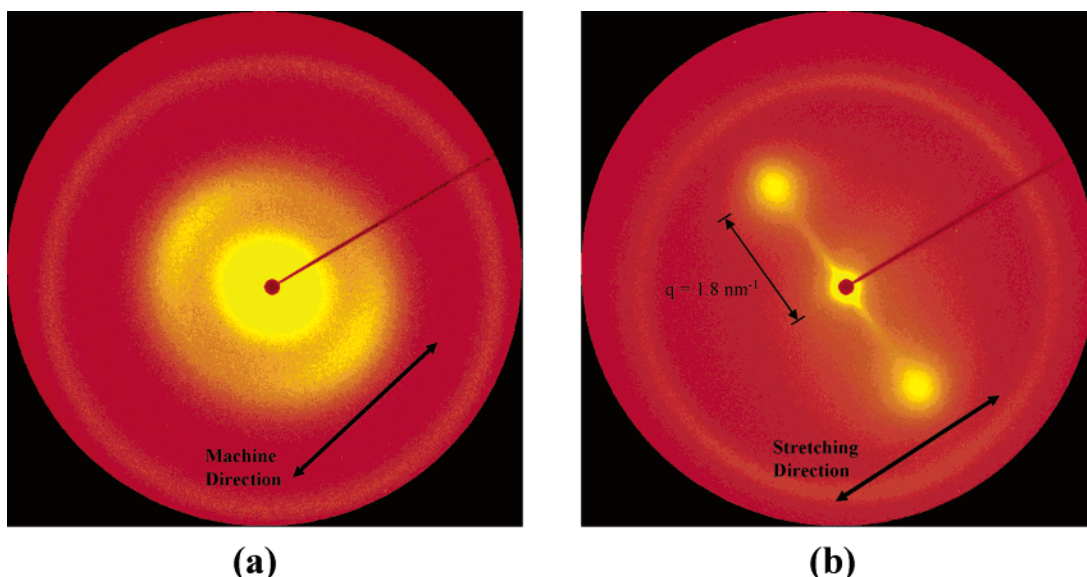


Figure 3. 2-D SAXS scattering patterns of (a) as-received Nafion, showing a slight morphological anisotropy in the ionic domains from the membrane calendaring process, and (b) uniaxially oriented Nafion ($\lambda_b = 5.4$).

cluster morphologies in an attempt to control and tailor the properties of Nafion films and membranes.

2.3. Evaluation of Nafion Morphology through Studies of Oriented Membranes

Given the morphological complexity of Nafion membranes and the limited structural information that can be extracted from the relatively diffuse scattering profiles, the elucidation of detailed morphological models has required the study of controlled morphological manipulations by processes including solvent swelling and mechanical deformation. Over the years, a variety of groups have demonstrated that the application of uniaxial extension provides a particularly useful means of evaluating the size, shape, and spatial distribution of crystallites and ionic domains in Nafion. Moreover, structural information obtained from these studies has been used to differentiate the various morphological models that have been proposed for PFSIs.

Gierke et al. reported the first data showing the effect of tensile drawing on the SAXS profiles of the unhydrolyzed Nafion precursor and that of the hydrolyzed ionomer.¹⁷ For the oriented nonionic precursor, the low angle scattering maximum attributed to a periodicity associated with the organization of PTFE-like crystallites was observed only in the meridional scan, implying a periodicity in the long spacing along the fiber axis. In contrast, SAXS scans of an oriented, hydrolyzed ionomer showed that the ionomer peak was only observed in a scattering direction perpendicular to the draw direction, implying a periodicity normal to the fiber axis.

A similar analysis was conducted by Fujimura et al.³⁷ on cesium-neutralized Nafion with orientations up to $\lambda_b = 1.5$ (where λ_b is the ratio of the final extended length to the initial undrawn length). Over a range of orientations, the ionomer peak was observed to shift to lower angles and decrease in intensity in the meridional (draw) direction, while a shift to higher angles and an increase in intensity

was observed in the equatorial direction. Using the Bragg spacings calculated from the peak maxima, a nonaffine deformation behavior was observed between the microscopic and macroscopic dimensions. This observation led to a conclusion, similar to that proposed to explain solvent swelling behavior, that nonaffine behavior was inconsistent with an interparticle scattering model yet could be accounted for by deformation of a core-shell particle.

More recently, Moore and co-workers found that Nafion membranes, neutralized with tetraalkylammonium ions, could be oriented with high elongation at elevated temperatures (e.g., 200 °C for tetrabutylammonium form Nafion) to yield extremely anisotropic WAXD and SAXS scattering patterns.^{58–60} With uniaxial deformation (ranging up to $\lambda_b = 5.4$) at temperatures above the ionomers' α -relaxation (as determined using dynamic mechanical analysis) followed by cooling to room temperature, the oriented morphology was observed to be stable in the absence of stress. Using a 2-dimensional area detector, the scattering patterns were shown to increase in intensity at azimuthal angles perpendicular to the stretching direction (i.e., equatorial scattering) with a profound decrease in intensity (to the point of disappearance) at angles parallel to the stretching direction (i.e., meridional scattering) with increasing orientation.⁵⁸ At relatively high orientations (greater than ca. $\lambda_b = 2.0$), only equatorial spots at $q = 1.8 \text{ nm}^{-1}$ were observed (Figure 3). In contrast to the earlier studies of oriented membranes containing inorganic ions,^{17,37} the equatorial peak position of the TBA⁺ form membranes remained constant with elongation. A circular integration over all azimuthal angles of the scattering patterns was performed to calculate the relative invariant, Q , for samples having a range of elongations. A significant increase in Q with elongation was attributed to an increase in the extent of ionic aggregation with elongation to yield a matrix with fewer lone ion pairs in the highly oriented membranes.⁵⁸

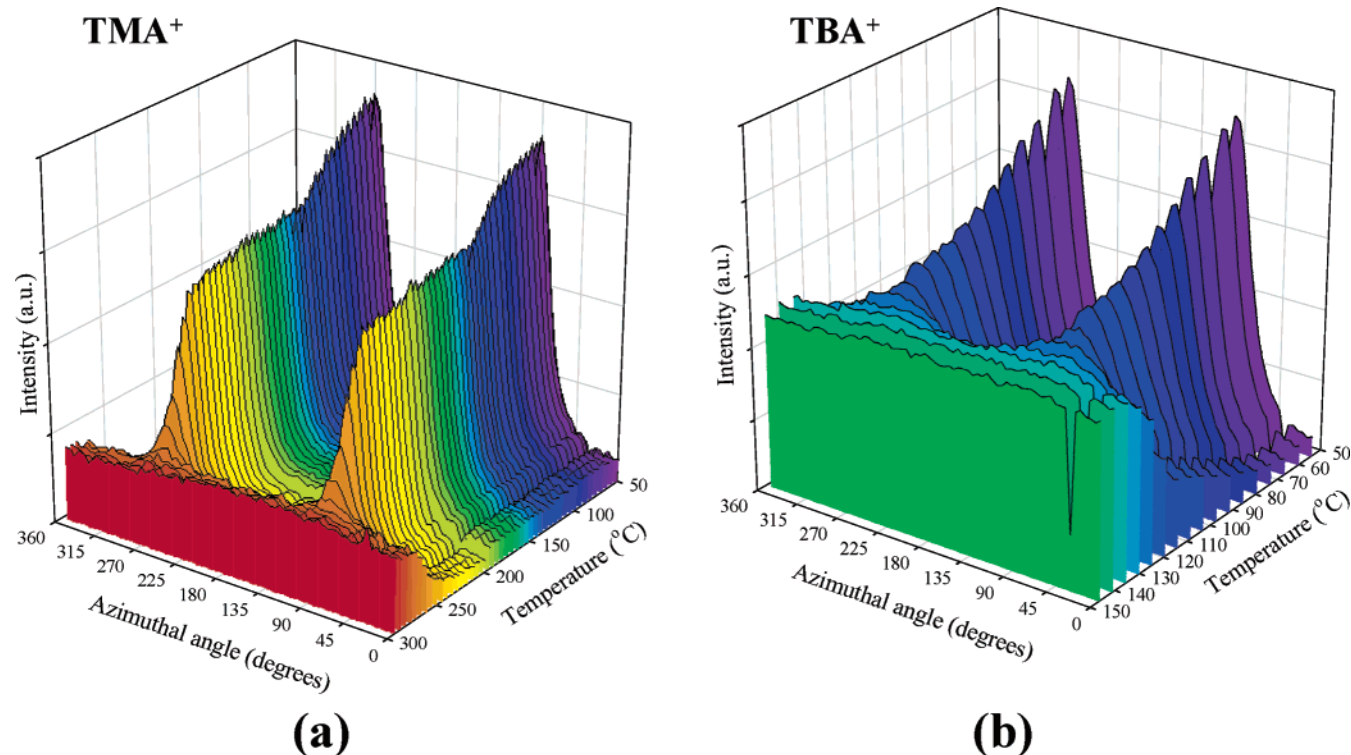


Figure 4. Azimuthally integrated SAXS profiles as a function of temperature for (a) TMA⁺ and (b) TBA⁺ forms of uniaxially oriented Nafion.

The thermal relaxation behavior of oriented Nafion membranes was also evaluated using time-resolved synchrotron SAXS analysis.⁶¹ For oriented membranes neutralized with tetramethyl- (TMA⁺), tetraethyl- (TEA⁺), tetrapropyl- (TPA⁺), and tetrabutylammonium ions (TBA⁺), the anisotropic scattering patterns were found to relax back to isotropic patterns as the samples were heated from 50 to 300 °C (see Figure 4). Moreover, the temperature at which the morphological relaxation occurred tracked with the size of the tetraalkylammonium ions, following the order TBA⁺ < TPA⁺ < TEA⁺ < TMA⁺. This relaxation behavior of the ionic domains was noted to be in excellent agreement with the order of the principle dynamic mechanical relaxations (α -relaxations) for these materials. Thus, the thermal relaxation of the scattering patterns was attributed to the onset of ion-hopping (i.e., the thermally activated process of redistributing ion pairs between aggregates in the electrostatic network in order to relieve local stress on the chain segments). With a weakened electrostatic network for the samples containing large tetrabutylammonium ions, the onset of ion-hopping is activated at lower temperatures, allowing for significant chain mobility and morphological reorganization.

Elliott and co-workers performed a detailed SAXS investigation of the morphology of Nafion membranes that were subjected to uniaxial and biaxial deformation.^{62,63} For as-received membranes, manufactured by Du Pont using an extrusion process, the cluster reflection was shown to exhibit a limited degree of arching in the direction perpendicular to the machine direction. Upon uniaxial extension, this arching was observed to increase in a manner consistent with previous studies. This arching was rationalized on

the basis of an interparticle scattering model and contrasted to the behavior predicted for an intraparticle model.⁶³ With the interparticle scattering model, the arching was explained by an increase in coherence of the intercluster spacings perpendicular to the draw direction, accompanied by a corresponding reduction in coherence in the parallel direction. In contrast, the observed arching with respect to the intraparticle scattering model was noted to be unlikely, since it would require an elliptical deformation of the clusters, as independent scatterers, and an electron density difference between the long and short axes of the elliptically shaped clusters. Using a model-independent maximum entropy method for reconstructing a 2-dimensional electron density map in real space from that corresponding to the scattering data, the intercluster spacings parallel to the draw direction were found to be almost random, while the spacings in the transverse direction were observed to display distinct periodicity.⁶¹ Furthermore, the clusters in the drawn sample were found to be somewhat agglomerated relative to their distribution in the as-received membrane. Based on this finding, the anisotropic shape of the small-angle upturn was attributed to scattering between oriented cluster agglomerates having periodic dimensions significantly larger than the intercluster spacings. For extruded membranes drawn perpendicular to the machine direction (i.e., a sequential biaxial draw), the anisotropic morphology was found to persist, but to an extent much less oriented than that observed for membranes drawn parallel to the machine direction. Relatively isotropic morphologies were obtained only when the membranes were processed with a simultaneous biaxial draw.

In a subsequent communication,⁶² Elliott and co-workers found that uniaxially oriented membranes swollen with ethanol/water mixtures could relax back to an almost isotropic state. In contrast, morphological relaxation was not observed for membranes swollen in water alone. While this relaxation behavior was attributed to the plasticization effect of ethanol on the fluorocarbon matrix of Nafion, no evidence of interaction between ethanol and the fluorocarbon backbone is presented. In light of the previous thermal relaxation studies of Moore and co-workers,⁶¹ an alternative explanation for this solvent induced relaxation may be that ethanol is more effective than water in weakening the electrostatic interactions and mobilizing the side chain elements. Clearly, a more detailed analysis of this phenomenon involving a dynamic mechanical and/or spectroscopic analysis is needed to gain a detailed molecular level understanding of this relaxation process.

Londono et al. reported the results of a synchrotron SAXS study of oriented Nafion membranes.⁶⁴ As the elongation was increased to 150%, meridional scattering of the ionomer peak disappeared while the intensity profile narrowed azimuthally about the equator. At 150% elongation, an equatorial streak, similar to that shown in Figure 3b, was observed and noted to resemble the SAXS pattern of drawn fibers containing a microfibrillar morphology. Using a finely collimated X-ray beam (100 μm) and stacked films, edge-on scattering patterns were obtained for orientations parallel and perpendicular to the stretching direction. The observation of an isotropic scattering pattern from the orientation parallel to the stretching direction confirmed the fibrillar morphology of oriented Nafion. Furthermore, based on this analysis, the authors suggest that the morphology of uniaxially drawn Nafion consists of oriented cylindrical or lamellar domains, rather than spherical clusters. From these scattering results alone, a definitive distinction between cylinders or lamella was not possible. Simultaneous SAXS/WAXD measurements were also collected in-situ during the orientation process. The (100) crystalline reflection of the PTFE-like crystallites was observed to narrow about the equator at a rate of almost double that of the orientation of the ionic domains. While the authors acknowledge the bilayer lamellar model proposed by Starkweather,⁴¹ the SAXS/WAXD results are stated to indicate that lamellar ionic domains may also be present in the amorphous phase. However, if the Starkweather model were strictly considered, such that the crystalline bilayers were intimately linked to the lamellar ionic domains, then the orientation of the ionic and crystalline domains should have tracked together with a one-to-one correlation.

Computational methods combined with a novel approach in the application of scattering physics were recently employed by Barbi et al. in a synchrotron SAXS study of the nanostructure of Nafion as a function of mechanical load.⁶⁵ A new method of multidimensional chord-distribution function (CDF) analysis was used to visualize the multiphase nano-

structure information of Nafion in direct space following established procedures used to study oriented semicrystalline polymers and strained elastomers. Based on the classical ionomer domain model of Gierke¹⁷ (i.e., ionic clusters as inverted micelles interconnected by channels), the deformation behavior of Nafion in the dry state was evaluated over a range of deformations from 0 to 125%. During the deformation, the channels between clusters are proposed to open and widen in the direction of strain and merge with adjacent domains to form slab-shaped domains that align together in the draw direction.⁶⁵ Using contour maps constructed from the CDF analysis, the average domain thickness D_t (i.e., the dimension perpendicular to the draw direction) and the maximum domain height D_h (i.e., along the draw direction) were determined. As the elongation was varied from 50% to 125% (near the break point), the domain thickness decreased from 1.9 to 1.5 nm, while the domain height increased from 3 to 6 nm. From this real space information, and the noted absence of autocorrelation peaks on the meridian, the ionic domains were concluded not to be cylinders. With respect to the polymer matrix, the crystalline domains were shown to be cylindrical in nature and undergo plastic deformation and parallelization upon elongation. At high elongations, the CDF analysis indicated a broad distribution of crystallite sizes with an ultimate inclination of 40° relative to the draw direction.

Recently, van der Heijden et al. have used simultaneous SAXS/WAXD to study the morphological variation in Nafion during the deformation process of uniaxial extension.⁶⁶ Using absolute values of the Hermans orientation factor, the orientations of both the ionomer and crystalline domains were quantitatively compared with respect to the draw ratio. The structural anisotropy at length scales between 0.2 and 4 nm was evaluated based on a ratio, α , of the crystalline to ionomer domain orientation factors. For draw ratios below 200%, α values were observed to be well below 1.0, indicating that the ionomer domains oriented more readily than the crystalline domains. Based on this observation, a simple model involving the deformation of spherical ionic domains into ellipsoidal shaped structures was rejected, since the clusters would not be expected to deform more than their surrounding matrix. Beyond 200% elongation, the α values approached 1.0, indicating that the crystalline and ionic domain orientation was correlated with respect to elongation. This two-stage orientation behavior was thus explained based on a new consideration of Nafion morphology (see below) as a collection of bundled, elongated polymeric aggregates containing relatively extended chain crystals. Upon stretching, two orientation mechanisms were postulated to occur simultaneously: at small draw ratios, the large bundles rotate such that the elongated aggregates in the bundles are more or less correlated in orientation, and at large draw ratios, the alignment of individual elongated aggregates is refined in the draw direction due to sliding and/or disentangling of the aggregates from each other. Further analysis of the crystalline morphology indi-

cated that the degree of crystallinity remained constant as a function of the draw ratio.

2.4. Current Models for the Morphology of Nafion

Since the early studies of Nafion morphology, numerous investigators have attempted to reconcile a wealth of structural information with observed properties (specifically, transport properties) in order to develop a well-defined morphological model for perfluorosulfonate ionomers. As noted in the studies above, the complicating factors associated with this endeavor include the random chemical structure of the copolymer, the complexity of co-organized crystalline and ionic domains, vast morphological variations with solvent swelling, the relatively low degree of crystallinity, and the diffuse, heterogeneous nature of the morphology that leads to a wide range of domain dimensions. While the majority of morphological information about Nafion has originated from small-angle scattering and wide-angle X-ray diffraction experiments, the simple fact remains that this polymer yields very little characteristic detail in the dimensions probed by these methods. Thus, the quest for a universally accepted model continues with a spirited debate in the current literature.

The principle scattering models for the morphology of Nafion that have been proposed to date include a cluster-network model proposed by Gierke et al.¹⁶ (Figure 1), a modified (depleted-zone) core-shell model proposed by Fujimura et al.^{36,37} (Figure 2b), a local-order model first proposed by Dreyfus et al.,^{44,67–69} a lamellar model proposed by Litt,⁷⁰ a sandwich-like model proposed by Haubold et al.,⁷¹ and a rodlike model proposed by Rubatat et al.⁷² Central to each of these models is the recognition that the ionic groups aggregate in the perfluorinated polymer matrix to form a network of clusters that allow for significant swelling by polar solvents and efficient ionic transport through these nanometer-scale domains. These models do, however, differ significantly in the geometry and spatial distribution of the ionic clusters. While the complications associated with modeling the spatial distribution of ions within a semicrystalline matrix are often either ignored or simply eliminated through various thermal treatments, the experimental evidence of PTFE-like crystals in Nafion is undeniable. Thus, the validity of a given model in *completely* describing the morphology of Nafion requires a reasonable account for the existence of crystallites in the presence of a pervasive ionic network.

The original cluster-network model proposed by Gierke et al.^{16,17,31,32} (also referred to as the cluster-channel model) has been the most widely referenced model in the history of perfluorosulfonate ionomers. Despite the very large number of papers and reports that have strictly relied on this model to explain a wide variety of physical properties and other characteristics of Nafion, this model was never meant to be a definitive description of the actual morphology of Nafion, and the authors recognized that further experimental work would be required to completely define the nature of ionic clustering in these ionomers.¹⁷ For example, the paracrystalline, cubic lattice

of close-packed spheres was only chosen to describe the spatial distribution of inverted micelle clusters for the convenience of simple space-filling calculations. The cluster dimensions obtained from these calculations were consistent with other experimental information (e.g., from TEM analysis); however, the observed spatial distribution of clusters was not, by any means, paracrystalline. Furthermore, the existence of 1 nm channels connecting the clusters was proposed in order to reconcile the highly permselective transport properties of Nafion containing inverted micelles.^{16,31} With channels, a network of clusters could exist with a percolation pathway through the membrane; however, no direct experimental evidence has ever revealed the existence of channels in these polymers. On the other hand, this cluster-network model was the first to attribute the SAXS maximum in Nafion to an interparticle origin, and it offered the possibility of slight morphological reorganization during solvent swelling.¹⁷ Both of these considerations have prevailed through the test of time and are currently featured in the modern understanding of this polymer.

In a manner following the scattering studies of other ionomeric systems, the intraparticle, modified core-shell model of Fujimura et al.³⁷ lost popularity through the late 1980s and has since been more or less discounted as a reasonable model for the morphology of Nafion. Recent SANS analysis of water-swollen Nafion was performed by Gebel and Lambard with a quantitative comparison of the core-shell models to other interparticle scattering models.⁶⁷ Using the depleted-zone core-shell model of Fujimura,³⁷ the theoretical profiles showed a poor fit to the experimental data, and the dimensional and contrast values extracted from the best fits were found to be unrealistic. Furthermore, the existence of isolated ion pairs constituting the matrix in the depleted-zone core-shell model was noted to be highly questionable in swollen membranes and confirmed to be improbable by ESR measurements.⁷³

In considering the ionomer peak observed for Nafion to be of an interparticle origin, a more quantitative approach to extracting detailed structural information from the scattering data involved the application of a modified hard sphere model.⁵² In the work of Kumar and Pineri⁴² (discussed above), the SAXS peak was accounted for quantitatively (in both position and intensity) as arising from the interference between clusters, assuming them to be noninteracting hard spheres. With calculations based on the modified hard sphere model,^{24,25} the theoretical peak value of the relative intensity invariant over an intermediate q -range was found to be within 15% of the experimentally observed intensity invariant for samples having different equivalent weights, different cationic forms, and different water contents. Recently, Orfino and Holdcroft used the modified hard sphere model to determine the characteristic dimensions associated with the ionic clusters in dry and hydrated Nafion.⁷⁴ With reasonable fits to the experimental scattering profiles, their model calculations indicated that the number density of clusters decreased from 3.2×10^{19} to 9.7×10^{18} clusters/cm³

upon hydration, while the cluster size increased from a radius of 1.12 to 2.05 nm. Although this observation is in agreement with the morphological reorganization proposed in the cluster-channel model of Gierke,¹⁷ a comparison of the model parameters determined for the radius of the ionic core and the radius of closest approach to the size of a single, hydrated ionic group led the authors to the conclusion that clusters could be simply bridged by single ionic sites rather than organized ionic channels.⁷⁴

The local-order model, first applied by Dreyfus et al. (see above),⁴⁴ is another interparticle scattering model used to define the spatial distribution of spherically shaped ionic clusters in Nafion. More recently, Gebel and Lambard demonstrated that the local-order model provided a better fit to SAXS and SANS profiles of hydrated Nafion than those of the depleted-zone core-shell and modified hard sphere models over the range of scattering vectors between 0.3 and 2.0 nm⁻¹.⁶⁷ At larger q -values, the deviation between the model fit and experimental data was attributed to the fact that the model assumes monodisperse clusters having a homogeneous electron density. While additional terms allowing for polydispersity in dimensions were noted to yield improvement in the model fits, the added adjustable parameters were deemed undesirable. Using a Debye-Bueche model to fit the small-angle upturn (i.e., a method found successful for other ionomer systems), heterogeneities having a correlation length on the order of 8 nm were found to best reproduce the excess intensity at low q -values. Although this dimension was noted to be surprisingly small for "large-scale" heterogeneities, the excellent agreement with the size of the correlation-hole in the radial distribution function of the local-order model was acknowledged. To extract further information from the scattering at low angles, an ultras-small-angle USAXS camera was used to significantly extend the low q -range.⁶⁴ While this analysis yielded correlation lengths for large-scale density fluctuations in excess of 300 nm, no detailed description of the morphological origin of these heterogeneities was offered, and their existence in contrast to the assumed "gaslike" order of the local-order model was not reconciled.

Gebel and Moore⁶⁸ also applied the local-order model to the SAXS and SANS study of a series of short-side-chain perfluorosulfonate ionomers, ranging in equivalent weights from 635 to 1269 g/equiv. These PFSIs differ from Nafion in the structure of their side chain, which contains only one ether linkage and two CF₂ units separating the sulfonate group from the perfluorinated backbone. Moore and Martin⁵⁵ reported the first SAXS and WAXD characterization of these new PFSIs, showing that these polymers possessed a morphology similar to that of Nafion, having both crystalline and ionic domain structures that varied with equivalent weight and water content. Subsequently, Gebel and Moore quantitatively analyzed this initial SAXS data in combination with new SANS data using the local-order model.⁶⁸ In agreement with the findings for Nafion,^{44,67} the local-order model was found to satisfactorily reproduce the scattering profiles for the short-side-chain ma-

terials, having intermediate equivalent weights. For the short-side-chain PFSIs having high equivalent weights, the model fits were found to deviate significantly from the experimental profiles. This observation was attributed to the relatively high crystallinity of the blocky ionomers;⁵⁵ long runs of PTFE units in the high equivalent weight ionomers yielded an intense crystalline peak at low q -values that influenced the observed position of the ionomer peak. Deviations observed for the low EW ionomer were attributed to the very large water uptake (~80 wt %) as a result of the absence of crystallinity.⁵⁵ For this system (i.e., the 635 EW ionomer), the highly swollen morphology was suggested to be more appropriately described as a polymer-in-water system.⁶⁸ Thus, based on recent studies of PFSI solutions and the reasonable fit of the scattering profile to the form factor of cylinders, the morphology of the swollen 635 EW system was proposed to resemble a connected network of rods,^{51,52} as opposed to a locally ordered distribution of spherical clusters. This new concept for the morphology of PFSIs will be discussed in more detail below.

Through consideration of the morphological and dimensional changes that had been observed in SAXS analyses of Nafion during swelling and deswelling experiments, Litt⁷⁰ proposed a reevaluation of Nafion morphology that could provide a simpler rationalization of the literature than the current interparticle models based on spherical clusters.^{17,37,44} The principal concern addressed by this proposal was that a major reorganization of the ionic domains is required to explain the fact that the observed Bragg dimensions from the ionomer peak varied almost linearly with water content as opposed to the 1/3-power dependence expected for isotropic (affine) swelling of spherical structures. Furthermore, since the swelling/deswelling behavior is observed to be reversible, the extent of morphological reorganization required with the cluster-network model was argued to induce nonrecoverable plastic flow. Using the SAXS data of Gierke et al.¹⁷ over a limited range of water contents, Litt showed that the d spacings are proportional to the volume of absorbed water.⁷⁰ Based on this observation, a lamellar model consistent with the bilayer structure suggested by Starkweather⁴¹ was proposed for the morphology of Nafion. In this model, the ionic domains are defined as hydrophilic "micelle" layers separated by thin, lamellar PTFE-like crystallites. As water absorbs between the lamella and separates them, then the increase in d spacing between ionic domains is expected to be proportional to the volume fraction of water in the polymer and the swelling behavior should be completely reversible, thus eliminating the requirement of morphological reorganization.

While the lamellar model proposed by Litt⁷⁰ provides a convenient and simple explanation for the swelling behavior of Nafion, an important morphological feature observed in the SAXS and SANS profiles of PFSIs, namely the low angle maximum attributed to the crystalline, interlamellar long spacing, is ignored in this analysis. In studies of short-side-chain PFSIs, Gebel and Moore⁶⁸ found that the

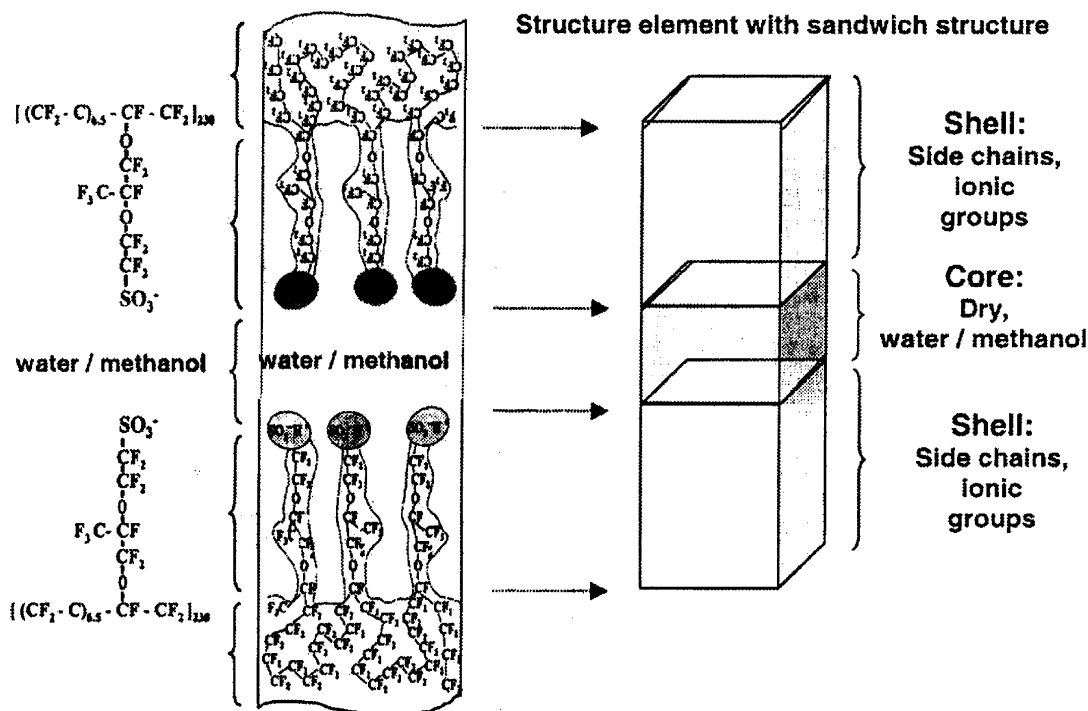


Figure 5. Sandwich-like structural element proposed for the morphological organization of Nafion. (Reprinted with permission from ref 71. Copyright 2001 Elsevier.)

swelling behavior of the ionic domains in these PFSIs is identical to that observed for Nafion; however, the interlamellar spacings shift with water content in a manner significantly different from that of the intercluster spacings. This observation was also confirmed by Young et al. through SANS studies of Nafion swollen with a variety of polar organic solvents.⁷⁵ Since the lamellar model essentially stipulates a parallel shift for the two maxima attributed to a lamellar structure of the ionic domains imposed by the semicrystalline character of the polymer, the observation of dissimilar shifts indicates that the lamellar model is an oversimplification in the global description of the morphology of Nafion. In an attempt to reconcile the dissimilar shifts with the constraints of the lamellar model, Young et al.⁷⁵ have proposed a preferential partitioning of solvents into regions of the structure that do not give rise to the ionic scattering maxima (presumably domains of amorphous fluorocarbon chains between crystallites). Nevertheless, this consideration implies that at least a portion of the crystallites in Nafion are separated by nonionic regions, which is different from the case of the crystallites that impose the lamellar ionic structure as explicitly dictated by the lamellar model. To date, no such morphology has been observed for Nafion.

A variation of the lamellar model was recently proposed by Haubold et al.,⁷¹ in which synchrotron SAXS studies were performed on acid form Nafion 117 samples. The molecular weight of these samples was reported to be $250\,000\text{ g}\cdot\text{mol}^{-1}$, and the experiments were conducted on dry samples in air and samples equilibrated with water, methanol, and a range of water/methanol mixtures using an in situ flow cell. The most fundamental result of this study is that the data show the usual ionomer peak at $q = 1.4\text{ nm}^{-1}$, which gives a Bragg spacing of $d = 2\pi/q \approx$

4.0 nm , in harmony with the results of all other SAXS investigations. The scattering cross section data was fitted to a layered model whose basic structure element (i.e., the scattering particle) is a “sandwich” (Figure 5). The outer portion of this sandwich (the “shell”) consists of the side chains, including the sulfonic acid groups, and the inner liquid portion (the “core”) consists of the water/methanol molecules. To provide channels that serve as conduction pathways for protons through the membrane, these structural elements were proposed to be juxtaposed in a linear fashion so that the liquid core regions are contiguous.

The structure factor chosen for this “sandwich” model is that of a rectangular parallelepiped whose dimensions are those of the monodisperse sandwich particles with an overall random orientation.⁷¹ A least-squares fit of the model scattering cross section to the experimental data yielded the dimensions of the core thickness, c , the combined thickness of the two shells, s , as well as the lateral dimensions a and b . Also issuing from the fit were the electron density contrasts for the core and shell regions. From the model fits, the basic structure element was shown to have lateral dimensions a and b between the values of 1.5 and 4.5 nm, and the total thickness of the sandwich, $c + s$, was about 6.0 nm. Fitted values of s , c , a , and b , were also plotted versus the volume percent of methanol in water, which showed that c decreased while s increased with increasing percent methanol. The molecular interpretation of this observation was that as the methanol composition increased from 0 to 100%, the spacing between $-\text{SO}_3\text{H}$ groups on the two different shells (the region in which the solution is located) decreased from approximately 2.7 to 1.3 nm, while the shells ($s/2$) extended from approximately 1.7 to 2.5 nm. The latter result implies a change in conformation and/or packing of side chains and main chains; however,

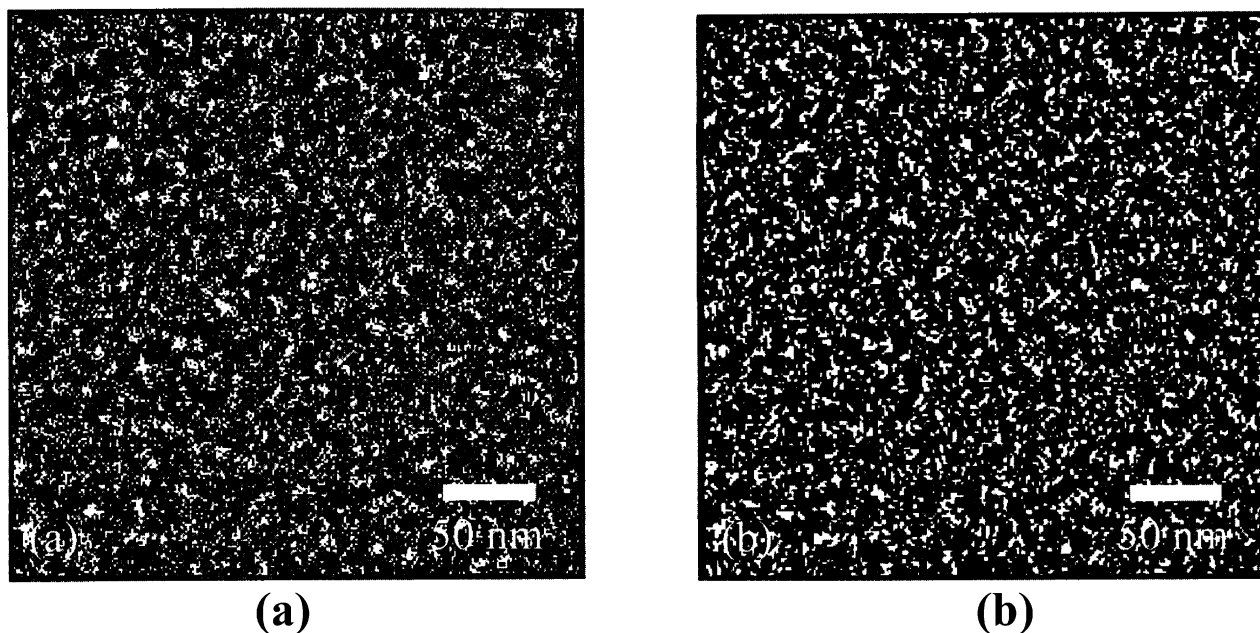


Figure 6. MaxEnt reconstruction of SAXS data from as-received Nafion equilibrated under (a) ambient humidity and (b) 100% RH. (Reprinted with permission from ref 63. Copyright 2000 American Chemical Society.)

the scattering contrast (relative to the average electron density throughout the membrane) for the shell versus percent methanol was found to be relatively constant. Thus, the authors concluded that methanol “leaves the side chains nearly unaffected”, although the meaning of this in consideration of the extension of the side chains is unclear. While this sandwich model was presented within the context of direct methanol fuel cell membranes, it does not offer a complete, unambiguous 3-dimensional pattern of hydrophobic/hydrophilic organization, but rather of local structure. Nor is there any information regarding rearrangement of the main chains, sections of which are known to organize into limited crystalline regions.

A methodological improvement in the analysis of SAXS data of Nafion has recently provided a new perspective on the spatial distribution of clusters in PFSIs. Elliott et al.⁶² have reported SAXS studies of water-swollen Nafion 115 in the acid form and various cation forms in which the membrane water content was quantitatively adjusted using an environmental sample holder with controlled humidity. The radially integrated SAXS profiles show the usual cluster reflection that moves to lower scattering angle with increasing humidity as well as the usual small-angle upturn at low scattering vector magnitudes. From the behavior of the cluster peak position (d -spacing) versus volume fraction of absorbed water, it was concluded that cation exchange does not affect the hydrated morphology. In direct contradiction to both the lamellar morphology, as suggested by Litt,⁷⁰ and other models based on individual three-dimensional clusters (i.e., noninteracting hard spheres),⁴² it was further noted that d was neither directly proportional to the water volume fraction nor proportional to the cube root of this quantity.

Using a novel, model-independent maximum entropy method to interpret the SAXS data, Elliott et al.⁶³ presented a self-consistent morphological para-

digm for PFSIs, which was capable of reconciling the microscopic and macroscopic swelling behavior of these materials. The maximum entropy (MaxEnt) method was used in this analysis to determine the most statistically probable structure for Nafion from the experimental SAXS data. Through this analysis, 2-dimensional SAXS patterns (in reciprocal space) were transformed to generate real space, two-dimensional projections of electron density distributions within a representative volume of the membrane. The technique of spatial filtering was also used to highlight particular features of the electron density maps with respect to different features of the underlying SAXS patterns in discrete scattering vector ranges. Specifically, a low pass filter was applied to mask the cluster reflection, while a high pass filter was used to mask the small-angle upturn prior to applying the maximum entropy data manipulation.

Interpretation of the MaxEnt electron density maps, termed “reconstructions”, led to the conclusion that the most statistically probable scattering model for Nafion is of an ion clustered morphology with a hierarchical scale of structures.⁶³ Figure 6 shows a maximum entropy reconstruction of SAXS data for Nafion H⁺ under ambient humidity and 100% RH. The clusters in these “images” are the white spots and are often seen as agglomerated (clusters of clusters), and more so for the 100% RH case. With an increase in water uptake, the MaxEnt reconstructions showed that the average cluster separation increases with a concurrent decrease in the cluster number density. An important fact is that the “microscopic swelling”, defined in terms of the Bragg spacing for the cluster reflection, does not transform in an affine manner with the macroscopic swelling. Particularly, the relative intercluster expansion is greater than that of the bulk sample dimensions. This behavior was explained as a consequence of the

decrease in the number density of clusters with swelling.

The distribution of clusters observed in the MaxEnt reconstructions was also shown to be nonuniform, suggesting an agglomeration or clustering of clusters.⁶³ By applying a low pass filter (to highlight long-range structure), this agglomeration was linked to the small-angle upturn observed in the SAXS profiles. With confirmation from the MaxEnt analysis of oriented samples (see above), the small-angle upturn was concluded to be produced by the independent scattering from cluster agglomerates yet fundamentally caused by ionic aggregation. Thus, the principal scattering features of Nafion (i.e., the small-angle upturn and the ionomer peak) were noted to be produced by two distinct scattering mechanisms operating on different size scales.

The evolution of PFSI structure from the dry state through the water-swollen state to solution was studied by Gebel using small-angle scattering methods.⁷⁶ With respect to recent studies suggesting that PFSI solutions contain rodlike structures,^{51,52} the aim of this investigation was to gain an understanding of the morphological changes that occur as the ionomer is converted from the highly swollen state to solution during the dissolution process, and *visa versa* during the solution-casting process. Using a high temperature swelling process, water-swollen membranes with water volume fractions ranging from $\phi_w = 0.3$ to 0.93 were obtained. Similarly, homogeneous, aqueous solutions with concentrations up to a polymer volume fraction $\phi_p = 0.12$ were prepared, allowing for an overlap in polymer volume fraction between the solution and swollen membrane states. For the water-swollen membranes, the scattering profiles showed the prominent shift of the ionomer peak to lower q -values with increasing water content, in agreement with previous studies. A plot of the microscopic degree of swelling (defined as the increase in the Bragg distance of the ionomer peak maximum relative to the Bragg distance extrapolated for the dry membrane) versus the macroscopic linear expansion over the large range of water contents revealed a significant change in swelling behavior (i.e., a change in slope) at a linear expansion of 30%. In a double logarithmic plot of the Bragg distance versus the polymer volume fraction, ϕ_p , the change in slope was found to occur at $\phi_p = 0.5$. For low water contents, the slope of this plot was equal to -1.33 , while, at high water contents ($\phi_p < 0.5$), the slope dropped to -0.5 . This behavior was thus attributed to an inversion from a water-in-polymer state at low water contents to a polymer-in-water state at high water contents. The asymptotic behavior of the scattering curves for the water-swollen membranes was also evaluated following the Porod law in order to extract values for the specific surface (i.e., σ , equal to the area of the polymer–water interface per polar headgroup) of the scattering particles. For all samples, the asymptotic behavior was the same, and the average Porod limit yielded a specific surface value of $\sigma = 55 \text{ \AA}^2$. This observation, in agreement with other studies involving a low range of water contents, confirmed the strong significance of this parameter

in defining the structure of swollen membranes and further supports the conclusion that considerable structural reorganization occurs during the swelling process in order to keep constant the specific surface with increasing cluster size.

The slope of -0.5 in the double logarithmic plot of the Bragg distance versus the polymer volume fraction for the highly swollen membranes was noted to be consistent with a dilution of rodlike polymer aggregates.^{51,52} Furthermore, the small-angle scattering profiles of Nafion solutions and the highly swollen membranes were virtually superimposable in the q -range from 0.7 to 2.0 nm^{-1} , suggesting that the local structure on the scale of a few nanometers was identical. Since previous studies of these solutions provided strong evidence for the existence of rodlike aggregates,^{51,52} this observation led to the conclusion that the morphology of highly swollen membranes could be considered as a network of rodlike polymer particles. The deviation of the scattering curves at small angles ($q < 0.7 \text{ nm}^{-1}$) was attributed to the presence of nodes in the network structure and to large scale heterogeneities. It is important to note that this connected network of rodlike structures connected by nodes was proposed earlier by Lee et al.⁴⁵ to explain their SANS data probing the local water structure in Nafion.

Based on the results of this scattering analysis of Nafion over a wide range of water contents, combined with energetic considerations, Gebel proposed a conceptual description for the swelling and dissolution process shown schematically in Figure 7.⁷⁶ In this qualitative model, the dry membrane is considered to contain isolated, spherical ionic clusters with diameters of $\sim 1.5 \text{ nm}$ and a center-to-center separation distance of $\sim 2.7 \text{ nm}$. With the absorption of water, the clusters swell to hold pools of water surrounded by ionic groups at the polymer–water interface in order to minimize the interfacial energy. As the water content increases to between $\phi_w = 0.3$ and 0.5, structural reorganization occurs to keep constant the specific surface area, and the onset of percolation is achieved by the formation of connecting cylinders of water between the swollen, spherical clusters. At ϕ_w values greater than 0.5, an inversion of the structure occurs such that the structure resembles a connected network of rods. Finally, as the membrane “dissolves” into solution, the rodlike structures separate to yield a colloidal dispersion of isolated rods. While this model offered a plausible mechanism for the evolution in structure from the widely accepted concept of isolated clusters for membranes containing relatively low water contents to rodlike structures in solution, no thermodynamic justification for the phase inversion process at $\phi_w = 0.5$ was offered. Moreover, the fact that the scattering profiles near this phase inversion point did not show a significant change in contour is difficult to rationalize.

To further probe the phase behavior of hydrated Nafion, Rollet et al.⁷⁷ used a contrast matching method in the SANS analysis of Nafion membranes neutralized with tetramethylammonium ions. With 12 hydrogen atoms per counterion, the $\text{N}(\text{CH}_3)_4^+$ ions

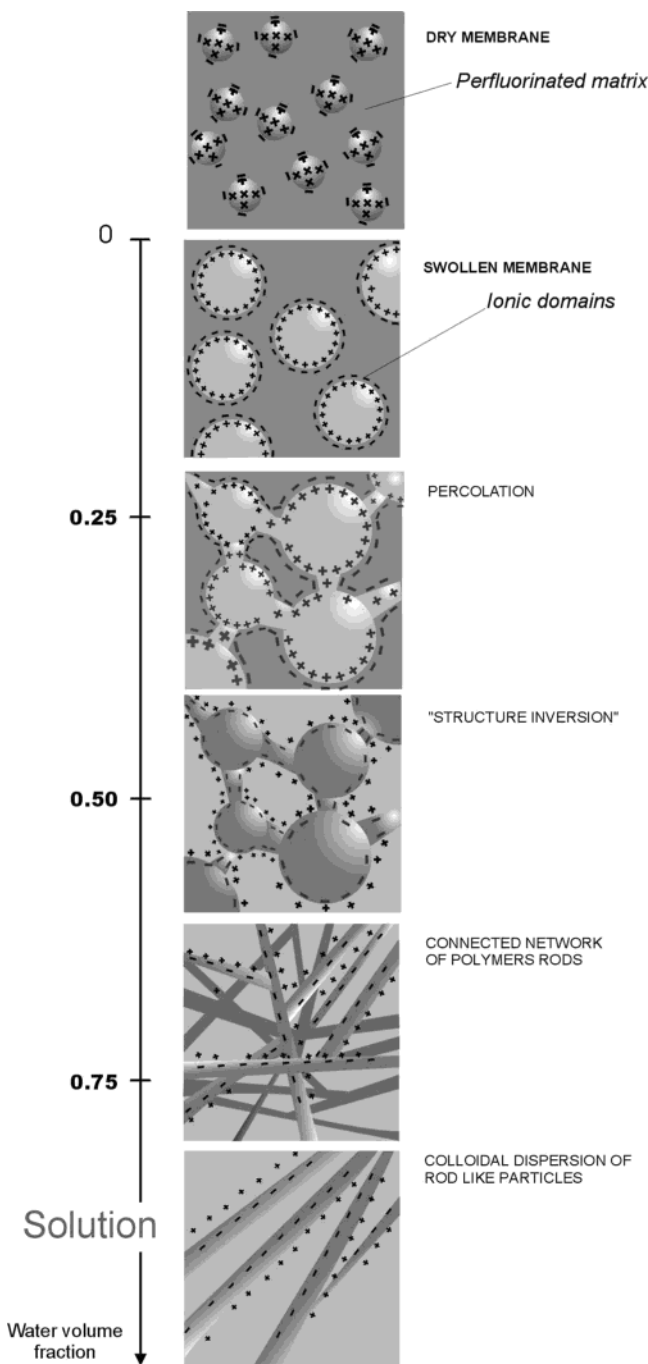


Figure 7. Conceptual model for the morphological reorganization and continuity of the ionic domains in Nafion as the dry membrane is swollen with water to the state of complete dissolution. (Reprinted with permission from ref 76. Copyright 2000 Elsevier.)

were found to be excellent neutron scatterers that provided a third source of scattering contrast, thereby acting as a useful morphological probe at the interface between the water and polymer domains. By varying the water composition with a range of $\text{H}_2\text{O}/\text{D}_2\text{O}$ mixtures, the contrast profile of the scattering domains was evaluated to gain a new insight into the structure of Nafion. The relative magnitudes of scattering features in the SANS profiles were shown to vary systematically with the $\text{H}_2\text{O}/\text{D}_2\text{O}$ composition, indicating that the $\text{N}(\text{CH}_3)_4^+$ ions were condensed in a thin layer with the sulfonate groups at the interface between the hydrophobic polymer parts and the

water domains. Through the assumption of spherical aggregates and the recognition that no structural change occurs when H_2O is replaced by D_2O , the structure factor contribution to the scattered intensity was eliminated by dividing the SANS profiles obtained with various $\text{H}_2\text{O}/\text{D}_2\text{O}$ mixtures by the intensity profile for Nafion in pure water.⁷⁷ The resulting normalized profiles were shown to present a clear minimum near $q = 1.5 \text{ nm}^{-1}$ that shifted toward smaller q -values as the composition of D_2O decreased. In considering the form factor for spherical core-shell particles, the two opposing geometries (i.e., a water core surrounded by a counterion shell or a polymer core surrounded by a counterion shell) were used to simulate SANS curves comparable to the experimental data. While the general shape of the curves for both simulations resembled the experimental data and showed a clear minimum near $q = 1.5 \text{ nm}^{-1}$, only the “polymer core surrounded by a counterion shell” geometry matched the shift of this minimum toward smaller q -values. Thus, based on this analysis, the authors concluded that the morphology of hydrated Nafion is best described as polymer aggregates surrounded by water.⁷⁷ Although an attempt was made to model both spherical and elongated particles using a similar approach, the authors acknowledged that a conclusive distinction between these shapes was not possible given the limited q -range of the experimental data.

In a second paper, Rubatat and co-workers⁷² used a combination of small-angle X-ray and neutron scattering techniques, including USAXS, to probe characteristic dimensions in hydrated Nafion over the range from 1 to 1000 nm. Through a combination of the USAXS and SAXS data, the entire scattering curve of Nafion was presented to show the extended small-angle upturn attributed to long-range heterogeneities in electron density, the low angle maximum attributed to supralamellar dimensions of the crystalline domains, and the ionomer peak attributed to intercluster interferences. In addition, double logarithmic plots of the scattering data $I(q)$ versus q showed two regimes of linear intensity decay; at low angles, the data followed a q^{-1} power law, while, at high angles, the intensity decay followed the expected q^{-4} power law indicative of a sharp interface for the scattering particles. The q^{-1} regime was noted to fit the behavior expected for scattering from rodlike particles over the range of wave vectors from $2\pi/L$ to $2\pi/D$, where L and D are the rod length and diameter, respectively. Based on the observed span of scattering vector in this regime, the rodlike particles were estimated to have dimensions of $D \approx 6 \text{ nm}$ and $L \geq 100 \text{ nm}$.

Scattering data over the extended range of q -space were also collected from Nafion samples containing a wide range of water contents ($\phi_w = 0.05\text{--}0.84$).⁶⁹ While systematic shifts in the intensities and positions of the structure maxima (i.e., the crystalline and ionomer peaks) were observed and consistent with those found by others, the general shapes of the scattering profiles for all samples were quite similar. This observation supported the assumption that the swelling process simply involves a dilution of the



Figure 8. Schematic representation of an entangled network of elongated rodlike aggregates in Nafion. Long-range heterogeneities arising from bundles of locally ordered aggregates are proposed to give rise to the low angle increase in scattered intensity. (Reprinted with permission from the original author.)

scattering entities rather than inducing a strong structural reorganization of the cluster morphology, as suggested earlier by Gebel.⁷⁶ In plotting the characteristic (Bragg) distances, $2\pi/q^*$, corresponding to the two structure maxima, versus the polymer volume fraction, two microscopic swelling regimes were observed, in agreement with that found by Gebel.⁷⁶ For high ϕ_p , the swelling process was observed to follow a power law close to ϕ^{-1} , in agreement with the results of Fujimura^{36,37} and Litt.⁷⁰ For low ϕ_p (below $\phi_p = 0.6$), the swelling process was observed to change to a power law close to $\phi^{-0.5}$, suggesting a dilution of cylindrical shaped particles. To reconcile the shift in swelling behavior observed at $\phi_p \approx 0.6$ with the suggested rodlike morphology of the scattering particles, the authors proposed that the aggregates are more ribbonlike than rodlike, with a cross-sectional thickness and width close to 2 and 8 nm, respectively.⁷² At low water contents, the ribbons are considered to pack face-to-face in a manner that allows for an initial dilution law with an exponent of -1 . However, at high water contents (low ϕ_p), where the distance between aggregates is greater than 8 nm, the orientation distribution around the long axis becomes isotropic in a manner that allows the aggregates to be considered as cylinders with a dilution law following an exponent of -0.5 .

Therefore, in the context of a morphology considered to be fundamentally characterized by the presence of elongated aggregates, the authors propose that the intermediate q -range provides information related to the size, shape, and spatial distribution of the aggregates, while the very small q -range (i.e., the small-angle upturn) may be attributed to larger bundles of aggregates (see Figure 8) with a long-range heterogeneous distribution.⁷² Between these regions in q -space lies information related to the distribution of crystallites in Nafion. Unfortunately, the degree of crystallinity in Nafion is low (e.g., 8–12 wt %³⁶), and thus, little conclusive information about

this morphological feature has been extracted from these scattering studies. As noted in this study, the swelling behavior observed for this scattering feature is surprisingly large (i.e., increases in interdomain distances from 10 to 100 nm with increasing water content) relative to that expected for expansion of interlamellar dimensions. Clearly, additional investigations of this morphological feature are warranted in order to more fully understand the origin of this scattering maximum. If the crystalline domains are contained within the rodlike aggregates, as previously proposed,⁴⁹ then the interlamellar dimensions should track with a corresponding increase in the rod length. On the other hand, the interlamellar correlations may be of an interaggregate origin, and the dimensions should thus track with some function of the interaggregate spacing. To date, this question remains to be answered.

2.5. The State of Understanding from X-ray and Neutron Investigations

Over the period of about two decades, numerous models have been proposed for the morphology of Nafion based on information gathered from small-angle scattering and wide-angle diffraction studies. While these distinctly different models have varied significantly in quantitative and qualitative detail, many have weathered the test of time and remain the focus of debate in the current literature. In all these studies, one fact remains constant; the morphology of Nafion is complex. Fortunately, state-of-the-art scattering methods and data analysis techniques are providing a wealth of new morphological information that may be correlated with other morphological and physical property studies to bring forward a deeper understanding of the complex nature of Nafion.

In reviewing the evolution of information that has been reported from these morphological studies, it should be recognized that each of the principal models for the morphology of Nafion, while distinct in their conceptual design, contains relevant aspects of structure that collectively facilitate a more global understanding of the molecular organization of perfluorosulfonate ionomers. By recognizing the specific perspective by which a particular model was developed, a number of interesting disparities between the different models may be reconciled. For example, a relatively new rodlike model has been recently modified to include the possibility of ribbonlike aggregates that may assemble locally,⁷² at low water contents, in a lamellar fashion. By narrowing the perspective to a limited range of water contents, suddenly the rodlike and lamellar models are in agreement. In a similar fashion, the excellent mechanical integrity of swollen Nafion membranes may be attributed to entanglements of the proposed elongated polymeric aggregates in the solid state. At these entanglement or crossover points, local nodes may exist⁷⁶ such that, at moderate water contents, the swollen nodes may appear as isolated clusters. This perspective reconciles the rodlike and cluster-network models.

The morphological information and interpretations currently reported for Nafion still support the concept

of a connected network of ionic domains through which polar solvents and ionic species permeate. The principal focus of these important investigations continues to be aimed at understanding the structural nature of the ionic domains, such as the size, shape, and spatial distributions of the clusters. One consensus that appears to be developing in the current literature is that the ionic domains in hydrated Nafion possess some degree of anisotropy in shape and heterogeneity in their spatial distribution. In contrast to a regularly ordered morphology, this general conception of a more irregular, heterogeneous structure is consistent with the random chemical structure of PFSIs. As we learn more about the organization of these ionic domains, however, the simple concept of "ionic clusters" in these materials becomes more convoluted. Although the ions clearly cluster as a result of the nanoscale phase separation between polar and nonpolar constituents of the copolymer, the notion of discrete ionic clusters or contiguous ionic domains depends on the perspective of the method used to probe the morphology and the chemical composition of the membrane (e.g., the state of hydration). Nevertheless, the current models and their detailed methods of structural analysis now constitute useful tools that may be applied to precise evaluations of morphology–property relationships in these benchmark materials. Moreover, these tools may be used to characterize trends in controlled morphological manipulations of PFSIs through various processing procedures (e.g., solution-casting, thermal treatments, mechanical deformation, etc.) that may prove to enhance the membrane properties over those of as-received Nafion.

The nature of the crystalline component in Nafion has received much less attention than that of the ionic domains, and thus, the relevance of this morphological feature to the technologically important properties of the membranes is still unclear. Since the initial studies of Nafion morphology, the crystalline component has been recognized as an important structural feature and often considered as a necessary component that provides mechanical integrity and a barrier to solvent swelling. With respect to current models, however, the crystallites may be considered to exist within elongated polymeric aggregates or as critical structures that impose the organization of the ionic domains. In the rodlike models, the crystallites may play a minor role to that of entanglements in affecting the mechanical behavior of the swollen membranes. On the other hand, the lamellar model suggests that the crystallites are the principal factor in limiting ionic domain swelling. Clearly, further work is required to resolve this important issue. In addition, as Nafion is the benchmark in studies of many new membrane materials for fuel cell applications, the role of crystallinity (if needed at all) in affecting desirable membrane properties must be addressed.

3. Microscopy Studies

Microscopic studies, regardless of the method of producing images, have an advantage in being able to provide a direct visualization of the sizes, shapes,

and geometrical distribution of ionic clusters, crystallites, and the continuous perfluorinated matrix. The usual problems regarding sample thickness and provision of sufficient electron density contrast, as well as possible artifacts, are present. The SAXS and SANS methods of structural inquiry have advantages that are specific to the nature of the underlying wave–particle interactions. On the other hand, the results are usually prejudiced by the need to assume a particular model, which must necessarily be simple so that the most basic geometrical parameters can be extracted.

Ceynowa performed electron microscopic studies of 60–80 nm thick microtomed Nafion 125 membranes that were converted, for the purpose of affecting electron density contrast, to the Pb^{2+} form, and all of the excess cations and co-ions were removed.⁷⁸ It is the heavy metal that provides electron density contrast between the phase in which it resides and the surrounding phase. These membranes were then exposed to ethanol and 1,2-epoxypropane, although these solvents would not have remained in the samples under the vacuum in the microscope column. The micrographs consisted of uniformly distributed "points" that were presumed to be ion clusters that were 3–6 nm in diameter.

Fujimura et al., in addition to their SAXS studies, performed TEM investigations of thin sections of 100 EW Nafion in the cesium ion form.³⁷ The important details of sample preparation were not provided in this paper, although it is likely that the samples were sectioned from membranes rather than being films cast from solution. The heavy Cs^+ counterion associated with the sulfonate groups provides electron density contrast so as to highlight the cluster regions. It should be appreciated that these samples were only ~60 nm thin, so that, in principle, if the characteristic intercluster spacing is ~4 nm, there will be only ~15 clusters to span the thickness of this sample. A micrograph of this sample shows isolated particles that are, on average, a few nanometers in diameter.

Xue et al. also performed TEM investigations of Nafion 117 morphology.⁷⁹ Solution-cast films, of thicknesses in the range 50–100 nm and stained by RuO_4 , showed good contrast. It was explained how this staining agent would be selectively incorporated in the side chain domains, notwithstanding the fact that none of the usual unsaturated $\text{C}=\text{C}$ bonds for staining reactions exist in these regions. FTIR and X-ray fluorescence analyses showed that this was the case based on the fact that residual water, which would be found in the most hydrophilic regions, was oxidized to give RuO_2 . Therefore, the observed features would likely be clusters. Three phases were observed on the basis of white, gray, and dark regions in micrographs: Spherical clusters, in the diameter range 25–50 Å, were surrounded by interfaces and were uniformly dispersed throughout an organic matrix across the field of view. While the concept was earlier advanced by Yeager et al.,¹⁸ Xue et al. claimed to be the first to view three phases in Nafion using the TEM technique.

Rieberer and Norian investigated unstained microtomed Nafion 117 samples using TEM.⁸⁰ The thinner edges of the 50 nm thick sections of the K⁺ form were used so as to probe regions having thickness on the order of 10 nm. Other samples consisted of films cast from ethanol solutions. The solution-cast samples were exchanged to the Cs⁺ form to affect good electron density contrast. In both cases, steps were taken to minimize beam damage to these thin sections, as explained in the paper. TEM images of the Cs⁺ form samples showed clusters having sizes in the range 1–5 nm, the average of which is around the value of intercluster Bragg spacings that was derived from SAXS studies. Bright regions, due to phase contrast fringes, were said to be nonionic channel areas representing a third phase of the system. The microtomed samples showed the same features as those that were solution-cast. These studies included X-ray energy dispersive spectroscopy (EDS) and energy loss spectrometry (EELS) microanalyses of elemental composition. In particular, the Cs-to-S mole ratio was found to be close to unity, showing essentially complete ion exchange so that all of the sulfonate groups are accounted for in the clusters seen on the micrographs.

Porat et al. performed TEM (zero-loss bright field) studies of very thin Nafion films that were cast from ethanol/water solutions, and some of the conclusions are as follows.⁸¹ It was suggested that the backbone had a planar zigzag conformation in large orthorhombic crystallites as in polyethylene, in contrast with the helical conformation found in poly(tetrafluoroethylene). This is an interesting result, although there are no other studies that support this view. Sulfur imaging indicated the presence of sulfonate clusters that are 5 nm in size.

Lehmani et al. studied the surface morphology of dry and hydrated acid form Nafion membranes using atomic force microscopy (AFM) in tapping mode.⁸² The digital images were also analyzed for surface roughness. The results for “cleaned” samples that were dried under vacuum at 80 °C show “supernodular aggregates” of spherical domains having diameters of ~45 nm. These domains, that appear rather distinct on the images, are of a size scale that is greater than the Bragg spacings derived from the SAXS profiles of these materials. It is unclear as to whether these features are strictly a surface phenomenon and/or the result of sample preparation. The surfaces probed were the actual membrane surfaces rather than those of a fresh surface of a film cross-section that was produced by cutting or freeze fracture. Thus, the observed structures may not be representative of the membrane interior.

On a finer level, spherical grains that have an average diameter of 11 Å are seen. A section analysis, which consisted of a plot of image contrast intensity versus distance, indicated that there is a mean periodicity of around 49 Å, which is close to the values of the SAXS Bragg spacing usually associated with intercluster distances. This, as well as other microscopic studies, favors the model of phase separation as opposed to the core–shell model as applied to the interpretation of scattering data. The hydrated

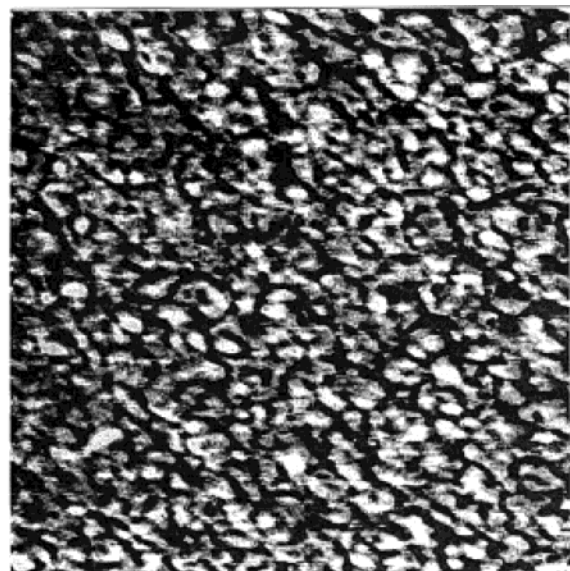
sample was prepared by placing a drop of water on it, and the AFM apparatus was kept in a constant humidity chamber. The supernodular structure was preserved, and the surface was less rough than that of the dry sample.

McLean et al. used AFM to elucidate the surface and near-surface ionic domain and semicrystalline morphologies of Nafion 117 in the K⁺ form, as well as Surlyn and sulfonated poly(styrene-*co*-ethylene/butylene-*co*-styrene) (Kraton) ionomers to which comparisons were made.⁸³ In AFM, the tapping mode phase generates image contrast on the basis of small regions being hard versus soft or, in a general sense, sharp viscoelastic gradients. Similar to the method of dynamic mechanical analysis, but on a smaller scale of interrogation, the phase angle that is plotted in two dimensions across the surface refers to the lag between the oscillatory motion of the cantilever to which a probe tip is attached and the oscillating input signal to the piezoelectric drive for the cantilever.

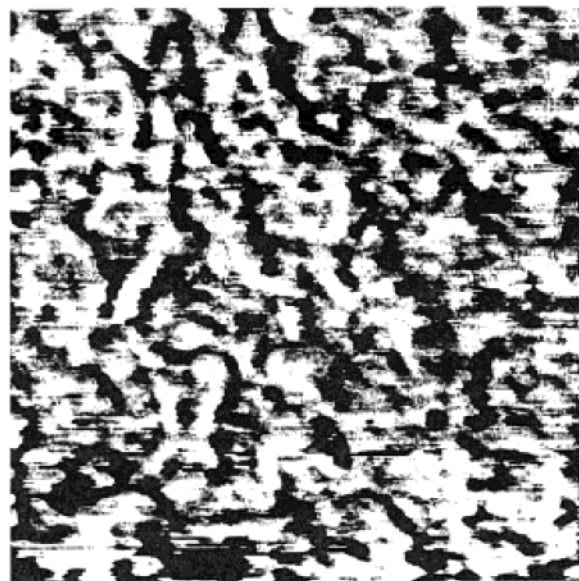
The stiff regions observed in the studies of McLean et al. were assigned to fluorocarbon crystalline domains, the size of which was around 10 nm. The crystalline packing was referred to as lamellae which are not organized into stacks, as is the case for the Surlyn ionomers that were studied. An interesting outcome of the “normal” tapping studies was the discovery of a very thin (~5 Å) fluorine-rich layer over the surface in which the contrasted soft regions are amorphous.

Other experiments involved lower oscillation amplitude tapping on the same sample after a normal tapping experiment was conducted over the surface. The authors suggested that attractive tip interactions with ionic domains dominate the phase signal under these conditions so as to produce greater contrast in the sense of phase difference. In this way, the ionic domains are seen more clearly. The low amplitude experiments revealed ionic domains of size 4–5 nm, which is in agreement with the results of earlier TEM experiments.^{37,81} The ionic domains, appearing as irregularly shaped, were not resolved to a degree to which distinct boundaries and interphase as well as amorphous regions could be seen because these features overlapped and artifacts of the AFM method relating to feature edges must be considered. No long-ranged patterned organization of the clusters was seen, which is in agreement with the observation of a well-studied broad, single SAXS peak attributed to polar–nonpolar phase separation in these materials.

Images were also obtained for Nafion K⁺ samples that were soaked in deionized water using low oscillation energy so as to sense hydrated ionic clusters. An ambient humidity conditioned (control) sample exhibited 4–10 nm in diameter clumps of multiple (unresolvable) ionic domains. Upon exposure to water, the ionic features became enlarged in a way that they were elongated and appear somewhat as channels having a width of 7–15 nm, as seen in Figure 9. While Figure 9 might offer a view of contiguous hydration pathways, the morphology particularly is that of the K⁺ ionic form so that caution must be exercised in applying this information in rationalizing the proton conductance and other prop-



A



B

Figure 9. Low oscillation energy tapping mode phase images of a K^+ form Nafion 117 membrane. In part A, sample was exposed to ambient, room temperature humidity (ionic species are in the light regions). In part B, sample was exposed to deionized water. The images are $300\text{ nm} \times 300\text{ nm}$, and the phase range is $0\text{--}80^\circ$. (Reprinted with permission from ref 83. Copyright 2000 American Chemical Society.)

erties of sulfonic acid form Nafion within the context of PEM fuel cells.

In addition to providing a “direct” visualization of ionic clusters, the discovery of the thin fluorine-rich layer may have important implications with regard to the liquid/vapor sorption of these materials. To be sure, the nature of this layer would depend on the specific liquid or vapor environment contacting the membrane surface. In particular, the molecular polarity of the environment and its influence on surface tension would be involved. The difference between the liquid water versus saturated water vapor sorption was mentioned in this report. Also, the contact angle experiments of Zawodzinski et al.

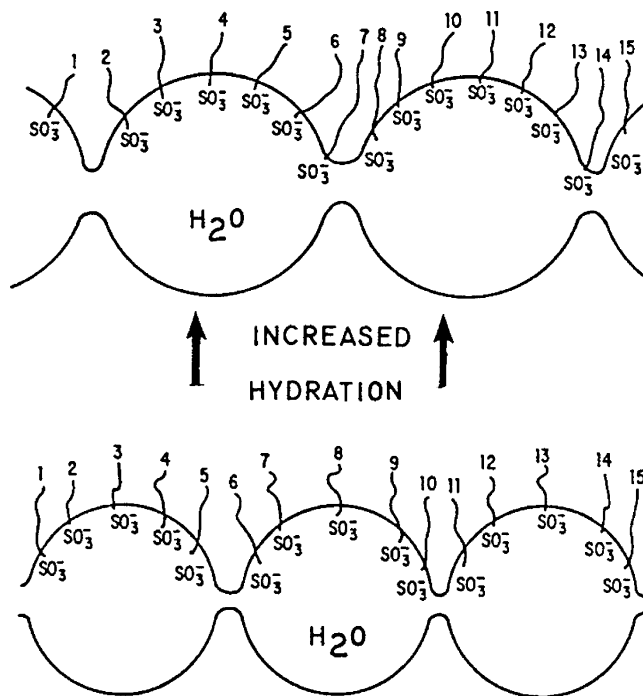


Figure 10. Evolution of a smaller number of larger clusters with increased hydration of Nafion ionomers, according to Gierke, Munn, and Wilson. (Reprinted with permission ref 17. Copyright 1981 Wiley.)

suggest that the surface of Nafion is of very high fluorocarbon composition.⁸⁴ This phenomenon, which has been known for some time, is referred to as “Schroeder’s Paradox”.^{85,86}

McLean et al. offer interesting comments that have implications regarding molecular transport. It was mentioned that polar–nonpolar interfacial tension would restrict the formation of high surface/volume narrow channels and drive the system to larger ionic domain dimensions. In fact, a simple model calculation by Gierke et al. implied that increasing hydration would cause a smaller number of larger clusters, that is, cluster coalescence,¹⁷ and the morphology of the water soaked K^+ form sample seen in Figure 10 supports this idea. Presumably this occurs by individual ion-hopping events or cluster coalescence, or a combination of both. From a thermodynamic perspective, this process might be viewed as a continuous and spontaneous minimization of the overall hydrophilic–hydrophobic interfacial free energy by decreasing the cluster surface/volume ratio. To be sure, the concept of “interface”, in the usual continuum sense, becomes blurred at this fine ultrastructural level and the “roughness” of the hydrated phase has been discussed by a number of authors.

It was also mentioned by McLean et al. that ions and polar solvent molecules must necessarily diffuse across thin amorphous fluorocarbon or interfacial regions between swollen polar domains. However, all of this does not require the need for channels with diameters of 10 \AA that are coated with SO_3^- groups for long-range transport. In any case, a simple consideration of the steric volume of SO_3^- groups in relation to the size of these channels leads to the conclusion that more than one group would have difficulty fitting into this very small volume. Related

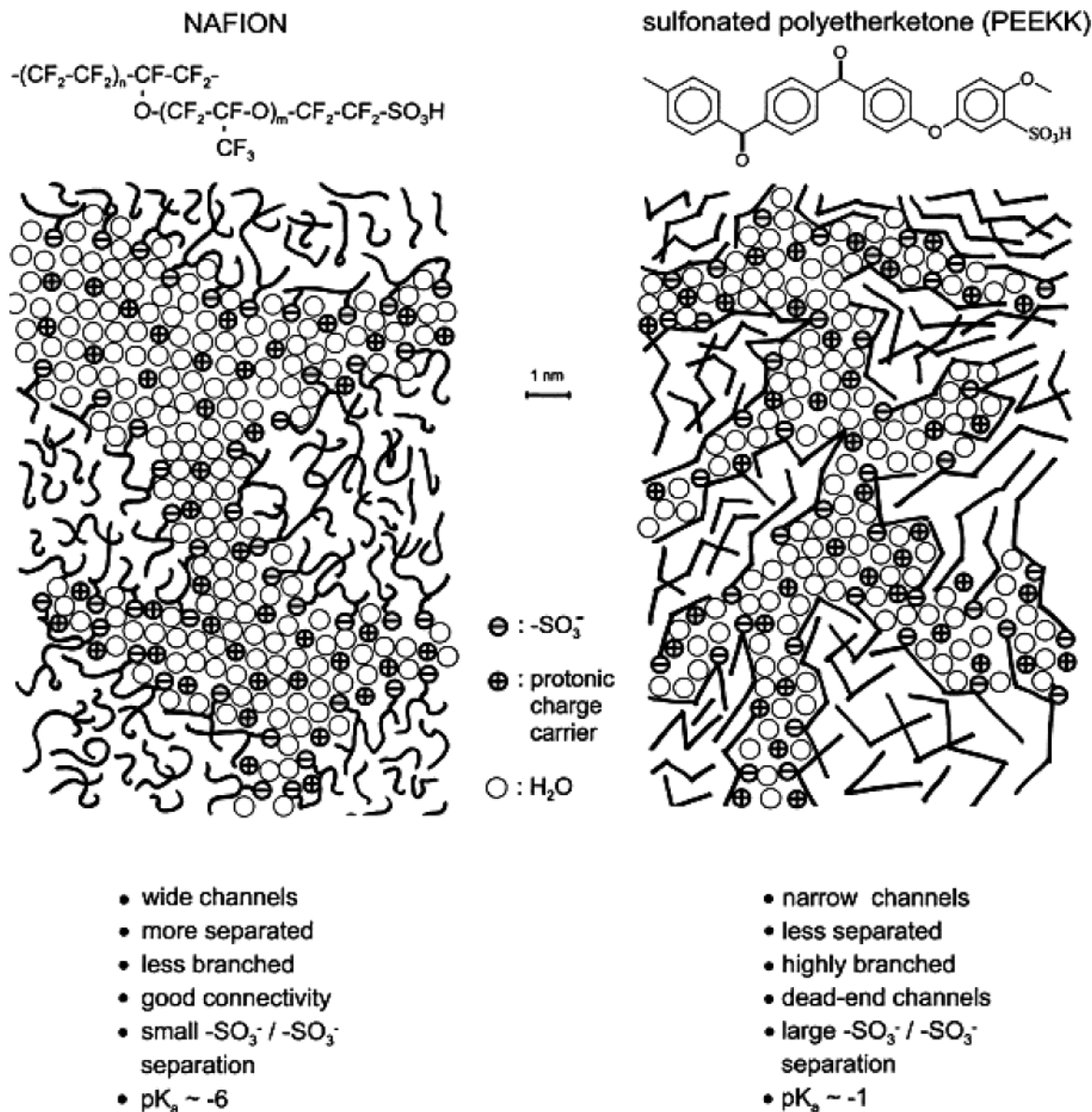


Figure 11. Stylized view of Kreuer of the nanoscopic hydrated structures of Nafion and sulfonated polyetherketone. (Reprinted with permission from ref 91. Copyright 2003 Elsevier.)

to this discussion is the conclusion of Tovbin,⁸⁷ which was based on the X-ray scattering results of Ozerin et al.,⁸⁸ that the channels through the perfluorocarbon regions are around 50% wider than those proposed by Gierke et al.

As mentioned earlier, Orfino and Holdcroft performed SAXS studies of acid form Nafion 117 samples that were in the dry and wet (19% of total swollen weight) states.⁷⁴ One of the conclusions was that, upon hydration, the number of ionic clusters decreases while their size increased, which also supports the concept of the evolution of a smaller number of larger clusters, as advanced by Gierke et al. and later factored into the equilibrium swelling model of Mauritz and Rogers that will be described later.⁸⁹ An important goal of this study was to determine the nature of the ubiquitous "ionic channels". In a wet membrane, 89% of the ionic sites were calculated as residing in the cores whose average diameter was 4.10 nm. There are 74 SO_3H groups per cluster, and the average length of channels between adjacent

clusters was found to be between 0.30 and 0.88 nm. Owing to these very small channel lengths, it was concluded that the cores can be connected by only a single ionic site so that the concept of a pore has no meaning on this scale.

James et al. also performed AFM tapping mode phase investigations of Nafion 115 membranes while the samples were in an environmental chamber of controlled humidity.⁹⁰ The data from their experiments were presented in a somewhat different fashion from that usually seen in the literature. Rather than mapping the phase angle ψ , $\sin \psi$, which is directly proportional to the energy loss, was mapped. This energy loss is due to either viscoelastic or tip adhesion effects. An increased viscoelastic energy change would involve local material softening due to water incorporation. An adhesion energy change would involve enhanced attraction between the tip probe and inserted water structures. The authors argued that, at the frequency of the cantilever, the viscoelastic effect would be negligible and the adhe-

sive mechanism predominates. Their studies indicated that while the number of clusters decreased, the size of the average cluster increased with increasing humidity, which, again, is reinforced by the conclusions of others as discussed throughout this section. The images showed clusters with sizes in the range 5–30 nm. The sizes at the upper end of this range are considerably greater than those proposed on the basis of SAXS studies, and these large features were attributed to aggregates of clusters of size 3–5 nm. The larger structures were rationalized as cluster agglomerates, as also proposed by Elliott et al. as a result of their SAXS studies.⁶³ These AFM studies also detected features that are the consequence of extrusion of the precursor form.

Kreuer discusses the structure of Nafion as compared to the structure of lower cost, thermally stable, oxidation resistant, sulfonated poly(ether ketone) membranes within the context of fuel cells.⁹¹ While it is not intended to discuss the latter nonperfluorinated materials here, Kreuer's review contains a good summary of the state of knowledge of Nafion up to the time of his writing. The nanoscopic view, depicted in Figure 11, is described as an arrangement of low dimensional polymeric objects (which might be called clusters), the spaces between which are filled with water (channels). This picture is based on the SAXS studies of Gebel.⁷⁶

However, Kreuer states that SAXS information, by itself, cannot resolve the question of whether this model is more appropriate than the inverse micelle model of Gierke et al., that, in a general sense, would possess more morphological order than that reflected in the SAXS scattering profiles.¹⁷ Regardless of issues regarding the interpretation of SAXS data, it is worth noting that the nanoscale morphology seen in Figure 11 is rather similar to that seen in the AFM images of McLean et al.⁸³ The concept of water as being an extended second phase is reasonable considering the low degree of morphological order. In summary, compared with poly(ether ketone), Nafion has wide versus narrow water channels, the hydration pockets are more separated, the percolated hydration structure is less branched with good connectivity, and there are no dead end channels; there is less hydrophobic–hydrophilic interface, and the inter-sulfonate group separation is less. These differences in morphology between the two membranes were explained as being the consequence of having a less hydrophobic backbone, sulfonic acid groups that are less acidic than those attached to a perfluorocarbon structure, and a reduced flexibility of the backbone for the case of sulfonated poly(ether ketone).

4. The Nature of Water, Other Solvents, and Ions in Nafion

In 1972, when the main thrust for these then-new materials was the development of efficient polymer membranes for chlor-alkali cells, the E. I. du Pont Co. reported much information, mostly in the form of product literature, in the form of empirical equations regarding the water mass and volume uptake of sulfonate form Nafion as a function of EW (in the range 1000–1400), some alkali metal counterion

forms, and the molarity (0–14 M) of aqueous electrolyte solutions in which the films were equilibrated.⁹² At that time, it was already understood that the properties of these materials were very sensitive to swelling history so that these equations applied for the “standard pretreatment” of boiling in pure water for 30 min. Information was also presented on water absorption at room temperature versus the temperature of initial equilibration (uptake decreases with increasing initialization temperature), as well as percent swelling in organic solvents, as well as mixed solvents, at room temperature. Compared with the conventional sulfonated cross-linked polystyrene ion exchange membranes, Nafion swells to a greater extent in a number of organic solvents than it does in water. This information was useful in estimating dimensional changes which were reduced by fabric reinforcement in chlor-alkali electrochemical cells. While the general trends described by these equations will hold for current grades of extruded Nafion films, their use in an absolute sense might be questioned and should especially be avoided for solution-cast membranes, especially those of low EW.

Yeo investigated the swelling of Nafion sulfonate membranes in the acid as well as alkali counterion forms, in a number of hydrogen bonding solvents.^{93,94} Percent mass uptake versus solvent solubility parameter (δ) curves appeared to have two maxima and therefore dual cohesive energy densities, each of which was said to correspond to a distinct morphological feature. It was suggested that the peak at low δ corresponds to interactions with the tetrafluoroethylene regions, while the peak at high δ reflects more polar solvent molecules that would prefer to interact with the ionic regions.

Gebel et al. also performed swelling studies of Nafion 117 membranes.⁹⁵ They measured sample expansion along three directions—along and perpendicular to the machine direction, as well as along the thickness direction—after equilibration in the given solvent and also calculated the actual number of solvent molecules per SO_3^- group at swelling equilibrium. It was concluded that the Gutmann donor number of the solvent, which is related to cation solvation energy and has units of $\text{kcal}\cdot\text{mol}^{-1}$, is a parameter that is more important than the solvent solubility parameter. Nor did the data correlate well with solvent dielectric constant or interfacial surface tension. Moreover, a plot of expansion versus solubility parameter was seen to not be in harmony with the dual cohesive energy density concept of Yeo, as the data of Gebel et al. appeared rather scattered. In the view of Gebel et al., at the time of their writing, the solvent was considered to be exclusively contained in the clusters.

Duplessix et al. used water vapor pressure isotherm (i.e., water uptake vs external relative humidity) data combined with simultaneous isotherm differential microcalorimeter analysis to determine the average heat of absorption per water molecule for 1200 EW acid form samples.²⁹ Hysteresis was seen between sorption and subsequent desorption curves at 25 °C, and nonzero water content remained at zero relative humidity, indicating the presence of tightly

bound water. Average heat of water absorption versus water content curves showed that the former remains at a constant value of around $-12 \text{ kcal}\cdot\text{mol}^{-1}$ up to an uptake that corresponds to about 5 H_2O molecules per SO_3H group, where the negative sign of this energy indicates exothermicity. It was a significant fact that this binding energy, which must be associated with water of hydration, is the same for samples dried at room temperature as it is for samples dried at 220°C . At higher water uptakes that cause polymer swelling, this energy continuously decreases to a value that is around $4 \text{ kcal}\cdot\text{mol}^{-1}$, which is approximately the strength of a hydrogen bond in liquid water. The decrease in energy occurs at a lower content for the sample dried at 220°C , which implies a polymer structural rearrangement with change in pretreatment.

Rodmacq et al. (same CENG group) applied the same analyses to the Na^+ - and Fe^{2+} -neutralized forms, the latter of which permits the use of Mossbauer spectroscopy.³⁰ The vapor pressure isotherms at room temperature for both ion forms were seen to be similar. Heat of absorption versus water content plots for the Fe^{2+} salts dried at room temperature indicate that the energy of absorption of the first few water molecules is $13 \text{ kcal}\cdot\text{mol}^{-1}$ (essentially the same as that for the acid form), and this somewhat constant energy then drops at higher water contents. The low water content value is lower at $10 \text{ kcal}\cdot\text{mol}^{-1}$ for the Na^+ form although no reason was offered to account for this difference. It must be said that the results of these Mossbauer studies, as well as the results of other similar studies of Nafion, have more to say about the state of Fe in this environment than about the morphology of the host polymer.

Zawodzinski et al. determined the water uptake of acid form Nafion 117 at 30°C in experiments that equilibrated membrane samples in a sealed relative humidity environment that was controlled by LiCl solutions of known tabulated water activity or equilibrium partial pressure p/p_0 .⁹⁶ Vapor pressure isotherm curves were determined by measuring mass uptake, expressed in terms of number of moles of H_2O per mole of SO_3H groups = λ versus p/p_0 . The plot showed a somewhat small increase in λ with increasing p/p_0 until an uptake of around 6 $\text{H}_2\text{O}/\text{SO}_3\text{H}$ was reached, after which the increase was considerably greater. The results can be interpreted in terms of a condition of tightly bound, SO_3H -associated water in the initial stage and the evolution of more loosely bound water in the latter stage. These results are in essential harmony with those of the similar studies of Duplessix et al. for the acid form.²⁹ Zawodzinski et al. also compared the water uptake of membranes exposed to saturated water vapor with the uptake resulting from contact with liquid water and discovered that the former was less than the latter.⁹⁷ This is the case despite the fact that water activity in both cases is, on the basis of macroscopic thermodynamics, theoretically equal to 1.00. This was discussed in the above section on Microscopy Studies in relation to the paper of McLean et al., in which the existence of a thin fluorine-rich layer was discovered in their AFM investigations.⁸³ In theory, while such a hydrophilic

water barrier would influence the rate of water uptake, the equilibrium water uptake, which was reported by Zawodzinski and others, should not be affected in this way. Clearly, more research is required regarding this phenomenon and its influence on properties.

Later, Hinatsu et al. studied the uptake of water, from the liquid and vapor states at various temperatures, in acid form Nafion 117 and 125, and Aciplex and Flemion membranes, although the latter two similar products will not be discussed here.⁹⁸ These studies were motivated by a concern over the deleterious effects, involving either overly dry or overly wet membranes, on electrical conductivity within the context of polymer electrolyte fuel cells and polymer electrolyte water electrolyzers.

The membranes used in these studies had undergone a rather rigorous cleaning procedure. The liquid uptake studies were performed by simple, careful weight uptake experiments over the range $25\text{--}130^\circ\text{C}$. All water vapor uptake versus relative humidity isotherm studies were conducted at 80°C using a thermostated glass apparatus involving a water vapor reservoir, a quartz spring attached to a sample basket for mass uptake, and a pressure gauge.

The results of the water equilibrium uptake studies that were conducted at room temperature (25°C), for samples that were predried in a vacuum at 25 , 80 , and 105°C for various times, are as follows. Upon immersion in distilled water, the samples that were dried at room temperature attained and maintained the same uptake versus predrying time. On the other hand, the water contents of the samples that were dried at 80 and 105°C underwent a rapid decrease versus drying time, with the greatest decrease for the highest temperature. This behavior was interpreted in a general way as open microstructures caused by the formation of large, hydrated ion clusters upon swelling and "pore" shrinkage and reorientation of the side chains upon drying, the latter of which is reversed upon reexposure to water at elevated temperatures. Perhaps another way of stating this would be to say that the structures have been "annealed". In the usual sense, this involves improved molecular packing, that is, a decrease in free volume that is encouraged by thermal kinetic energy by heating. Thus, the sample dried at 105°C would have been in a state closer to a true equilibrium condition of optimal main and side chain packing and therefore exhibited the least water uptake.

Cleaned membranes that were dried at 80°C were referred to as the "N" (normal) form, and those dried at 105°C , as the "S" (shrunken) form. Membranes prepared by preboiling were referred to as the "E", or expanded, form. These symbols are mentioned here because they were used in other reports to refer to membranes prepared under similar respective conditions.

Liquid water uptake versus temperature curves were established over the temperature range $25\text{--}130^\circ\text{C}$ for Nafion that was vacuum-dried at the above two temperatures (S and N forms) as well as for a sample that was preboiled in water for 2 h (E form). Uptake increased with increasing immersion tem-

perature for both forms over the entire temperature range, with the N form value being greater than that of the S form at a given temperature, but the preboiled sample uptake was constant up to 100 °C. The lower uptakes for the S form can be attributed to a condition of more densely packed main chains and side chains affected during predrying. However, at immersion temperatures higher than 100–110 °C, the uptake for the different forms becomes the same, and this “transition” temperature range was said to correspond to the glass transition of acid form Nafion, as this relaxation was reported and termed in the early paper of Yeo and Eisenberg.⁹⁹ The conclusion is that, after the passage of the membrane through this transition, its thermal history was erased.

The water uptake isotherm curves of Hinatsu et al., at 80 °C, for very well dried membranes, were reflective of initial hydration of sulfonic acid groups for the slow curve rise region at low RH, followed by swelling during the high rise region. These authors suggested that the difference in uptake for the liquid versus vapor phase is more complex, involving an additional, condensation process on the interior pore walls (a “pore”, presumably was intended to be a cluster) in the latter, whereas sorption from the liquid phase is “direct”. On the other hand, it might be argued that hydrogen bonds must be broken in the liquid phase before sorption occurs whereas isolated water molecules can be sorbed from the vapor phase without this requirement. In any case, the cause of the differences between the sorption of saturated water vapor and liquid water (both having a theoretical water activity of 1.00) does not seem to be entirely understood at present.

The authors also mention the interesting result that uptake from water vapor at 80 °C was less than that at lower temperatures, as reported by others, and that this difference was not due to the predrying procedure.¹⁰⁰ It was suggested that water would condense on the membrane surface with more difficulty at the higher temperature and that this would retard sorption. This situation is of obvious significance with regard to humidified membranes in fuel cells. Also, as seen in other studies, the water uptake increases with decreasing EW.

Futerko and Hsing presented a thermodynamic model for water vapor uptake in perfluorosulfonic acid membranes.¹⁰¹ The following expression was used for the membrane–internal water activity, a_1 , which was borrowed from the standard Flory–Huggins theory of concentrated polymer solutions:¹⁰²

$$a_1 = (1 - \phi_2) \exp[(1 - 1/r)\phi_2 + \chi\phi_2^2]$$

ϕ_2 is the polymer volume fraction, χ is the polymer–solvent (water) interaction parameter, and r is the polymer equivalent unit/mole of water volume ratio that is calculated on the basis of the densities of dry polymer and water as well as the EW and molecular weight of water. $\phi_2 = r/(r + \lambda)$, where λ is the number of water molecules per sulfonic acid group.

A number of concerns can be raised over the use of this simplistic equation that was derived for

concentrated polymer solutions which, at best, can be applied to amorphous polymers with randomly distributed solvent molecules rather than systems having two phases of very different chemical compositions—in this case, a sharp contrast between strongly hydrophobic and strongly hydrophilic regions. Moreover, the strong interactions among water molecules, ion exchange groups, ether groups in the side chains, and the hydrophobic backbone in a phase separated system cannot be represented by the single quantity χ that, additionally, was originally intended to account for weak interactions.

The Flory–Huggins equation was modified to account for “proton-transfer complexes” of the sort $\text{SO}_3^- \cdots \text{H}_3\text{O}^+$. In short, a fraction of the water content was viewed as being strongly bound in these complexes, and this reduces the effective water concentration in the membrane. One might view the water molecules bound to these complexes as not being osmotically active, as would be “free” or mobile water. This reasonable concept was based on the IR studies of Zecchina et al.^{103,104} If the fraction of SO_3H groups that exist in these complexes is λ_c , then ϕ_2 increases to the effective value of $(r + \lambda_c)/(r + \lambda)$. Then, the constant for the equilibrium $\text{SO}_3\text{H} + \text{H}_2\text{O} \leftrightarrow \text{SO}_3^- \cdots \text{H}_3\text{O}^+$ was given by $K = \lambda_c / [(1 - \lambda_c)a_1]$.

The simultaneous solution of the equations for a_1 , ϕ_2 , and K will yield an a_1 versus λ curve if all the underlying parameters were known. To this end, Futerko and Hsing fitted the numerical solutions of these simultaneous equations to the experimental points on the above-discussed water vapor uptake isotherms of Hinatsu et al.⁹⁸ This determined the best fit values of χ and K . χ was first assumed to be constant, and in improved calculations, χ was assumed to have a linear dependence on ϕ_2 , which slightly improved the results in terms of estimated data fitting errors. The authors also describe methods for deriving the temperature dependences of χ and K using the experimental data of other workers.

The authors discuss Schroeder’s paradox, referred to elsewhere in this review, and the fact that liquid water uptake increases but saturated water uptake decreases with temperature. And, at low temperature, the water uptake by membranes in contact with saturated vapor is greater than that by membranes in contact with liquid water, which suggests a fundamental difference in membrane microstructure for the two situations. An energy level diagram of thermodynamic states versus temperature was proposed, based on this Flory–Huggins-based model.

By their nature, and in contrast with microscopic and scattering techniques that are used to elucidate long-ranged structure, spectroscopic methods interrogate short-range structure such as interactions between fixed ions in side chains and counterions, main chain conformations and conformational dynamics, and the fundamental hopping events of water molecules. The most common methods involve infrared (mid-IR and to a much lesser extent near- and far-IR) and solid-state NMR spectroscopies, although other approaches, such as molecular probes, have been utilized.

The long-ranged transport of ions, hydrated protons, water, and other solvent molecules through Nafion depends on the morphology on the dimensional scale interrogated by SAXS, SANS, TEM, and AFM methods. This is the scale at which critical issues involving the size of, shape of, and spacing between the ionic domains are important. To formulate a realistic transport model, detailed knowledge of the long-range spatial organization of these domains, the manner in which regions of concentrated hydration structures are incorporated in these domains, and the contiguous interdomain water structure is essential. These aspects must be understood in order to account for the obstacles to migration and how these obstacles form a percolation topology that is expressed in measured ionic conductivities, diffusion coefficients, and other transport parameters. While these *geometrical* considerations are important, it is also important to understand the nature of fundamental interactions experienced by these migrating species with functional groups on the polymer. In particular, different ion exchange groups will cause different degrees of swelling as well as different Coulombic and hydrogen bonding interactions with counterions and solvents. These interactions, that are operative on the scale of less than ~ 10 Å, are appropriately studied by spectroscopic means.

In an early study, Mauritz et al. investigated anion-cation interactions within Nafion sulfonate membranes versus degree of hydration using FTIR/ATR and solid state NMR (SSNMR) spectroscopies. An understanding of the dynamic ionic-hydrate molecular structures within and between the sulfonate clusters is essential for a fundamental understanding of the action of these membranes in ion transport. This information can be directly related to the equilibrium water swelling that, in turn, influences molecular migration.

This FTIR spectroscopic study was aimed at monitoring the effects of monovalent alkali counterion type (Li^+ , Na^+ , K^+ , Rb^+) and degree of hydration upon the vibrational state of the fixed sulfonate groups in 1100 EW membranes in which the cation/sulfonate ratio was 1:1.¹⁰⁵ The location and width of the peak for the $-\text{SO}_3^-$ symmetric stretching vibration are sensitive to these variables due to an induced polarization of S-O dipoles in the sulfonate group by the electrostatic field of the adjacent cation. This peak wavenumber, ν_s , is relatively independent of water content and cation type at high degrees of hydration but shifts to higher values and broadens as the water content decreases. These changes were interpreted in terms of increased sulfonate-cation Coulombic interactions as water is removed. The relative population of solvent-separated ions decreases as the fraction of contact ion pairs increases. The shift is largest for Li^+ , which has the greatest hydration number and highest surface charge density. Smaller shifts are observed for the Na^+ and K^+ forms, and none are observed for Rb^+ , which hydrates poorly, if at all, and has a low surface charge density.

Caution should be applied in interpreting ATR spectra because this is a surface technique that only interrogates structure within a distance of a few

microns beneath the surface. Moreover, thin, transparent solution-cast films may not have the same morphology as those of extruded sheets.

SSNMR studies based on ^7Li , ^{23}Na , and ^{133}Cs nuclei for 1100 EW samples whose sulfonate groups were exchanged with these cations (no excess counterions or co-ions being present) were conducted versus water content.^{106,107} The spectra reflect the influence of the immediate chemical environment about these cations that have spins greater than $1/2$ and, therefore, possess quadrupole moments. It is the interaction of these quadrupole moments with local electric field gradients that influences the chemical shift (δ) and line width of the observed resonance. In this case, the electric field is mainly due to $-\text{SO}_3^-$ anions as shielded by water molecules.

For ^{23}Na a plot of δ versus $\text{H}_2\text{O}/\text{Na}^+$ mole ratio = r is essentially flat at high water contents until r is lowered to where there are less than ~ 6 H_2O molecules per $\text{SO}_3^- \text{Na}^+$ ion pair. At higher water contents, most $-\text{SO}_3^- \text{Na}^+$ pairs are separated by liquidlike water molecules, but since the hydration number of Na^+ is 4, a considerable population of cations must exist in contact ion pairs for $r < 6$. In fact, δ greatly increases when r decreases from 6, providing evidence for contact ion pairs. On the average, there are not enough water molecules present to form complete hydration shells that would provide electrostatic shielding around the Na^+ ions. Contact ion pairing was discussed many years ago to rationalize the decrease in ionic mobility in simple electrolytes with increasing concentration.¹⁰⁸ The FTIR and SSNMR spectroscopic results presented here also are in harmony with a four-state model of ionic-hydrate association-dissociation equilibrium between bound and unbound cations in simple electrolyte solutions, as proposed by Eigen et al.^{109,110} The broadening of the symmetric SO_3^- FTIR peak upon membrane drying is considered as evidence of a multistage association-dissociation equilibrium subject to restrictions imposed by the polymer host. A molecular based model for ion conductivity in Nafion would have to incorporate this mechanism.

The chemical shift and line width observed for each water content were taken as weighted averages of the values in the free and bound states, and from two equations expressing these averages, P_b and P_f , the mole fractions of bound and free Na^+ ions, respectively, were extracted. P_b significantly increases as the approximate hydration number that might be expected for a $\text{SO}_3^- \text{Na}^+$ pair is approached from the direction of considerable hydration.

The ^{23}Na NMR parameters of Nafion are not greatly affected by changing EW in the range of water content where valid comparisons are possible,¹¹¹ and this reflects the short-ranged nature of these dynamic ionic-hydrate structures.

The behaviors of the ^7Li and ^{133}Cs resonances for membranes incorporating these counterions are qualitatively similar to that for the samples incorporating the ^{23}Na probe. δ for the Cs^+ form undergoes a significant shift at the lowest water content, which is reasonable considering the low hydration capacity of this large cation.

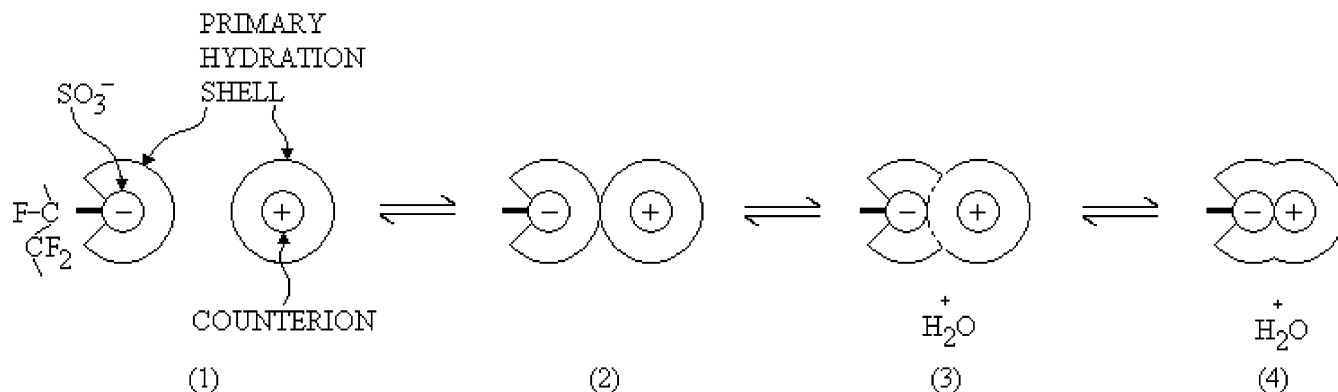


Figure 12. Four state model of the hydration-mediated counterion–side chain association–dissociation equilibrium, of Mauritz. (Reprinted with permission from ref 107. Copyright 1982 American Chemical Society.)

The interpretation of these SSNMR results is in agreement with that issuing from the FTIR studies of the same systems, as discussed earlier.

Mauritz et al., motivated by these experimental results, developed a statistical mechanical, water content and cation-dependent model for the counterion dissociation equilibrium as pictured in Figure 12. This model was then utilized in a molecular based theory of thermodynamic water activity, a_w , for the hydrated clusters, which were treated as micro-solutions. a_w determines osmotic pressure, which, in turn, controls membrane swelling subject to the counteractive forces posed by the deformed polymer chains. The reader is directed to the original paper for the concepts and theoretical ingredients.¹⁰⁷

Another noteworthy early IR spectroscopic study of Nafion (125 and 152) membranes, in the acid as well as various counterion forms, was that of Heitner-Wirguin, who assigned a number of characteristic bands and compared the spectra to those of sulfonated polyethylene (Redcat) membranes.¹¹²

Falk et al. conducted early FTIR studies of the structure of water in this ionomer, and the papers of these investigators serve as an excellent resource for the various band assignments, as tabulated in the book edited by Eisenberg and Yeager.¹⁹ The results of these studies were significant on a quantitative basis, in part, due to their careful control of water content by a vapor equilibrium technique that allowed for reproducibility as well as precise determination of the H₂O/SO₃⁻ ratio.¹¹³

Falk inspected the fundamental bands of the HDO isotope of water in Na⁺ form Nafion (125 and 142) sulfonate membranes. The bands of HDO are simpler and lend themselves to less ambiguous interpretation than the bands of H₂O or D₂O, as either the D–O or H–O stretching band can be studied in isolation for low and high D/H ratios, respectively. At low water contents (1.6 H₂O/SO₃⁻ mol/mol), both the O–H and O–D stretching bands occur as doublets (3660, 3520 cm⁻¹ and 2695, 2588 cm⁻¹, respectively), and at higher frequencies than those of HDO in liquid water. The conclusion was that O–H groups in water molecules exist in two different molecular environments at low water contents. In particular, the low frequency component was associated with hydrogen bonded O–H groups, while that at high frequency reflected non-hydrogen bonded O–H groups, perhaps

belonging to H₂O molecules at the hydrophobic–hydrophilic interface.

Falk, based on his FTIR studies of H₂O-, D₂O-, and HDO-containing Nafion, also rationalized that hydrated clusters either were much smaller than those proposed by Gierke et al.¹⁷ or possessed a shape that deviated greatly from sphericity such that fluorocarbon structural fragments intrude into cluster regions. In retrospect, this early view is more commensurate with recent visualizations based on subsequent experimental structural evidence, especially the structures displayed in pictures by Kreuer.⁹¹ Despite the considerable hydration capacity of Nafion, hydrogen bonding between water molecules in maximally hydrated samples is considerably less extensive than that in liquid water. This situation might be rationalized in terms of a high surface-to-volume ratio (S/V) for clusters of this size as well as the fact that when H₂O molecules are confined in such small spaces, a large relative population must reside at hydrophobic–hydrophilic interfaces, especially if the interfaces are irregular.

The idea of convoluted or rough interfaces is in contrast with the view of Rollet et al., who concluded that the ionic domains are spherical (In fact, this was an assumption in a local-order model.) and that interfaces between hydrophobic and hydrophilic phases are sharp, although this situation changes when the temperature is greater than 60 °C.¹¹⁴ This conclusion is based on the results of SANS investigations of Nafion 117 membranes as a function of temperature, nature and charge of the counterion, concentration of electrolyte solutions in which the membranes were equilibrated, and membrane pretreatment.¹¹⁴ These particular conclusions were based on an analysis of scattering data in the Porod region where the intensity scales as q^{-4} . These authors offer the general conclusion that the nanostructure of Nafion is governed by interfacial phenomena.

Spectra at higher water contents indicated an increasing relative population of water molecules in O–H···O hydrogen bonds, and the shift of the low wavenumber O–H stretching component to lower frequencies reflected increasing strength of the hydrogen bonds. The fact that the peak wavenumber of the high frequency component was constant is harmonious with the notion that these groups have O–H- -CF₂ juxtapositions. At least qualitatively, the

ratio of the integrated absorbances under the O–H–CF₂ and O–H···O peaks should yield information on the geometry of the aqueous domains in terms of surface-to-volume. For a water uptake corresponding to 2 H₂O molecules per SO₃[−] group, 24% of OH groups do not participate in hydrogen bonds. For high water contents, however, the peaks were not able to be resolved.

Kujawski et al. used FTIR/ATR spectroscopy to study side chain interactions with the alkali counterion series in Nafion 117 membranes that were equilibrated in water, ethanol, and 2-propanol.¹¹⁵ These results were compared against the spectra of a membrane consisting of an interpenetrating network of polyethylene and sulfonated poly(styrene-*co*-divinylbenzene) (PESS). The behavior of the symmetric stretching band of the sulfonate group of Nafion showed that, for dry membranes, the smaller the counterion radius, the stronger is the ion pair interaction, as earlier noted by Lowry and Mauritz¹⁰⁵ and Falk et al.¹¹⁶ In the Li⁺ form equilibrated in pure 2-propanol, ν_s was affected in a fashion similar to that caused by pure water. On the other hand, this band was unaffected by the alcohol in the PESS membrane, meaning that the SO₃[−]Li⁺ ion pairs were not dissociated in this hydrocarbon system. The implication is that Li⁺ cations were solvated by 2-propanol molecules in Nafion but not in PESS and the strong alcohol affinity of the perfluorinated ionomer was due to the greater acid strength of the SO₃H groups. For water–isopropanol mixtures, ν_s was noted to be constant over the composition range. This was interpreted to mean that the strengths of hydrogen bonding of the alcohol and water molecules with the sulfonate group are practically identical. However, the membrane internal composition of the binary solution may not be the same as that of the external solution in which the membrane was equilibrated, and partition coefficients were not determined.

Cable et al. similarly studied the influence of hydrophobic as well as hydrophilic counterions on characteristic vibrations of the sulfonate and the two perfluoroether groups in the side chains of Nafion 117 membranes using FTIR/ATR spectroscopy.¹¹⁷ The symmetric SO₃[−] stretching band for dry Na⁺ form membranes shifted to higher wavenumbers with increase in degree of neutralization by this cation but, in contrast, shifted to lower wavenumbers with increasing neutralization with tetrabutylammonium cations (TBA⁺). The latter behavior was attributed to diminished polarization of the SO₃[−] groups by the hydrophobic TBA⁺ cations that have a low surface charge density as opposed to the influence of the stronger electrostatic fields posed by the smaller Na⁺ counterions that have a larger surface charge density.

Cable et al. also noted two distinct bands in the region 1000–950 cm^{−1}, in which resides the absorption envelope for the symmetric C–O–C stretching vibration. This spectral feature was earlier observed by Heitner-Wirguin¹¹² as well as Lowry and Mauritz.¹⁰⁵ Heitner-Wirguin noted a small shift in this band when the Na⁺ counterion is replaced by transition metal counterions. The spectra of Lowry and Mauritz for dry Li⁺, Na⁺, K⁺, and Rb⁺ forms

show the low wavenumber component as a shoulder at ~970 cm^{−1} on the dominant peak at ~980 cm^{−1}. The ~970 cm^{−1} peak becomes more prominent and better resolved with hydration, particularly for the Li⁺ and Na⁺ forms, and the evolution of this low wavenumber component with increasing degree of hydration is especially evident for the Li⁺ form. These facts were taken to suggest that parts of the perfluoroether side chains penetrate the ionic clusters rather than forming a neat inverted micelle as depicted in the Gierke model. A closer inspection of the spectra in this region shows a fainter shoulder on this absorption envelope at 995 cm^{−1}, which was verified by Falk and later seen by Cable et al., although the origin of this peak has not been addressed.¹¹⁸

Cable et al. observed that the low wavenumber component (965 cm^{−1}) increased in wavenumber with increase in degree of Na⁺-neutralization of dry samples and that this shift correlates with the increasing peak wavenumber shift of the symmetric stretching vibration in SO₃[−] groups. On the other hand, the high wavenumber component (980 cm^{−1}) does not shift with either counterion type or hydration. The general view is that a portion of the ether groups in the side chains are strongly influenced by the state of ion pair association while the ether groups near the backbone are shielded from these interactions. In addition to consideration of through-space Coulombic field perturbations on the C–O–C vibration, through-bond inductive effects, that is, vibrational coupling within the span of a few bonds from a polarized SO₃[−] group, should also be considered as a mechanism. These conclusions are supported by the fact that the FTIR spectrum of a corresponding sulfonyl fluoride Nafion precursor film, that did not have cluster morphology, exhibited only a single ether band at ~980 cm^{−1}.

The frequency of the symmetric stretch does not vary with degree of neutralization for hydrated membranes, which was attributed to the shielding of sulfonate anions from the electrostatic field of the Na⁺ ions.

Risen et al. investigated cation–anion interactions using far IR spectroscopy (50–300 cm^{−1}) to study Nafion sulfonate membranes that were neutralized by cations in the series Na⁺, K⁺, Rb⁺, and Cs⁺ and the series Mg²⁺, Ca²⁺, Sr²⁺, and Ba²⁺, as well as the acid form.¹¹⁹ The spectra in this region for hydrated samples show a broad but well-defined band below 300 cm^{−1} that is not present for the acid form. For both the monovalent alkali and divalent alkaline earth series, the band monotonically shifts to lower frequencies, f , such that $f \propto M^{-1/2}$, where M is the cation mass, and the slope of the line is greater for the divalent series. These facts identify this band with harmonic oscillations of the cations in the force field of the fixed SO₃[−] anions. Moreover, the force constant is essentially the same for each ion in the monovalent series and, likewise, the force constant is essentially the same for each ion in the divalent series. Based on the slopes of these lines and harmonic oscillator theory, the force constants for the members of the monovalent cation series are less than those of the divalent cation series. This fact

reflects stronger cation–anion Coulombic interactions owing to the greater charge of the divalent ions.

Interestingly, this “ion motion band” is not influenced by water as seen in dehydration studies. While sample preparation details were given in this report, the exact water contents of these samples were not stated; rather, samples were referred to as “dry”, “partially dry”, or “hydrated”. While far IR spectroscopy has not been exploited in the study of Nafion, it is clear that information regarding cation–anion binding and vibrational frequencies would be of great importance in understanding and modeling ion-hopping kinetics, using activated rate theory.

Another study involving cation–sulfonate interactions in Nafion (1200 EW) is that of Yeager, who investigated the property of equilibrium ion exchange selectivity at 25 °C.¹²⁰ The results of this study are relevant with regard to the use of this ionomer as a chromatographic medium or as a membrane through which more than one cation is simultaneously transported. The degree of H⁺ exchange in the acid form was determined for mono- and divalent cations and expressed in terms of ion exchange selectivity coefficients, $K_{H^+M^+}$, and $K_{H^+M^{2+}}$, respectively, that involve the equivalent ionic fraction of the given ion, M⁺, in the ionomer, the external solution molarity, and the cation activity coefficient. One result is that, for the alkali metal series Li⁺, Na⁺, K⁺, Rb⁺, Cs⁺, as well as Ag⁺, and Tl⁺, there is a larger spread in $K_{H^+M^+}$ values than that seen for conventional cross-linked sulfonated polystyrene ion exchange resins. The spread for the alkaline earth series is smaller than that for the alkali metals. In both cases, selectivity decreased with increasing membrane hydration. Also, it was seen that exchange of alkali metal cations from anhydrous methanol solutions was very similar to that for the aqueous solutions.

Yeager suggests that the major factor involved in the ion exchange selectivity of Nafion is the positive entropy change associated with the replacement of H⁺ with the metal ion, which is accompanied by water release and polymer contraction.

Barnes studied the nature of water in Nafion 117 membranes in various alkali metal cation forms using near-IR (NIR) spectroscopy.¹²¹ Advantages of the use of this spectral range (in this case, over the wavelengths 1100–2500 nm) are that there are no obscuring CF₂ overtone bands and that band shifts due to hydrogen bonding are greater than the characteristic bands that are seen in the mid-IR range. The NIR water bands of interest are the combination bands 1890 nm (type I: non-hydrogen bonded water) and 1920 nm (type II: hydrogen bonded water with bond angles around 110°), as discussed by Luck.¹²²

Both type I and type II water forms were detected, and the I/II mole ratio was rather constant at 1:2.2 for the Na⁺ form having the low H₂O/SO₃[−] mole ratios of 0.06, 0.5, and 1.2. These numbers were derived from the areas under the two deconvoluted peaks. The ratio of type I to II water molecules decreases in the order for the series Na⁺ > K⁺ > Rb⁺ > Cs⁺, which is reasonable considering that the cation hydration number decreases in this order and shows the structure-breaking action of cations with

high surface charge density. The somewhat linear plot of type I water versus square of the cation radius was taken to suggest that water molecules are not only distributed around cation–anion associations, but a fraction resides close to the perfluorinated backbone, as earlier suggested by Falk et al.¹²³ and Yeager et al.¹²⁴ In fact, The NIR spectrum of PTFE homopolymer showed that type I water is the only form found in this matrix.

The molecular mobility of water in Nafion was investigated using NMR spectroscopy, by Starkweather and Chang,¹²⁵ Boyle et al.,¹²⁶ and Bunce et al.¹²⁷ The overall conclusion of these studies was that water possessed less mobility than that of liquid water and that there were cooperative motions among the molecules and strong interactions with the ion exchange groups.

Sivashinsky and Tanny, in an early paper, used ¹H NMR to study water in Nafion 125 that had been boiled and then converted to the Na⁺ form by soaking in aqueous NaCl.¹²⁸ The water content was such that H₂O/SO₃[−] was 16:1 (mol/mol), which corresponds to a condition where there are a considerable number of water molecules in excess of those that would be tightly bound in hydration shells around the ions. It is unclear in this document as to whether excess electrolyte was leached from these samples, but it is a reasonable assumption. The theoretical model of Bloembergen, Purcell, and Pound for the temperature dependence of relaxation processes for water adsorbed on a surface was seen to fit their data.¹²⁹ From the minimum in a T_1 (spin–lattice relaxation time) versus reciprocal temperature plot at ~250 K, a correlation time ($\tau_c = 1.7 \times 10^{-9}$ s) was extracted that was 2 orders of magnitude larger than that for supercooled water, but 4 orders of magnitude shorter than that for ice at the same temperature.¹³⁰ This was taken to imply that the structure of water that is mobile at ~250 K is more akin to that of a supercooled liquid or what might be thought of as a glass. Also, free induction decay studies versus temperature did not reflect freezing in the sense of a first-order phase transition. A conclusion based on the T_1/T_2 value at the T_1 minimum was that water molecules existed in a number of environmental states. Coupled with heat of fusion data obtained from DSC experiments, it was concluded that the presence of small “pores” and interaction between the water and the matrix were the most important structure-determining factors.

Boyle et al. also performed ¹⁹F NMR investigations of the fluorocarbon backbone in 1100 and 1500 EW acid form samples in the hydrated state in the temperature range −120 to 160 °C.¹³¹ No effort was made in sample preparation to remove impurities from these samples, which can be problematic. The interpretations of the results for 1100 EW are as follows. T_2 data for a low degree of hydration (7%) showed that the backbone motions are considerably slower than those in the SO₂F precursor form in the high temperature region, which was said to reflect constraints posed by ion clustering, as there are no clusters in the precursor form. For a water content of 25%, there is greater motion in the temperature

range in which these motions are activated, and this was ascribed to a plasticizing effect of the water, presumably in terms of weakening electrostatic interactions in the clusters. The T_2 behavior for the 1500 EW samples up to +120 °C shows greater mobility than that for the 1100 EW sample that had comparable water content. In essence, the explanation for this was that there are fewer clusters in the 1500 EW sample that would constrain matrix motion.

Pineri et al. correlated the results of DSC, NMR, ESR, water sorption isotherms, and dynamic mechanical analyses of hydrated acid form Nafion 120 membranes that had undergone temperature cycling.¹³² They concluded that water sorption properties have a strong dependence on temperature. Desorption occurs during cooling from room temperature for contents greater than around 8 wt %, and this is followed by freezing. Also, the water vapor pressure decreases during this cooling to establish a new thermodynamic equilibrium. Desorption was seen to take place above what was then termed the “glass transition of the ionic phase” (~220 K) during the heating of a liquid nitrogen cooled sample that had 15 wt % water. Earlier, Starkweather and Chang similarly referred to a “glass transition of the aqueous domains” based on dynamic mechanical and dielectric relaxation experiments, as well as proton NMR spectroscopy.¹²⁵ After this desorption event (from the “ionic phase”), the water was said to freeze, as evidenced by a DSC exothermic peak, and this also results in an increase in elastic modulus. An endothermic peak was said to correspond to a frozen-to-mobile transformation in the hydration microstructure, and the fractions of desorbable and non-desorbable water were calculated as a function of water content. Pineri et al. were in disagreement with the conclusions of Sivashinsky and Tanny¹²⁸ in that the former believed that their DSC peaks reflected a first-order transition having to do with the sorption or desorption of water into or out of the ionic phase but disregarded the idea of a pore-size effect. Characteristic water desorption times and changes in the number of mobile protons were determined at different temperatures using proton NMR spectroscopy. It should be cautioned that these results have significance within the context of the particular manner in which these samples were prepared. For example, the membranes were not boiled, as usual, as part of an initialization process.

Yoshida and Miura also studied the nature of water, in terms of freezing and non-freezing fractions, in 1100 EW samples in the Li^+ , Na^+ , K^+ , NH_4^+ , and alkylammonium counterion forms, using DSC.¹³³ The degree of neutralization of the sulfonic acid groups for all the cations was around 90%, and the measurements were performed on samples of various water contents over the temperature range 100–50 K. For example, cooling curves starting at 310 K (37 °C), at the rate of 10 K/min, for the Li^+ form, showed exothermic peaks—first-order transitions—whose magnitudes were enhanced, and the peak temperatures increased with increasing water content. The peak widths decreased in this order of cation type but were not as narrow as that of pure water. These peaks,

beneath the freezing temperature of pure bulk water, were said to be due to water crystallizing in the membrane. Heating curves showed a single endothermic peak at around 270 K (−3 °C) that was attributed to water melting. These peaks shifted to lower temperature, broadened, and became more asymmetric with decreasing water content. It is reasonable that smaller “ice” crystals that would exist at lower water content on this dimensional scale would have lower crystallization and melting temperatures for the usual surface/volume considerations, as discussed in crystallization theory.

These investigators classified the incorporated water molecules into three categories: nonfreezing, freezing bound, and free water. The freezing bound water peak at the lowest temperature was distinct, but the peaks for nonfreezing and free water were difficult to separate and the combined area under them was simply treated as being due to “free water”. The heat of fusion of pure water and the areas under the exothermic peaks were used to calculate relative free versus freezing bound water content, and the total amount of freezing water was estimated from the area under the single melting endotherm peak. In plots of the amounts of the three types of water with increasing total water content, it is seen that a threshold must be exceeded before freezing water can exist.

Nonfreezing water molecules were considered to exist in hydration shells around the given cation. Presumably, mobility restrictions placed on ion-contacting water molecules, posed by the strong electric fields, prevent these water molecules from crystalline packing, as in the so-called “structure-breaking” effect in simple aqueous electrolytes. The amounts of nonfreezing and freezing bound water decreased with decreasing “hydration radius”. While not explicitly defined in this paper, “hydration radius” apparently refers to the radius of the bare cation plus the thickness of a well-defined hydration shell, as this quantity was said to decrease in the order $\text{K}^+ < \text{Na}^+ < \text{Li}^+$ and the hydration numbers decrease in this order.

This is another study that illustrates that the ensemble of water molecules can be partitioned into different classes. The state of a water molecule depends on whether it is directly interacting with a cation—and is a function of cation type—and on the total water content, which, when low, will not provide for enough molecules to form distinct crystallites.

The properties of Nafion at freezing temperatures can be quite relevant, for example, within the context of fuel cells in vehicles with regard to cold-starting, as well as the degradation of membrane/electrode assemblies due to the freezing of in situ water.

Miura and Yoshida also investigated the changes in the microstructure of 1100 EW Nafion sulfonate membranes, in alkali, ammonium, and alkylammonium cation forms, that were induced by swelling in ethanol using DSC, dynamic mechanical analysis (DMA), SAXS, and electron probe microanalysis (EPMA).¹³⁴ These studies were performed within the context of liquid pervaporation membranes that could potentially be used to separate ethanol from water

in azeotropic mixtures. The treatment consisted of drying membranes from a water-swollen state and an ethanol-swollen state. The membranes were swollen for 1 week in these liquids at 296 K, after which they were dried under vacuum at room temperature for 1 week.

The DMA results showed a large difference between the relaxations of the water-treated and EtOH-treated membranes for some of the cation types (and only slight differences for the others). It should be cautioned that the assignment of the $\tan \delta$ peaks in this paper should be reconsidered in the light of the more recent studies of Moore et al.¹³⁵ It was suggested that these viscoelastic changes reflected a condition where ionic clusters undergo rearrangement by swelling in EtOH, and it was deduced, based on their SAXS analysis, that, when Na^+ and ammonium were the counterions, the sizes of the ion clusters in the EtOH-treated-dried membranes (SAXS Bragg spacing of 2.8 nm) were smaller than those in the water-treated-dried membranes (SAXS Bragg spacing of 3.3 nm). EPMA sulfur mappings on the surfaces of a Na^+ form membrane showed dots about 100 nm in size that were attributed to aggregates of clusters, although the images are not of such a quality as to ascertain the structure of these units. A digital image analysis provided information on the number density, size, and shape distribution of these cluster aggregates. The results of this analysis were that the number of cluster aggregates in the EtOH-dried sample was less than that for the water-dried sample and that the dispersion of cluster aggregates was more homogeneous with EtOH treatment. These authors speak of the relaxation of stresses that are frozen in during membrane processing, as caused by the incorporation of EtOH, and this is said to be responsible for the changes in structure and properties.

MacMillan et al. studied the dynamics of water molecules in Nafion 117 using ^1H , ^2H , and ^{19}F NMR spectroscopy.¹³⁶ Special care was taken to remove impurities from samples, including paramagnetic contaminants as well as oligomers and precursor fragments, which often does not occur in sample preparation.^{137,138} A transition in relaxation behavior at a characteristic temperature T_t was observed. T_t is defined as the temperature at which the slopes of the T_1 (spin–lattice), T_2 (spin–spin), and $T_{1\rho}$ (rotating frame spin–lattice) relaxation times versus $1000/T$ curves undergo a sharp change. For a hydration level of 15.9%, T_t is approximately -10 °C. T_t shifts to higher values with decreasing degree of hydration. Sorbed water molecules behave much as in the bulk and are not greatly modified by their polymer environment. The activation energy is small, which reflects high rotational mobility with low hydrogen bond density for $T > T_t$. It is worthy to note that Escoubes and Pineri reported an endothermic peak seen in the microcalorimetric studies of Nafion having 15% water at around -15 °C, which is close to T_t .¹³⁹

^{19}F T_1 and T_2 values indicate that the polymer relaxation is unaffected by the presence or absence of water. These results differ from the NMR results

of Boyle et al., which indicated increased mobility with hydration.¹³¹

It was suggested that there is a range of temperatures over which SO_3H groups go from being fully dissociated to being fully associated upon cooling, and this temperature range depends on the properties of the water at a given degree of hydration.

For T below this range, a large population of protons appears to be in a solidlike environment and contribute to the T_2 and $T_{1\rho}$ relaxation.¹⁴⁰ The motional correlation time, τ_c , was assumed to have an Arrhenius dependence on T . On T_2 and $T_{1\rho}$ versus $1000/T$ plots, a change in slope was associated with the onset of acid group reassociation. The activation energies for molecular reorientation were rather large, to the extent that up to four hydrogen bonds must be broken to affect this motion. This suggested a highly ordered supercooled fluid of hydrogen bonded water, although the molecular mobility of water in this system is much greater than that in ice. The belief was expressed that water forms complex cage-like structures, or clathrates, of a number of molecules. τ_c at 253 K monotonically decreased from 6.6×10^{-7} to 6.5×10^{-12} s as the average number of H_2O molecules per SO_3H group increased from 1.1 to 11.6, which would indicate greater rotational mobility. It was concluded that supercooling occurs at much lower temperatures than those for water that resides in regular shaped pores,¹⁴¹ and this was attributed to irregularly shaped clusters within Nafion, a concept that was perhaps earliest expressed by Falk.^{113,118} This picture is somewhat different from that of Yoshida and Miura, who spoke of water crystallizing in the usual sense. It must be remembered that their results were for cation exchanged, rather than acid form, samples, and protons from the acid groups can be directly incorporated into the water molecule structure, whereas cations interact with water molecules by forming hydration shells.¹³³ MacMillan et al. considered that the high surface/volume aspect of water clusters inhibits the formation of ice. A simple model that relates correlation time to pore radius showed that the cluster surface varies as $r^{2.5}$ rather than r^2 , which means that the surface/volume is greater than that on the basis of a solid sphere, hence, the term “fuzzy sphere”.

It will be recalled that Sivashinsky and Tanny also favored the idea of supercooled water whose structure is influenced by being in pores as opposed to the idea of freezing water.¹²⁸ While the NMR experiments of Sivashinsky and Tanny were performed on the Na^+ form, τ_c at ~ 250 K was 1.7×10^{-9} s, which is in the midrange of those obtained by MacMillan et al. for different water contents. It is difficult to imagine water as forming ice in the usual bulk sense in these confined spaces having high surface/volume.

Cation–sulfonate interactions, as well as proton mobility, are also expressed in the electrical conductance behavior of these membranes. Many studies of this property have been reported, and there is no attempt in this review to cite and describe them all. Rather, a few notable examples are chosen. Most testing is done using alternating current of low voltage to avoid complications in the form of chemical

changes at membrane–electrode interfaces that might occur with direct current.

Cahan and Wainright showed that there is an inherent problem with two electrode cells in that membrane/blocking electrode interfacial impedance interferes with the measurement of the bulk impedance at low frequencies and that use of the four electrode system eliminates this problem.¹⁴² In the absence of this interfacial effect, conductivity is independent of frequency from the dc range up to at least 10^5 Hz. These conclusions were reinforced by the impedance studies of Fontanella et al. in which the electrodes were of both large and small area in a two-electrode configuration.¹⁴³ Thus, the four electrode configuration is generally preferred, although the measured values reflect conductivity along the plane of the membrane rather than along the more relevant thickness direction. There is also the issue of conductivity anisotropy in the plane of the membrane that is generated by melt extrusion of films. A study by Gardner et al. demonstrated that this is in fact the case.¹⁴⁴ There is also the question as to whether the in-plane conductivity is the same as that along the perpendicular direction.

Environmental control that fixes a known concentration of solvent in the membrane under test is also important. The reader is encouraged to consult the review, and references therein, of conductivity measurement techniques by Doyle and Rajendran.¹²

Gavach et al. studied the high frequency electrical resistance of Nafion 117 membranes in various monovalent counterion forms using an ac impedance analyzer. For low water contents, the resistance was seen to increase to very high values as the water content decreased, which can be attributed at least in part to ion pair formation as oppositely charged ions become increasingly less separated by water molecules. The alkaline cation series follows a trend opposite to that for the ion mobilities in pure water.¹⁴⁵ Later Gavach et al. performed this analysis for various counterion forms as a function of water content.¹⁴⁶ Curves for specific conductivity versus number of moles of water molecules per SO_3^- group exhibited an overall organized trend of upward displacement in the following order for the cation forms: $\text{Al}^{3+} < \text{Mg}^{2+} < \text{Mn}^{2+} < \text{Ca}^{2+} < \text{K}^+ < \text{Na}^+ < \text{Li}^+ < \text{H}^+$. There is a clear correlation with cation valence.

For a given cation at relatively high degree of hydration, there is a simple monotonic line, in some cases with slight curvature, on the Z' versus Z'' diagram, and this corresponds to a pure resistance, not strongly linked to morphology, in a situation where ions can readily hop between clusters in this swollen state. But, when the degree of hydration is lowered, there is, in addition, a semicircle that develops, and this is suggested to be due to a capacitive effect owing to an accumulation of ions on each side of intercluster channels that have been significantly narrowed. While not stated in this article, the semicircle can be considered to reflect a form of fluctuating interfacial polarization with a characteristic relaxation time during which cooperative charge motions accumulate and dissipate during

half of the period of electric field oscillation. The effects of percolation and ion pairing are significant at lower hydration levels.

Using a simple electrostatic interaction-based model factored into reaction rate theory, the energy barrier for ion hopping was related to the cation hydration radius. The conductance versus water content behavior was suggested to involve (1) a change in the rate constant for the elementary ion transfer event and (2) a change in the membrane microstructure that affects conduction pathways.

Earlier, Gavach et al. studied the “superselectivity” of Nafion 125 sulfonate membranes in contact with aqueous NaCl solutions using the methods of zero-current membrane potential, electrolyte desorption kinetics into pure water, co-ion and counterion self-diffusion fluxes, co-ion fluxes under a constant current, and membrane electrical conductance.¹⁴⁷ “Superselectivity” refers to a condition where anion transport is very small relative to cation transport. The exclusion of the anions in these systems is much greater than that as predicted by simple Donnan equilibrium theory that involves the equality of chemical potentials of cations and anions across the membrane–electrolyte interface as well as the principle of electroneutrality. The results showed the importance of membrane swelling; there is a loss of superselectivity, in that there is a decrease in the counterion/co-ion mobility, with greater swelling.

The situation for hydrated Nafion in the acid form, or as containing aqueous acids or strong bases, is more complex because protons and “defect protons” (i.e., OH^- ions), migrate according to a somewhat different mechanism. Proton transfer in either case occurs throughout and between clusters of hydrogen bonded water molecules to a degree that depends on the relative water content.

While it is beyond the scope of this review to elucidate details of the current views of proton transport across hydrogen bonds in aqueous systems, the reader is referred to the paper by Eikerling et al.¹⁴⁸ These authors describe the three main options as follows: (1) An excess proton can be a part of an H_3O^+ ion in which all of the three protons are equivalent. (2) The proton is placed between the two water molecules in the hydrogen bond in an H_5O_2^+ grouping, in the view of Zundel.¹⁴⁹ (3) The proton is a part of an Eigen H_9O_4^+ cluster comprised of an H_3O^+ ion and three H_2O molecules strongly attached to each of the three protons of the H_3O^+ species.¹⁵⁰

Eikerling, in this paper, presents a phenomenological model for proton conductivity and mobility in a hydrated Nafion channel and incorporated this model into a statistical model of a multichannel structure consisting of hydrophobic regions throughout which are water-filled channels (pores). A shortcoming of this model is that polymer structure is not factored into the calculations. Mechanisms for proton transport along the negatively charged surface and “bulk” of a pore are factored in. The surface mechanism has a higher activation energy but a higher concentration of charge carriers, and the balance between surface and bulk effects depends on the surface density of SO_3^- groups and pore size. The model accounts for

the effect of proton localization sites, dependent on EW, and pore water content and overall swelling. Theoretical estimates of the membrane conductivity agree with experimental data. In another paper, Eikerling and Kornyshev describe a theoretical treatment of activated proton transfer in a single pore with sulfonated groups on the surface.¹⁵¹

Aldebert et al. studied the room temperature conductance of 1100 EW Nafion membranes using a method that also measured the swelling due to a contacting liquid.¹⁵² The membranes tested were in the H⁺ as well as Li⁺, Na⁺, and Rb⁺ forms, and the solvents used were water, ethanol (EtOH), *N*-methylformamide (NMF), and propylene carbonate (PC). Prior to use, the membranes were boiled in nitric acid, washed with distilled water, and dried. The conductance, measured versus time from the onset of swelling, showed plots in which there was an abrupt rise so that a hold-up time, t_0 , could be extracted by extrapolating the fast rise portion of the curve back to zero conductance on the time axis. This is similar to the time lag method for measuring gas diffusion coefficients in membranes.¹⁵³ Ultimately, the curves approached asymptotic behavior. Cation diffusion coefficients were derived using the equation $x^2 = 8Dt_0$, where x is the thickness of the membrane before swelling. D for membranes contacting water was seen to decrease with increasing counterion radius and with the Guttman donor number of the solvent. This can be accounted for in the usual sense by the fact that larger cations solvate less and so become less mobile. D for the H⁺ form ($1.08 \times 10^{-6} \text{ cm}^2 \cdot \text{s}^{-1}$) was close to the value for pure water ($0.83 \times 10^{-6} \text{ cm}^2 \cdot \text{s}^{-1}$), and this was taken to mean that protons are highly "solvated". D for the Li⁺ form decreased in the following order for the solvents: H₂O > EtOH > NMF > PC. This can be rationalized in terms of the relative affinity of these solvents for the cation. Because D is defined within the context of early-time data—that is, before the conductance reaches an asymptote—it might be questioned as to whether D for the cation forms truly represents a value representative of a membrane in equilibrium with the solvent because diffusion coefficients in swollen systems can be reduced by plasticization effects.

Cappadonia et al. studied the electrical conductivity of acid form Nafion 117 membranes using an impedance analyzer as a function of temperature and water content over the range 0–29.8 g of H₂O/100 g of Nafion.^{154,155} It was seen that there is a high temperature regime over which the activation energy is low and decreases with increasing water content. In a low temperature range, the activation energy is higher and also monotonically decreases with increasing water content. The temperature for this conductance discontinuity occurs at around 260 K for water contents greater than 8 g of H₂O/100 g of Nafion. It was expressed that the most probable cause for this transition was freezing water. This idea was said to be reinforced by the DSC results of Chen et al., who noted an endothermic peak in Nafion samples, having comparable water content, beginning at ~253 K.¹⁵⁶ The freezing point depression, as

in other studies, was attributed to water having to crystallize in very confined spaces.

Fontanella and co-workers studied the effect of high pressure variation on the conductivity as well as the ¹H, ²H, and ¹⁷O NMR spectra of acid form Nafion117 membranes that were exposed to various humidities.¹⁵⁷ Variation of pressure allows for a determination of activation volume, ΔV , presumably associated with ionic and molecular motions. Conductivities (σ) were obtained from complex electrical impedance diagrams and sample geometry, and ΔV was determined from the slope of linear isothermal $\ln \sigma$ versus p graphs based on the equation $\Delta V = -kT[d \ln \sigma/dp]_T$, where p is the applied pressure. At room temperature, ΔV was found to be $2.9 \text{ cm}^3 \cdot \text{mol}^{-1}$ for a sample conditioned "in atmosphere" and was $6.9 \text{ cm}^3 \cdot \text{mol}^{-1}$ for a sample that was conditioned in 25% relative humidity, where the latter contained the lesser amount of water.

Activation volumes were derived from pressure dependent NMR experiments using the equation $\Delta V = -kT[d \ln T_1/dp]_T$, where T_1 is the spin-lattice relaxation time. ΔV values for the ¹H and ²H NMR experiments were close to each other as well as to the values based on conductivity. These results imply that the electrical transport is correlated with water molecule rotation. There is a trend of increasing ΔV with decreasing water content.

Paddison et al. performed high frequency (f) dielectric relaxation studies, in the Gigahertz range, of hydrated Nafion 117 for the purpose of understanding fundamental mechanisms, for example, water molecule rotation and other possible processes that are involved in charge transport.¹⁵⁸ Pure, bulk, liquid water is known to exhibit a distinct dielectric relaxation in the range 10–100 GHz in the form of an ϵ'' versus f peak and a sharp drop in the real part of the dielectric permittivity at high f .¹⁵⁹ A network analyzer was used for data acquisition, and measurements were taken in reflection mode.

Not surprisingly, ϵ' and ϵ'' increased with increasing water content, but especially when the water content reached 6 and 13 H₂O/SO₃H (mol/mol). This, by the usual argument, may reflect a situation where, at these hydration levels, there are water molecules beyond those that are ion-bound that are free to rotate and therefore increase the overall polarizability. There appear to be no peaks that rise above the considerable noise in the loss spectra, as seen in the spectra for pure water. The low f behavior of the ϵ'' versus f curves exhibits a $1/\omega$ ($\omega = 2\pi f$) dependence, so that specific conductivity values could be extracted in the usual way. These conductivities compare favorably with those obtained by Zawodzinski et al.¹⁶⁰

Alberti et al. investigated the influence of relative humidity on proton conductivity and the thermal stability of Nafion 117 and compared their results with data they obtained for sulfonated poly(ether ether ketone) membranes over the broad, high temperature range 80–160 °C and RHs from 35 to 100%.¹⁶¹ The authors constructed a special cell used in conjunction with an impedance analyzer for this purpose. Data were collected at high temperatures within the context of reducing Pt catalyst CO poison-

ing in direct methanol fuel cells at higher temperatures as well as the accompanying problem of membrane dehydration.

Nafion exhibited better proton conductance, especially at low RH, but the differences diminish or even vanish with increasing RH and increasing temperature. An interesting finding is that when RH is held constant, the conductivity remains constant over the temperature range 80–160 °C. It was suggested that the conductivity increase that would be “expected” (presumably, on the basis of faster proton hopping kinetics in the absence of a matrix)—but not seen—with increasing temperature is counteracted by a membrane microstructure change that reduces the mobility and/or concentration of the charge carriers, and an increase in polymer crystallinity was offered as a possible cause.

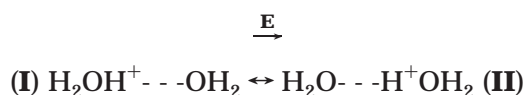
Alberti et al. also describe experiments dealing with reversibility during heating–cooling cycles at constant RH, as well as membrane swelling and chemical degradation, and the reader is referred to this report for the various interesting details.

Proton transfer in hydrogen bonds, referred as the Grotthuss mechanism in older treatises on reaction rate theory,¹⁶² and H₂O molecule rotational motion as well as the structural reorganization and diffusion within extended hydration structures are important fundamental molecular events within the context of membrane applications that depend on proton conductance. Membranes in H₂–O₂ fuel cells are of great current interest in this regard. These molecular events also underlie the function of membranes in the arena of membranes in chlor-alkali electrolytic cells,¹⁶³ water electrolyzers for the production of H₂,¹⁶⁴ and membranes used in Donnan dialysis processes that are used to strip metal ions, such as those of copper and nickel, from electroplating waste solutions.¹⁶⁵ Yeager and Gronowski provide a good listing of such applications, a number of which involve Nafion.¹⁶⁶ Related to this is the strong acidity of Nafion in the protonated form and its use as a solid substrate in organic synthesis as a superacid catalyst.^{167–169}

Of particular relevance (and often overlooked in the polymer community) is the work of Zundel et al., who conducted fundamental studies of the relationship between H⁺ conductivity and the IR spectra of aqueous acidic media, including cross-linked sulfonated polystyrene (SPSA) in the acid form versus degree of hydration.^{170,171} There is an IR spectral feature in the form of a continuous superposition of absorbance that begins in the region of O–H stretching for H₂O (~3500 cm⁻¹) and extends to lower wavenumbers, which is referred to as “continuous absorption”. In acids this continuum is caused by the rapid fluctuation of protons (rate ~ 10¹⁴ s⁻¹) due to a combination of their tunneling and barrier hopping in the hydrogen bond of H₅O₂⁺ groupings. Interaction between hydrogen bonds of different groupings via proton dispersion forces causes this continuum of vibrational energy levels owing to a distribution of distances between, and orientations of, hydrogen bonds in the network. The hydrogen bonds in these groupings are very polarizable, being 1–2 orders of

magnitude larger than the usual electronic polarizabilities. Thus, the state of these bonds is very sensitive to their environment, and the presence of ions can induce considerable polarization that suppresses continuous absorption. H₅O₂⁺ groupings are linked via H bridges with other H₂O molecules or with –SO₃⁻ acceptor groups. Protons are transferred over larger distances when these groupings shift within the extended hydration network by thermal rearrangement, and the rate-determining step of H⁺ migration is this structural diffusion.

Eigen addressed this topic in earlier literature¹⁷² although structural diffusion, according to Zundel, is more complex than the simple rotation of H₃O⁺ to affect favorable bond orientation for H⁺ transfer to a neighboring H₂O molecule. The large polarizability of hydrogen bonds in H₅O₂⁺ groupings was said to account for the high H⁺ conductivity of hydrated SPSA membranes as well as other acidic systems.¹⁷³ In the absence of an electric field, **E**, there is a dynamic equilibrium between two proton boundary structures, but when **E** is present, the weight of boundary structure II is increased because the hydrogen bond is easily polarized. Furthermore, the



proton can rapidly transfer within H₃O⁺ to one of the outer H atoms in boundary structure II (H⁺OH₂ → HOHH⁺) and another H⁺ transfer can take place with a third adjacent H₂O molecule and thermal rearrangement causes H₅O₂⁺ groupings to become redefined. This is the essence of so-called “structural diffusion”. Because H⁺ motions are coupled and these groupings exist within a more extended hydration environment, proton conductivity is in fact a cooperative process¹⁷⁴ that is sensitive to structuring influences within the supportive medium. In the case of –SO₃⁻–H⁺OH₂ groupings in SPSA, the time-averaged position of H⁺ is biased toward the water molecule at low degrees of hydration,¹⁷⁵ and if H₂O/SO₃H ≥ 2, excess protons will shift from acid–water H bonds to H bonds between H₂O molecules and the IR continuous absorption and H⁺ conductivity become great.

Ostrowska and Narebska noted an infrared continuous absorption in hydrated acid form Nafion 120 membranes that began at 3400 cm⁻¹ and extended toward low wavenumbers.¹⁷⁶ This feature was not present in dry membranes and, based on the work of Zundel et al., was proposed to be due to the existence of H₅O₂⁺ and H₉O₄⁺ groups, in which there are easily polarizable hydrogen bonds. This paper by Ostrowska and Narebska is also useful, as it contains a number of band assignments for Nafion.

Mauritz and Gray analyzed the IR continuous absorption of hydrated Na⁺OH⁻ and K⁺OH⁻-imbibed Nafion sulfonate membranes for the purpose of correlating this phenomenon to the current efficiency (cation transference number) of chlor-alkali electrochemical cells.¹⁷⁷ In this case, the similar issue of OH⁻ (“defect proton”) conductivity is important. A distinct continuous absorption appeared in the spec-

tra, as seen for membranes equilibrated in different high concentrations of aqueous Na^+OH^- and K^+OH^- . The continuous absorption arises from easily polarized hydrogen bonds in H_3O_2^- groupings and reflects the mobility and concentration of OH^- ions as influenced by the electrostatic fields about K^+ ions. This view was reinforced by the fact that the continuous absorption versus $[\text{OH}^-]$ profile correlated inversely with the experimental current efficiency versus $[\text{OH}^-]$ profile. Also seen in the spectra was a shoulder on the high wavenumber side of the main O–H stretching peak which is the signature of non-hydrogen bonded OH groups.

A more recent view of proton transport is that of Kreuer, who, compared with the Zundel-based view, describes the process on different structural scales within phase separated morphologies. The smallest scale is molecular, which involves intermolecular proton transfer and the breaking and re-forming of hydrogen bonds. When the water content becomes low, the relative population of hydrogen bonds decreases so that proton conductance diminishes in a way that the elementary mechanism becomes that of the diffusion of hydrated protons, the so-called "vehicle mechanism".^{178,179}

The next level is concerned with transport within "channels" as depicted in Figure 11. The condition in these regions is described in terms of charge distributions as deriving from solutions of the Poisson–Boltzmann (P–B) equation. This P–B approach can be questioned for a number of reasons, the first of which is that the equation is rooted in macroscopic-continuum-based electrostatic theory. In spaces that are only somewhat greater than 1 nm in width, there is molecular granularity rather than the required continuum and the dielectric constant is a ubiquitous parameter although approximate treatments can be made. Moreover, the imposition of a simple geometry for the channels for the purpose of solving the P–B equation ignores the complexity of the regions that are, in fact, ill-defined and most likely of complex shapes.

The highest level, at structural scales > 10 nm, is that over which long-range transport takes place and diffusion depends on the degree of connectivity of the water pockets, which involves the concept of percolation. The observed decrease in water permeation with decreasing water volume fraction is more pronounced in sulfonated poly(ether ketone) than in Nafion, owing to differences in the state of percolation.¹⁸⁰ Proton conductivity decreases in the same order, as well.

Another important property of Nafion is that of water diffusion. A number of studies of this property have appeared in the literature, and some notable examples are as follows.

Yeo and Eisenberg investigated the diffusion of water in Nafion by sorption from the contacting liquid into dry samples and measuring weight uptake versus time over the temperature range 0–99 °C.¹⁸¹ The resultant diffusion coefficients (D) increased from about 10^{-6} to 10^{-5} cm^2/s with increasing temperature, and the activation energy was determined to be 4.5 kcal/mol.

Takamatsu et al. studied the diffusion of water into the acid as well as mono-, di-, and trivalent salt forms of 1155 and 1200 EW samples.¹⁸² The gravimetric uptakes of membranes immersed in distilled liquid water versus time were determined. Three approximate diffusion formulas were applied to the data, and all yielded essentially the same result. The $\log D$ versus $1/T$ plots, over the range 20–81 °C, yielded activation energies of 4.9 and 13.0 kcal/mol for the acid and K^+ forms, respectively. Diffusion coefficients of various mineral cations that permeated from aqueous electrolytes were considerably smaller than that of water. Also, $\log D$ was seen to be proportional to the quantity q/a , where q is the charge of the cation and a is the center-to-center distance between the cation and fixed anion in a contact ion pair.

Yeager and Steck derived diffusion coefficients for water in totally hydrated Nafion120 membranes that were exchanged with alkali metal cations, using a radiotracer technique.¹⁸ At 25 °C, D for the Na^+ form was 2.65×10^{-6} cm^2/s and the values for the K^+ and Cs^+ forms were somewhat smaller, which would seem to reflect the lower maximal degree of hydration of these forms.

Yeager et al.,¹⁸³ again based on radiotracer studies of the self-diffusion of different ions ($^{22}\text{Na}^+$, Cs^+ , $^{36}\text{Cl}^-$, $^{35}\text{SO}_4^-$, $^{125}\text{I}^-$) in 1150 and 1200 EW Nafion membranes that were in contact with dilute and concentrated electrolytes, were the first to introduce the concept of mixed interphase regions of intermediate polarity. In dilute solution, room temperature studies,¹⁸⁴ Cs^+ and I^- ions were rationalized as having more tortuous diffusion pathways than Na^+ ions and water molecules. For concentrated solutions at 80 °C, Cl^- and SO_4^{2-} ion diffusion coefficients are smaller than that those for Na^+ ions, and D for Cl^- ions is greater than that for the SO_4^- anions.

In this conceptual (nonmathematical) model there is the view of hydrophobic semicrystalline perfluorocarbon regions and irregular-shaped aggregates of fixed ions. Small cations and water molecules reside mainly in the ion cluster centers and diffuse along different pathways than those for large cations having low hydration energies and anions which were thought to preferentially migrate through an intermediate phase containing a few water molecules and a few side chains. The high diffusion rates and low tortuosity of Na^+ ions and water molecules are explained by the nonspherical shapes of the clusters.

This view stands in contrast to the condition of having well-defined spherical clusters and sharp phase boundaries as depicted in the model of Gierke et al.

Millet determined self-diffusion coefficients for Na^+ and Cs^+ ions in hydrated 1200 EW membranes using conductivity measurements and the Einstein equation, $D_+ = u_+ kT$, where u_+ is the absolute mobility of the given cation.¹⁸⁵ u_+ can be derived from the equivalent conductivity according to $\Lambda = \sigma_+/C_+ = Fu_+$, where σ_+ is the specific conductivity, C_+ is the cation concentration (calculated on the basis of the dry membrane density, EW, and the water content), and F is the Faraday constant. The values of D_+ determined via these conductivity measurements

were compared with those determined by the radio-tracer technique of Yeager et al.^{186–188} to test the validity of the Einstein equation for this system. The water contents of these membranes corresponded to H₂O/SO₃[−] mole ratios in the range 6.6–11.3 for the Cs⁺ form and 11.9–18.4 for the Na⁺ form at 25 and 40 °C. The results showed that the *D*₊ values compared well with those of Yeager et al.

Zawodzinski et al. determined ¹H diffusion coefficients, *D*, in Nafion 117 having water contents over a range corresponding to H₂O/SO₃H = 2–14 mol/mol using pulsed field gradient spin-echo ¹H NMR spectroscopy.¹⁸⁹ This study was conducted within the context of understanding the nature of water as well as water concentration profiles and water management in fuel cell membranes. *D* was extracted from the NMR data using the following equation:

$$\ln \left[\frac{A(g)}{A(0)} \right] = -\gamma^2 D g^2 \delta^2 \left(\Delta - \frac{\delta}{3} \right)$$

A(*g*) is the signal intensity observed with an applied gradient *g*, *A*(0) is the intensity in the absence of an applied gradient, γ is the nuclear gyromagnetic ratio, and δ and Δ are time intervals of the pulsed field gradient spin-echo sequence.

D, measured in this way, ranged from 0.6×10^{-6} to 5.8×10^{-6} cm²/s over this range of water content in increasing order.

While *D* issuing from these experiments is not strictly the diffusion coefficient of water per se, but rather that of ¹H throughout the ensemble of environments in the hydration microstructure, these authors rationalized that it could in fact be identified with *D* at both high and low water contents. It should be appreciated that self-diffusion coefficients measured in this way reflect fundamental hopping events on a molecular scale.

Later, Jones, Inglefield, and co-workers performed fundamental solid-state NMR studies of acid form 1100 EW Nafion. Pulse field gradient NMR experiments interrogated the translational motions of water, ethanol, and fluorocarbon components in their systems.¹⁹⁰ ¹⁹F spin diffusion studies yielded important information on the size of the backbone (CF₂)_{*x*} and perfluoroalkyl ether regions in the hydrated and dry conditions.¹⁹¹ Static (nonspinning) ¹⁹F studies indicated the location of molecular penetrants within the nanophase-separated morphology. The reader is referred to the original paper for the explanations of this method, model assumptions, and so forth. One basic assumption is that the side chains form a distinct domain separate from a distinct domain consisting of the perfluorinated polymer backbone. The interpretation of the results is as follows. The spin diffusion results indicated domains in dry and solvent-swollen samples that are in the nanometer range, and this is commensurate with pendant group aggregation, which is in harmony with the structural view issuing from SAXS experiments on the same material. Although the NMR information does not provide information regarding the shape of the aggregates, interfaces are detected. The signature of an interface is graphical curvature that precedes the linear section of magnetization change versus square

root of time plots for spin diffusion. The spin diffusion results support the idea that the side chain phase is continuous with little tortuosity, which accounts for the rapid long-range transport of water and lower alcohols.

¹²⁹Xe gas, under pressure, was used by Jones, Inglefield, and co-workers as a probe of morphology based on the fact that its spectrum is sensitive to local molecular environment. Domains that are involved in penetrant uptake and diffusion can be inferred. The studies showed two overlapping resonances, one being assigned to an amorphous perfluoroethylene environment and the second to side chain domains. The latter regions are more heterogeneous, owing to the considerable line width.

Morphology based on chemical environment can be probed using ¹⁹F NMR spectroscopy because the chemical shifts of F atoms in the side chains are considerably separated from those in the backbone. Conformational dynamics as affected by domain-selective solvent incorporation are reflected in the widths of static ¹⁹F peaks. These conformational motions, in turn, can influence the migration of solvent penetrants.

Spin diffusion between the backbone and side chain resonances can be used to study domain size. For dry Nafion the side chain domains were found to be of the size 3.8 nm and these domains had a periodicity of around 10 nm. The first number is around that commonly associated with the diameter of a spherical cluster based on microscopic and scattering studies. The 10 nm spacing remains to be assigned to a structural feature. It is noted that the AFM studies of McClean et al.,⁸³ described earlier, identify fluorocarbon crystalline domains of size ~10 nm for the K⁺ form, and whether the coincidence of this number with the periodicity deduced by Meresi et al.¹⁹¹ is significant or fortuitous remains to be shown. Upon addition of 20 wt % water, domain size increases to 6.5 nm, but the periodicity is essentially unchanged. An ethanol uptake of 20 wt % causes a greater morphological rearrangement, giving a domain size of 11 nm and a periodicity of 19 nm. The repeat length is calculated using spin diffusion plots (linear extrapolation to zero magnetization on magnetization vs time plots). Static ¹⁹F line shapes showed that ethanol selectively plasticizes the side chain group domains.

NMR is the most fundamental *molecular-specific* probe of diffusion. Polymer motions and the spectroscopic signature of a given nucleus can be unambiguously related to a particular morphological domain. The size and time scale of the experiments are such that the fundamental hopping events of diffusing molecules can be sampled.

Plots of *D* versus water volume fraction¹⁹⁰ show that the concentration dependence of *D* is in fact described well by the Fujita free volume equation.¹⁹⁰ This was surprising considering that the underpinning of this equation simply involves available free volume for molecular hopping. The interpretation is that water molecules plasticize the perfluoroalkyl ether side chain domains and this increases *D* with increasing water content. *D* for water varied from

10^{-4} to 10^{-7} cm²/s, and these values are similar to those determined by Zawodzinski et al., as discussed above. Moreover, D for water versus temperature followed WLF behavior, which is also linked to free volume theory. D for ethanol was comparable to that for water although the concentration dependence was stronger and the free volume concept was not found to apply. This can be related to the fact that ¹⁹F spin diffusion and line shape analyses indicated larger morphological changes upon addition of ethanol as compared to water and greater plasticization of the side chain domains.

Sodaye et al. attempted to probe the free volume in various monovalent and divalent counterion forms of Nafion 117 that were swollen in water and alcohol using positron annihilation lifetime spectroscopy (PALS).¹⁹² The underlying concept is that free volume on the molecular level can influence polymer chain conformation and chain dynamics, which will affect transport and mechanical properties. While other techniques, such as gas diffusion, can indirectly interrogate materials for free volume, PALS is currently the only direct probe on an atomistic level. The details of this method will be omitted here, and it will simply be mentioned that the spectroscopic data are fitted to a quantum mechanical model that assumes spherical holes, of radius R , that are meant to represent free volume. The assumption of spherical holes is a limitation considering that the free space between polymer chains must not only be of complex geometry but must also be contiguous rather than existing in isolated discrete pockets of a dynamic nature. In short, there was seen to be a very small monotonic increase in R from 3.49 to 3.55 Å in proceeding from the H⁺ to Cs⁺ form. The free volume fraction was determined to be essentially unchanged across the range of alkali cations. The significance of these results can be questioned, given that the range of solvent swelling as well as solvent and ion diffusivity varies significantly over this range. Also, the difference in R between the water- and ethanol-swollen H⁺ forms (3.49 vs 3.67 Å) is somewhat insignificant. Thus, it must be concluded that these PALS experiments have not yielded information that correlates strongly with these critical properties of water-swollen Nafion, and this may be due in part to the overly simplistic model that was applied to the data.

A controversial model for the structure of Nafion is that which proposes a lamellar morphology, due to Litt.⁷⁰ Litt makes a number of arguments to support this model, but the most direct evidence consists of plots of the Bragg spacing, d , associated with clusters, versus water content, as seen in Figure 13. The plot comes from the paper by Gierke et al.,¹⁷ although this d versus water content behavior was also observed by Fujimura et al.³⁷ Litt points out that a lamellar structure would swell in only one dimension, which accounts for the linear d versus water content graphs. Swelling, on the microscopic level, occurs by having water incorporating between the lamellae, thereby pushing them farther apart. The bilayer structure presented by Starkweather⁴¹ is in fact commensurate with the model of Litt.

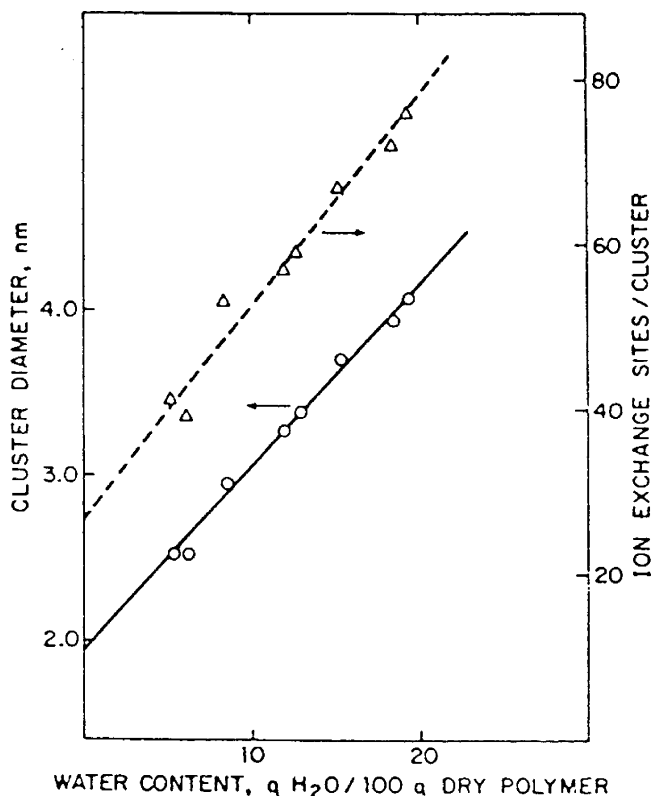


Figure 13. Dependence of cluster diameter and number of SO₃⁻ groups per cluster on water content in 1200 EW Nafion according to Gierke, Munn, and Wilson. (Reprinted with permission from ref 17. Copyright 1981 Wiley.)

Also, in support of the Litt model, Plate and Shibaev observed that hydrated membranes behave in a fashion as brushlike polymers. This suggested to these authors that Nafion has a multilayer structure such that water forms aggregates in lamellar domains,¹⁹³ and this view was said to be supported by the results of the neutron diffraction and Mossbauer spectroscopic experiments of Timashev.¹⁹⁴

This structural view can be compared with that of Gebel et al., who conducted SAXS and SANS studies of water-swollen (around 10–90 polymer volume percent) Nafion 117 in different cation forms.¹⁹⁵ The picture emerging from their studies consists of the aggregation of ionomer chains into elongated bundles which can be in the form of cylinders at high water content (2-D swelling) or ribbons (1-D lamellar swelling). Gebel et al. make the statement that “for high (polymer) volume fraction...the dilution process is similar to those of a lamellar structure...” These bundles have diameters that are ~40 Å, have lengths greater than 1000 Å, and are surrounded by “electrolyte”. This is an extension of the view of elongated aggregates in dilute perfluorosulfonate ionomer solutions. As noted earlier, in the scattering section of this review, Nafion does not form true solutions in the sense of having individual polymer chains freely intermixed with the solvent molecules.

Another spectroscopic method that has been used to study the multiphase structure of Nafion uses photophysical probes. This is well explained in a paper by Kalyanasundaram and Thomas, and references therein.¹⁹⁶ These authors studied the perturbations of the five predominant vibronic band intensi-

ties in fluorescence spectra of pyrene (Py), an aromatic chromophore, in a broad variety of organic solvents whose molecules have different dipole moments, as well as in micelles. The ratio of the intensity of peak 3 to peak 1 (I_3/I_1) decreases with increasing environmental polarity, and this ratio was the highest for perfluorinated saturated hydrocarbons.

Lee and Meisel incorporated Py, at levels of 10^{-3} M or more, into 1200 EW acid form samples that were swollen with water and with *tert*-butyl alcohol.¹⁹⁷ It was concluded based on the I_3/I_1 value for water swollen samples that the Py molecules were located in the water clusters and were most likely near fluorocarbon–water interfaces. It was also concluded, based on both absorption and emission spectra, that the probes had strong interactions with the SO_3^- groups that were exchanged with Ag^+ and Pb^{2+} cations in the case of water containing samples. Likewise, the pyrene molecules were rationalized as being surrounded by *tert*-butanol molecules in that case. However, excimer formation (due to the presence of adjacent pyrene molecules) in the *tert*-butyl alcohol system suggested the loss of cluster morphology.

Szentirmay et al. studied the microchemical environments of Nafion 117 in the acid and Na^+ forms using Py and $\text{Ru}(\text{bpy})_3^{2+}$ probes in fully hydrated ($\sim 40\%$) samples in various cation forms.¹⁹⁸ $\text{Ru}(\text{bpy})_3^{2+}$ emission spectra cannot be interpreted in terms of environmental polarity in as straightforward a fashion as in the case of Py, but blue shifts can reflect this aspect. One of the results of this study was that the microenvironment polarities were such that I_3/I_1 values for Py are between those for fluorocarbon and aqueous environments, and this conclusion was strengthened by the results of $\text{Ru}(\text{bpy})_3^{2+}$ probe studies, as well as the similar conclusion of Lee and Meisel. Another conclusion that was reached was that the SO_3^- clusters are chemically heterogeneous, an idea that was in line with the view of Yeager and Steck, who spoke of mixed interfacial regions.¹⁸

Robertson and Yeager used Py and $\text{Ru}(\text{bpy})_3$ probes for the purpose of locating the locations of Cs^+ and I^- ions in the nanophase-separated morphology.¹⁹⁹ It is known that these probes take residence in the intermediate polarity hydrophobic–hydrophilic interfacial regions. The studies concluded that Cs^+ ions were located in the aqueous regions, but I^- ions were in the interfacial regions.

It is perhaps a shortcoming of mobile probes that one must deduce where it is located based, for example, on the measured value of I_3/I_1 in the case of Py, and this presupposes that the basic features of the morphology are already known. One could not assign the probe location as being cluster domains if such domains had not been known to exist beforehand. Furthermore, the issue of whether large probe molecules perturb their molecular surroundings is the subject of debate. It would seem that the greatest benefit derives from establishing a semiquantitative degree of polarity of the phase in which the average Py molecule resides.

It is important to know whether complete ion exchange has been affected in a given sample, that

is, whether all of the sulfonic acid groups have been neutralized by the chosen cations of charge $+z$ e, as ion content can affect swelling, mechanical, and other properties. Young et al. determined the extent of ion exchange in Nafion 117 membranes in the K^+ , Cs^+ , Mg^{2+} , Ca^{2+} , Co^{2+} , Zn^{2+} , Cu^{2+} , Al^{3+} , and Fe^{3+} forms using cold-neutron-capture prompt γ neutron activation analysis (PGAA).²⁰⁰ PGAA is particularly suited for evaluation of chemical composition, being sensitive to trace ions and hydrogen, and is a nondestructive technique. In short, the nuclei of many elements in a sample placed in a neutron beam absorb neutrons and become an isotope of higher mass number in an excited state. Then, prompt γ rays are emitted by de-excitation of the compound nuclei and measured via a high resolution γ ray detector and the data appear as peaks on counts versus energy spectra, each element having a characteristic peak.

Four forms of membrane pretreatments were used, and the reader is referred to this report for the details of each. The as-received sample was seen to have K^+ contaminant, perhaps being a residue from conversion from the SO_2F form using KOH, but the samples that were pretreated using mineral acids were completely converted to the SO_3H form and the K^+ contaminant was removed in the process. The resultant acid forms were soaked in dilute (0.01 M) and concentrated (2 M) metal chloride salt solutions, and excess electrolyte was leached out of the latter by refluxing in DI/DS water. The peak intensity for a given atom was normalized to the peak intensity of sulfur, so that the average counterion/ SO_3 (mole/mole) ratio could be ascertained. In short, 94–100% of the SO_3H groups can be exchanged and conversions are slightly lower for the monovalent cations. This might be due to the lower hydration numbers, especially for the Cs^+ cation, and no data were reported for Li^+ and Na^+ ions that have greater hydration numbers. Also, it was shown that the excess chloride salts are in fact leached out of the membrane by refluxing with DI/DS water.

Other experiments were performed to affect partial ion exchange by soaking membranes in 0.01 M electrolytes in which the mole ratio of cation-to-sulfonate group was 1:2, 1:1, and 2:1. It was found that an external electrolyte concentration of 0.01 M was not high enough to totally convert all of the sulfonated groups to the desired cation form. An excess of 2:1 was found to be necessary for this purpose.

Increasing z increased the degree of exchange, as more than one sulfonate group can interact with a single cation.

These experiments are of significant value, as many studies have been reported in which complete ion exchange was assumed to take place but not verified.

As mentioned, this review is focused primarily on a survey of the vast literature dealing with the structure and properties of Nafion in the sulfonic acid and cation exchanged sulfonate forms. The literature on the carboxylate version is sparse and currently of lesser interest, as its application seems to be limited to membranes in chlor-alkali cells, and since it is a

less-strong acid than SO_3H , is not of interest in the arena of fuel cell membranes. It should be mentioned, however, that the carboxylate form is considerably more acidic than analogous hydrocarbon ion exchange resins. In this regard, the work of Yeager et al. in comparing cation and water self-diffusion coefficients, found by a radiotracer method, for the sulfonated and carboxylate forms of 1200 EW, is of importance.¹²⁴ In short, it was found that when the membranes are in contact with 0.10 M aqueous solutions of sodium and cesium chloride containing the ^{22}Na and ^{137}Cs isotopes in each respective case, cation diffusion proceeds faster in the carboxylate form, although this form has the lower water uptake. Yeager et al. also investigated and compared the sorption and transport properties of these two forms in concentrated aqueous NaCl and NaOH solution environments, and the differences were rationalized in terms of ion pairing.²⁰¹ The apparent $\text{p}K_{\text{a}}$ of the carboxylate form was determined to be 1.9, which is rather low and due to the electron withdrawing effect of fluorine atom substitution. Consequently, the carboxylic acid form can be totally neutralized in alkali electrolyte solutions.

The in-depth FTIR investigations, of Perusich, of the methyl ester ($-\text{CO}_2\text{CH}_3$), carboxylic acid, and potassium carboxylate forms should also be mentioned.²⁰² In addition to constructing a useful extensive tabulation of band assignments for these as well as the sulfonate materials, Perusich established quantitative expressions that allow for the computation of equivalent weight and acid content using the 555 cm^{-1} C–F and 982 cm^{-1} C–O–C ether bands, based on thin film absorbance measurements. This information is very useful for the accurate, reproducible, and rapid compositional measurements of this polymer. Also, the time evolution of bands during the conversion from the methyl ester to acid forms was reported.

5. Mechanical Properties

The mechanical properties of Nafion materials have not been of the most critical importance, as in the case of commercial thermoplastics or composite materials that are expected to be load-bearing. Rather, the primary focus has been on transport properties. To be sure, the mechanical integrity of membranes as mounted in cells, and under the perturbation of pressure gradients, swelling-dehydration cycles, mechanical creep, extreme temperatures, and the onset of brittleness and tear resistance, is important and must be taken into consideration.

The E. I. DuPont Co. presented empirical equations for the tensile strength, elongation at yield, and tensile modulus as a function of cation type, water content, and equivalent weight in the range $1000 \leq \text{EW} \leq 1400$ and at temperatures in the range $0 \leq T \leq 85\text{ }^\circ\text{C}$.²⁰³ These equations were shown in early product literature, as well.

Aside from this, the literature on the subject has largely been concerned with dynamic mechanical properties where experiments have been performed to gather data consisting of loss tangent ($\tan \delta$) and storage tensile modulus (E'). Rather than being

related to mechanical properties under considerable deformations within an application context, this information was used to identify thermomechanical transitions that were assigned to morphological features in the microphase separated morphology. The following is a historical presentation of these investigations.

In an early study, Yeo and Eisenberg noted a transition, labeled α , for the acid form ($\text{EW} = 1365\text{ g mol}^{-1}$) at around $110\text{ }^\circ\text{C}$ ($\tan \delta$ maximum).²⁰⁴ This relaxation was initially considered as the glass transition of the nonionic phase because, in these limited studies, water was seen to have only a minor effect on the magnitude or position of this peak. A β peak for the same dry acid form was seen at around $20\text{ }^\circ\text{C}$, which shifted to lower temperature with increasing water content, and this was discussed in terms of a glass transition of the polar regions. A γ peak at around $-100\text{ }^\circ\text{C}$ was mentioned as being of the same origin as in PTFE, that is, due to short-range molecular motions in the tetrafluoroethylene phase.

Later, Kyu and Eisenberg discussed dynamic mechanical relaxations for the same acid form of Nafion and re-examined their earlier interpretations.²⁰⁵ The γ relaxation retained its original interpretation. However, the α peak, having the greatest intensity, was reassigned as the glass transition of the polar regions because it had by then come to be seen as sensitive to ion type, degree of neutralization, and water content. The β peak was reassigned as the glass transition of the Nafion matrix.

Tant et al. reported a dynamic mechanical transition of around $100\text{ }^\circ\text{C}$ (maximum in G'') for acid form Nafion having 1140 EW.²⁰⁶ Since this transition also appeared for the sulfonyl fluoride precursor, but at a much lower temperature ($\sim 0\text{ }^\circ\text{C}$), they concluded that it involved main chain motions that are restricted by the conversion to the acid form. These motions were further restricted by the conversion to the Na^+ sulfonate form owing to strong ionic associations between the side chains. In contrast with the work of Kyu and Eisenberg, no transition appeared at $0\text{ }^\circ\text{C}$ in addition to that at $100\text{ }^\circ\text{C}$. While the equivalent weights of the samples utilized by Eisenberg and Kyu and Tant et al. were not quite the same, the notable difference in matrix T_{g} assignment is cause for confusion.

Miura and Yoshida²⁰⁷ noted a dynamic mechanical $\tan \delta$ peak at $120\text{ }^\circ\text{C}$ at 1 Hz, labeled α , for “dry” 1100 EW acid form Nafion. These investigators assigned this transition to motions within the polar clusters because it was sensitive to cation type.

Cable and Moore performed DMA (dynamic mechanical analysis) studies of various Nafion membranes including the acid form.²⁰⁸ A $\tan \delta$ peak with maximum at $110\text{ }^\circ\text{C}$, referred to as “ T_{g} ”, was seen, and there is a suggestion of a shoulder on the low temperature side that might arise from another mechanism. As this membrane was dried at only $60\text{ }^\circ\text{C}$, the possibility of residual water incorporation exists. Moore and Cable concluded that the α relaxation was due to chain motions within and/or near the ion-rich domains and that the β relaxation was

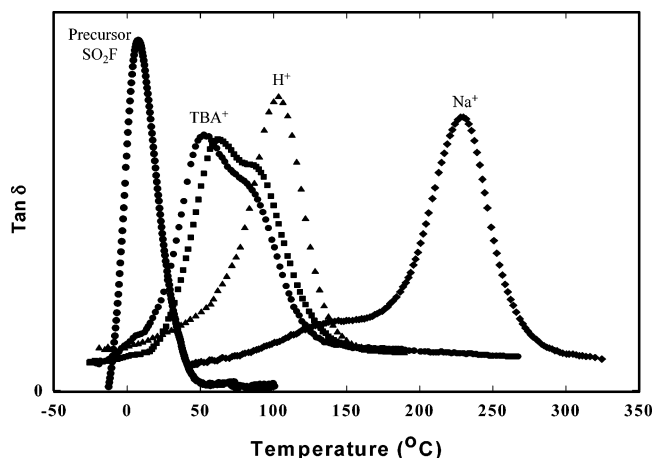


Figure 14. Dynamic mechanical data plotted as $\tan \delta$ versus temperature for Nafion in various forms.

due to chain motions of amorphous fluorocarbon units well removed from the ionic aggregates, that is, the matrix.¹³⁵ These investigators referred to chain motions within an electrostatic network rather than viewing the polar and fluorocarbon components as being isolated, discrete domains. This is in harmony with the view of Kyu and Eisenberg, who stated that "...whatever happens in one of the phases would be expected to have a strong effect on the other phase because of the intimate contact between the phases coupled with their small size." Mauritz and Young adopted this view in their DMA studies of Nafion/[organically modified silicate] nanocomposites.²⁰⁹

The effect of counterion type and size on the dynamic mechanical properties of Nafion has been studied recently by Moore and co-workers^{135,208} using a variety of organic, alkylammonium ions in comparison to the more conventional alkali metal ions. Figure 14 compares the $\tan \delta$ versus temperature plots of the Nafion precursor (i.e., the nonionic, sulfonyl fluoride form) to those of the ionomer in the H^+ , Na^+ , and tetrabutylammonium ion (TBA^+) forms. In the absence of electrostatic interactions, the sulfonyl fluoride precursor displays a single α relaxation near 0 °C. As a result of this low temperature relaxation, the precursor may be easily melt-processed into thin films for later membrane applications. However, once the polymer is converted to the sodium sulfonate form (by hydrolysis and subsequent neutralization), the ionomer yields a profound shift in the α relaxation to a temperature near 250 °C. Note that this form of the ionomer is no longer melt-processible due to strong Coulombic interactions that yield a dynamic electrostatic network (i.e., a physically cross-linked system) that persists to temperatures well above the melting point of the PTFE-like crystallites. In addition to the dominant α relaxation, a weak shoulder near 150 °C is observed and assigned to the β relaxation, in agreement with the work of Eisenberg.²¹⁰ For Nafion in the acid form, the α and β relaxations are observed at temperatures ~ 100 °C lower than that for the sodium sulfonate form of the ionomer. This shift to lower temperatures has been attributed to a reduction in the strength of the interactions between the SO_3H groups (i.e., comparably weak hydrogen bond interactions) relative to

the strong dipole–dipole interactions between the SO_3^-Na^+ groups.²⁰⁸

To further investigate the molecular origins of the α and β relaxations in Nafion, Moore and co-workers utilized a series of alkylammonium ions to systematically alter the dynamic mechanical response of the ionomer with respect to the strength of electrostatic interactions. When Nafion is neutralized to contain large tetrabutylammonium ions, the α and β relaxations are observed to shift to temperatures even below that of the acid form of the ionomer, as shown in Figure 14. Moreover, the magnitude of the β relaxation is seen to increase significantly to a level comparable to that of the α relaxation. This behavior was attributed to a weakening of the electrostatic interactions and a plasticization effect of the large organic counterions.²¹¹ Using a series of alkylammonium ions, from tetramethylammonium (TMA^+) to tetradecylammonium (TDecA^+), the α and β relaxations were found to shift monotonically over a range of temperatures from near that observed for the sodium form of the ionomer (i.e., with the small TMA^+ form) to near that of the α relaxation of the sulfonyl fluoride precursor (i.e., for the large TDecA^+ form). In addition, the magnitude of the β relaxation was observed to increase with counterion size to a point where it becomes the dominant relaxation for counterions larger than tetrahexylammonium. Based on these results and recent correlations of this DMA data with studies of molecular dynamics and morphological relaxations observed using variable temperature SS NMR and SAXS experiments,^{212, 213} the α relaxation is attributed to the onset of long-range mobility of both the main and side chains as a result of a destabilization of the electrostatic network (i.e., through the activation of a *dynamic* network involving significant ion-hopping processes). In contrast, the β relaxation is associated with the onset of segmental motions of chains within the framework of a *static* network of physically cross-linked chains.²¹⁴

6. Molecular Simulation of Structure and Properties

Mauritz summarized a number of molecular models of ionomer structure, including those pertaining to Nafion, that had had been formulated up to 1996.²¹⁵ Within the context of the title of this review, it should be appreciated that the results contribute to the "state of understanding" only if they are verifiable by careful experimentation. To be sure, theoretical predictions are welcome in the design of experiments and pointing the way toward useful applications.

The cluster-network model of Gierke et al. has already been discussed in the Introduction as being the first realistic model for rationalizing a number of properties of Nafion membranes.

Hsu, Barkley, and Meakin addressed the percolation aspect of hydrated clusters in relation to insulator-to-conductor transitions.²¹⁶ As the concentration of clusters on a hypothetical grid, that is, a three-dimensional lattice, increases, "islands" of clusters will grow in size and become interconnected. Eventu-

ally, a threshold volume fraction, C_0 , is reached where the pathways span the macroscopic dimensions of the grid—the percolation channels—and long-ranged ionic conduction is possible. The conductivity, σ , near and above C_0 obeys the following power law.

$$\sigma = \sigma_0(C - C_0)^n$$

This is a general equation that can be applied to any material that can support charge percolation. C_0 not only depends on dimensionality but also the manner in which the two components (one insulating, the other conducting) are dispersed, and the factor $(C - C_0)^n$ involves topological connectivity. The prefactor σ_0 depends on the particular conduction mechanism that operates within and between two adjacent clusters and involves interactions among ions, water molecules, and the ionomer. It is the one factor that involves the chemical identity of the system. This equation was tested by experimental measurements of σ for membranes of different equivalent weights and containing various uptakes of aqueous sodium hydroxide.

In short, C_0 was found to be 0.10, which is less than the value for a completely random system—which implies that the clusters were not randomly dispersed. A log–log plot of σ versus $C - C_0$ was found to be linear where n , the slope of the line, was 1.5, which in fact is in the established theoretical range of 1.3–1.7.

Of course, this equation and its theoretical underpinnings does not constitute a model as such and certainly does not address the structural specifics of Nafion, so that it is of no predictive value, as experimental data must be collected beforehand. On the other hand, the results of this study clearly elucidate the percolative nature of the ensemble of contiguous ion-conductive clusters. Since the time of this study, the notion of extended water structures or aggregated clusters has been reinforced to a degree by the morphological studies mentioned above.

In a related experimental study, Cirkel and Okada compared mechanical and electrical percolation that developed during the gelation of 3:1 (v/v) 2-propanol/water “solutions” of Nafion 117 in the acid and Na^+ forms.²¹⁷ Attention should be paid to the particular manner in which these samples were prepared, as different conditions may yield different results. Also, caution should be applied in comparing these results with those of percolation studies using preformed films, such as that of Hsu et al.²¹⁶

In relatively dilute solutions, Nafion is said to exist in the form of rodlike aggregates of practically the same size^{49,51} that are in equilibrium with loose ionomers⁷³ such that at higher concentrations the aggregates dominate.²¹⁸ The reader should consult the more recent papers of Gebel et al., cited earlier, for a more detailed view of Nafion “solutions”.

The relative viscosity η_r and storage modulus G' were determined by Cirkel and Okada in experiments using a rheometer in oscillatory rotational mode and Couette sample geometry as a function of Nafion volume fraction, φ , and angular frequency, ω , for the acid and sodium forms at 25 °C. Parallel experiments

were performed with an electrical impedance analyzer that measured conductivity, σ , vs ω for different φ values for an applied sinusoidal field.

The rheological properties change behavior, relative to more dilute solutions, above $\varphi = 0.2$, where non-Newtonian behavior is then exhibited. The power law dependence of η on φ is in harmony with the Zimm rather than the Rouse model, which suggests that hydrodynamic interactions between these polymers, in a mean field sense, are important. Electrical properties also begin to deviate for Nafion solutions above $\varphi = 0.2$, and mechanical percolation is essentially the same for the sodium and acid forms.

An interesting conclusion is that, as opposed to the Na^+ form, there is no electrical percolation threshold for the proton form, although conductive clusters must grow with increasing polymer volume fraction in both cases. In short, no clusters that span macroscopic dimensions form at a critical volume threshold for the acid form. These results are interpreted in two sketches, each having connected polymer strands above the percolation threshold so that there is mechanical percolation in either case. In one picture (Na^+ form), the sulfonate groups are evenly spaced so that electrical percolation exists, but for the acid form, these groups are more closely spaced in aggregates so as to cause voids along electrical pathways. It would need to be explained how, upon drying, the acid form gel evolves to form highly proton conducting membranes.

The concepts and techniques discussed by Cirkel and Okada are relevant with a view toward modifying the structure of solution cast Nafion membranes by manipulating counterion type, solvent, temperature, and other variables.

Hsu and Berzins used effective medium theories to model transport and elastic properties of these ionomers, with a view toward their composite nature, and compared this approach to that of percolation theory.²¹⁹

Hsu and Gierke presented an elastic theory for the clustering of ions in hydrated Nafion.³¹ This model presumes the existence of clusters and is unconcerned with the process of how clusters are actually created. Rather, it was intended to determine the equilibrium diameters of hydrated clusters given this assumed morphology. The equilibrium hydrated cluster diameter results from a minimization of a free energy composed of an elastic term and the non-specific interactions: $\text{SO}_3^- - \text{CF}_2$, $\text{SO}_3^- - \text{SO}_3^-$, $\text{H}_2\text{O} - \text{H}_2\text{O}$, H_2O at cluster surfaces, H_2O in the second layer from the cluster/hydrophobic surfaces, and H_2O in the bulk state. A severe limitation of this model is that it is semiphenomenological and therefore of little predictive value. This is so because prior knowledge of the dependence of the tensile modulus upon counterion type, water content, EW, and the diameter of an average dry cluster determined from SAXS studies, as well as the details of the experimental water vapor pressure sorption isotherm, is required in the calculations.

Mauritz and Rogers constructed a water vapor sorption isotherm model for ionomers with inherently clustered morphologies, as applied to Nafion mono-

valent cation–sulfonate forms.²²⁰ While it requires that all water molecules and fixed ions reside in clusters—a limitation—the theory provides for the variance of the average number of fixed ions in a cluster versus water content. The predicted quantities are the average number of sorbed water molecules per ionized side chain, n , the cluster radius extension ratio, λ , and the volume fraction of the cluster phase when the ionomer is equilibrated in either pure water or water vapor of relative humidity x . The driving force for cluster expansion is the osmotic pressure posed by visualized “ionic micro-solutions” within clusters, Π . Π was derived from a molecular theory of membrane–internal water activity that reflects (1) the hydration numbers of the ion exchange group and counterion, (2) the relative free versus bound water population, and (3) the sulfonate–counterion association–dissociation equilibrium, which depends on water content. Factor 3 was accounted for using a two or four state statistical mechanical model, involving hydration and ion pair energies, that was based on the earlier FTIR and solid-state NMR studies of Mauritz et al., of these materials.^{105,107} Π is resisted by a polymer contractile pressure, P , that is a function of a modulus, E , and λ , and equilibrium is considered as a condition where $\Pi = P$. A constitutive equation for λ versus n was assumed that allows for the evolution of a smaller number of larger clusters, as earlier described by Gierke et al.¹⁷

One of the limitations of this model is that the confinement of water molecules within clusters precludes its use within the context of water transport simulation because cluster-connective hydration structure is absent. Furthermore, water activity and contractile modulus are macroscopic based concepts whose application at the nanoscopic level is dubious. P is represented by a function borrowed from macroscopic elastic theory that contains E , and there is no microstructure-specific model for the resistance to deformation that can be applied to Nafion so that one is forced to use experimental tensile moduli by default.

Verbrugge and Hill presented a “macrohomogeneous” model for the transport of ions and solvent through ion exchange membranes using the Nernst–Planck equation.²²¹ No molecular mechanisms were factored into this model. These investigators did not feel that nanoscopic cavities that were connected by smaller charged pores existed, owing to the high radiotracer-based diffusion coefficients measured for bisulfate ions in Nafion 117 membranes, but they preferred a tortuous hydrophilic network phase of pores having diameters ~ 6 nm.²²² Pintauro and Verbrugge reported a model that calculated partition coefficients for a pore containing an electrolyte on the basis of adsorption onto the surfaces of pores that contain the fixed charge species.²²³ Bontha and Pintauro then applied this model to Nafion 117 membranes by treating them as arrays of parallel cylindrical pores.²²⁴ The Nafion model calculations accounted for electrostatic interactions between the pore surfaces and counterions, coions, and solvent molecules, as well as counterion/coion solvation free

energies. In this sense, the model was molecular-specific, but the use of the Poisson–Boltzmann equation to calculate the electrostatic potential in a pore can be questioned because this equation is based on the theory of macroscopic electrostatics but the pores are on the dimensional scale of atomic “granularity”. This model also has the feature of computing the dielectric constant as a function of radial distance in the cylindrical pore. The result indicated that water molecules are basically frozen in place near the pore wall due to the alignment of dipoles by the electric field, while near the cylindrical pore axis the water molecules exist in a state similar to bulk water. The reader is encouraged to compare these results with the results of Paul and Paddison, referred to later in this review, who also calculated pore permittivity versus radial distance in cylindrical pores using a more rigorous atomistic model. Despite the differences in the two approaches, the essential results are the same.

Eikerling et al. presented a random network and effective medium theory-based model of charge transport in “porous polymers”.²²⁵ The model adopts the view of clusters as being inverted micelles with connecting channels, much as in the Gierke model. There are three elementary types of bonds that are meant to represent conductances between bulklike water filled “blue (b) pores” and dry “red (r) pores”. The terminology is somewhat confusing, as a “pore” is meant to be a cluster and clusters are connected by “channels”. The pores have no chemical identity or structure other than having—or not having—excess water in the amount w . Both pore types contain water that is tightly bound by solvation of SO_3^- groups at the “inner pore surfaces”, and it is the excess water that can percolate when w is sufficiently high. There are “bonds” of random probabilities that connect the pores, and they are represented by elements consisting of three electrical resistors in series (i.e., pore–bond–pore), and the three conductivities add in the usual reciprocal fashion. These elements are linked to form an equivalent electrical circuit over the entire statistical ensemble. Kirchoff equations of simple electrical theory for this random network are solved in an approximate fashion by considering a single bond as being embedded in an effective medium of surrounding bonds. This is a site percolation problem in which the variable is x , the fraction of blue pores, and, as such, addresses the connectivity of the pore-channel network. The probabilities of b–b, r–r, and b–r bonds are given by x^2 , $(1 - x)^2$, and $2x(1 - x)$, respectively.

This model, when applied to Nafion as a function of water content, indicated a so-called quasi-percolation effect, which was “verified” by electrical impedance measurements. “Quasi-percolation” refers to the fact that the percolation threshold calculated using the single bond effective medium approximation (namely, $x_c = 0.58$, or 58% blue pore content) is quite larger than that issuing from a more accurate computer simulation. This number does not compare well with the threshold volume fraction calculated by Barkely and Meakin using their percolation approach, namely 0.10, which is less than the value for

a completely random system, which implies that the clusters are not randomly dispersed.²¹⁶

It should also be mentioned that capacitors were then added in parallel with the resistors in equivalent circuit elements because the frequency-dependent experimental electrical impedance data had a component that was 90° out of phase with the resistor.

The many details of this theory are omitted here. Nothing dealing with chemical groups and the forces that drive the morphology of ionomers is factored into this model, which limits its use in predicting fuel cell membrane performance. Moreover, it seems impossible to relate the quasi-percolation threshold to the real structure. Nonetheless, the view of conductance from the perspective of percolation is very appropriate.

Paddison and Zawodzinski performed fundamental calculations aimed at ascertaining side chain conformation.²²⁶ This fragment of the secondary structure is related to tertiary structure, that is, morphology, as it would determine, in large degree, how the side chains pack in micellar structures 40–50 Å in size. Packing, in turn, is related to hydration microstructure and the transport of ions and protons throughout these ionomers assuming that realistic hydration energetics are included in the calculations. These studies were conducted within the context of proton conducting membranes. The authors mentioned a particular need to establish a molecular basis for understanding electro-osmotic drag, that is, water transport as coupled with proton transport.

Self-consistent field, *ab initio* molecular orbital computations were performed on small molecules, namely $F_3C-O-CF_3$, to simulate the ether groups, and CF_3SO_3H , to simulate the ion exchange group at the end of the side chain. The energetics of a single H_2O molecule in the vicinity of these model compounds was determined to establish the water affinity of the ether and sulfonate groups. This water content is not high enough so as to cause swelling, and the single molecule is intended to be but a probe of its environment.

The calculations determined that the ether group was stiff and hydrophobic, but the SO_3^- group was strongly hydrophilic and flexible. However, the conclusion of ether group hydrophobicity may not be in harmony with the FTIR spectroscopic evidence of Lowry and Mauritz¹⁰⁵ as well as that of Moore et al.¹¹⁷ It was earlier mentioned that the band characteristic of this group has two components, at 965 and 980 cm^{-1} , for each of the two C–O–C groups in the side chain. By comparison, there is only one band in this region for the Dow short-side-chain membrane that only has one ether group. The band for the ether group closest to the sulfonate groups (965 cm^{-1}) shifts with water content, indicating either hydrogen bonding interactions with water molecules, through-bond inductive effects caused by proton dissociation in the SO_3H groups, or a combination of both. The ether group closest to the backbone, however, would seem to be shielded from water molecules. This result is also commensurate with the suggestion of Falk et al., based on their FTIR studies, referred to earlier, in

that the hydrophilic–hydrophobic interface is not sharp.

Using a molecular dynamics simulation (MM2) with no water molecules present, the side chain was predicted to be in a folded conformation at a temperature of 300 K. The C–O–C group was stiff, but the SO_3^- group, flexible. The folded conformation may simply be due to the artificial condition that the long side chain was isolated and not interacting with other side chains, and a curling of the unsolvated side chain having two ether oxygens would seem to be commensurate with minimizing interatomic energies. Discrete H_2O molecules should be packed around the side chains, rather than utilizing a dielectric continuum model of a solution environment to render the calculations realistic for a swollen state. A more realistic simulation would also involve more than one side chain.

Paddison, in later work, added more water molecules (up to 6) to the minimum energy side chain structure.²²⁷ Information relating to acid dissociation and local proton dynamics was obtained. One result of the calculations is that after the first hydration shell around the sulfonic acid group is complete, there is more effective shielding of the proton from the anion by the water molecules. Paddison stressed that this model, in which water molecules are clustered around a single sulfonate group, must be extended to include neighboring sulfonate groups so that proton transfer between them can be properly modeled.

Information extracted from the calculations for single acid molecule clusters was used, along with experimental information derived from SAXS measurements,^{17,228,229} in a water and proton transport model using a nonequilibrium statistical mechanical framework.^{230–232} Diffusion coefficients were calculated for Nafion 117 in cases where the number of water molecules per sulfonate group was 6, 13, and 22.5. More specifically, this model computes a “corrected” friction coefficient for the transport of H_3^+O in a hydrated pore/channel of cylindrical geometry. The diffusion coefficient is derived using the friction coefficient in the Einstein equation. Not accounted for, as mentioned by Paddison et al., is the contribution to mobility by proton hopping between water molecules, that is, the Grotthuss mechanism. The dielectric constant of water was assumed to be that of the bulk state, although Paul and Paddison presented a statistical mechanical model that determines the permittivity of water in hydrated polymer electrolyte membrane pores of cylindrical shape.²³³ Other assumptions of geometry and theoretical-computational details are beyond the scope of this review, and the reader is directed to the cited papers. The results of these computations were in agreement with diffusion coefficients obtained from pulsed field gradient NMR diffusion measurements.

Later, Paul and Paddison presented a statistical mechanical model that was used to calculate the dielectric permittivity in the water domains, that is, the pores, of Nafion.²³⁴ For computational purposes, a pore was taken as being of cylindrical geometry. The main prediction is that in a fully hydrated

membrane there is a central region within the pores where the water is similar to that in the bulk (i.e., has a dielectric constant ~ 80), but as one proceeds toward the pore walls, the water is increasingly more bound. This is essentially the same result predicted by Bontha and Pintauro using a different, less fundamental, modeling approach, as described earlier in this review.²²⁴

Niemark et al. investigated solvation and transport in Na^+ form Nafion using molecular simulations.^{235,236} Molecular mechanics energy optimizations of oligomers of 10 monomer units in a vacuum, as well as smaller oligomers that were solvated by water, methanol, and a water–methanol mixture, were performed using a potential force field based on electron density calculations, simulations of vapor–liquid equilibrium of lower perfluoroalkanes and ethers, and the thermodynamic properties of aqueous sodium sulfate solutions. The vacuum calculations yielded two conformations of the fluorocarbon skeleton, depending on the initial conformation in which the chain was placed before the simulation: either stretched for the initial all-trans conformation or highly folded and spiral-like for a randomly bent chain. When solvated, the oligomers, of smaller length, were more folded in water as compared to methanol and the side chain was stiff. H_2O and MeOH molecules formed hydrogen bonds with the oxygen atoms in the fixed SO_3^- anions, and these bonds have a lifetime considerably longer than the time scales required for rotational motions in the bulk. Water molecules could weakly hydrogen bond to the ether oxygen closest to the ion exchange group. For hydrated membranes having K^+ counterions, water did not form a continuous subphase, but isolated domains having less than 100 water molecules were predicted. It might be argued that a larger, more realistic ensemble of molecules and polymer molecular fragments would be required in a simulation to render this result credible, which is mentioned by Niemark. The statement is also made that it is not necessary to have a continuous hydrophilic phase in order to calculate water diffusion coefficients comparable to experimental values.

Khalatur et al. performed more aggressive molecular simulations of the structure of hydrated Nafion using integral equation theory.²³⁷ The details of the underlying theory, approximations, nature of force fields, computational algorithms, and so forth, are beyond the scope of this review and so will be omitted here. Semiempirical molecular orbital self-consistent field–rotational isomeric state calculations were performed in order to determine the equilibrium, energy-minimized conformations of fragments of the chain as well as “complexes” having a single water molecule probe. The polymer PRISM integral equation theory was used to calculate density–density intermolecular pair-correlation functions that reflect averaged particle density as a function of distance from any particle and determine the relation between the chemical structures of macromolecules and pair potentials and intermolecular correlation. While being essentially “atomistic”, the modeled structures had a measure of coarse-graining in that small

chemical groups were lumped together into effective spherical interactive force centers.

The calculations depicted a minimum energy conformation of an isolated side chain that is only slightly twisted, which was rationalized as being favorable with regard to the ability of water molecules to access the SO_3H groups. This structure was noted as being similar to the curled-up conformation determined by Paddison and Zawodzinski.²²⁶ Khalatur et al. also note that their energy-minimized side chain structure is rather different from that suggested by Litt in his lamellar model.⁷⁰

Another result is that water molecules preferentially reside at the terminus of the side chain (i.e., at the sulfonate group), which is not surprising, but also that the ether groups in the side chains are hydrophobic, which may be questioned by some investigators, as earlier noted in this review.

The addition of a small amount of water intensifies the drive for SO_3H group aggregation. Water, as predicted, is in a well-ordered state on local and mesoscopic scales, as evidenced by the NMR data of McMillan et al.,²³⁸ and is thought to exist in cagelike structures similar to clathrates. The water content in these calculations is above and below that corresponding to 4 H_2O molecules per SO_3H group, although it is unclear as to whether enough water molecules are present to allow for liquidlike water. Nor is it clear as to how many polymer chains are used in the calculations. In any case, the results reinforce the view of irregularly shaped cluster surfaces, or “fuzzy spheres” having a high surface area/volume aspect. This view is basically that of Falk¹¹³ and later Kreuer.⁹¹ These irregular or rough surfaces are amenable to the formation of water channels along which charge transport can take place.

None of the models address the question of how the main chains are packed, and details of crystallinity are neither factored into nor predicted by mathematical models of the structure and properties of Nafion. Chains packed in crystalline arrays are usually considered to be rigid within the context of certain properties; for example, with regard to diffusion, crystallites are viewed as impenetrable obstacles. ^{19}F NMR studies indicate otherwise. Molecular motions that do not significantly alter symmetry can in fact occur in polymer crystals. It would seem, for example, that the response of the Nafion structure to applied stress would depend on the flexibility of the polymer backbone, a certain fraction of which is incorporated in crystalline regions. On the other hand, Starkweather showed that the crystallinity and swelling of Nafion are not correlated.

At first thought, it might be considered that the steric restrictions posed by the large fluorine atoms would cause conformational rigidity due to restricted bond rotations. Hsu, however, showed that the conformations of the TFE chains in the crystalline regions in Nafion are in fact dynamic in that they can undergo helix reversals; that is, the handedness of the helix is easily reversed.²³⁹ These helix reversals are also seen in PTFE.²⁴⁰ This disorder phenomenon causes considerable conformational entropy and is

involved in the overall thermodynamics of the system. The principal IR spectroscopic signature of a helix reversal in PTFE is a very temperature-sensitive peak doublet in the range 600–700 cm^{-1} .²⁴¹ Temperature-dependent IR studies, conducted in the range –30 to 110 °C, showed an activation energy of only 1 $\text{kcal}\cdot\text{mol}^{-1}$. The overall conclusion is that fluoropolymer chains are rather flexible in the sense of torsion.

Jang et al. conducted full atomistic molecular dynamics simulations on two fictitious Nafion-like extreme chemical microstructures. One structure was an 80 unit chain consisting of a single block of 10 consecutive perfluorosulfonic vinyl ether (PSVE) units that were placed at the end of a single block of 70 TFE units. The other structure, referred to as “dispersed”, was also a chain of 80 monomer units in which single PSVE units were placed between blocks of 7 TFE units.²⁴² The total systems in either case consisted of four chains, and there were 15 water molecules per sulfonic acid group so that the total number of atoms in the simulations was 4568. The fundamental inter- and intramolecular interactions consisted of van der Waals, electrostatic, bond stretching, bond angle bending, and torsional bond rotation energetics.

These structures are fictional in the sense that these sequences do not correspond to the actual statistical polymerization based on the comonomer reactivity ratio, although it was said that the results have significance with respect to Nafion structural optimization and guidance in the search for Nafion replacements. Also, the non-insignificant degree of crystallinity of Nafion was not accounted for in the model.

The reader is referred to this paper for the details of the structure “annealing procedure”, equation of motion integration, and so forth.

While most of the conclusions are intuitive (e.g., predicted phase segregation), the results regarding interfaces are noteworthy. These regions were predicted to be heterogeneous in the sense of hydrophobic and hydrophilic patches. A hydrophilic patch consists of overlapping hydration shells about sulfonate groups while a hydrophobic patch consists of water-contacting perfluorocarbon groups. The calculations indicated that the interfaces are heterogeneous, much as suggested by Yeager some time ago, and that the diblock system has larger patches, that is, a greater degree of segregation, both ideas of which are intuitive.

While the computational-limited number of atoms is appreciated, the use of only four relatively short chains raises questions regarding the predicted morphologies. In principle, the sample space in these calculations is not large enough to generate an ensemble of periodic or quasi-periodic hydrophobic–hydrophilic phase components that would be sampled by high resolution TEM, AFM, or scattering techniques that reveal long-range structure.

Finally, simulations of the mean-squared displacement versus time for water and hydronium molecules were performed. The diffusion of water at this degree of hydration was seen to be greater for the more

segregated (diblock) structure. However, the diffusion of hydronium was determined to be insensitive to monomer sequence. It was pointed out that protons in these simulations are only allowed to move by the “vehicular” mechanism, that is, by translation as a part of an overall H_3O^+ molecule, whereas, in reality, protons can hop between adjacent water molecules via a combination of activated rate and tunneling processes.

Tanimura and Matsuoka calculated energy barriers for proton transfers in the small model compound associations ($[\text{CF}_3\text{SO}_3/\text{H}^+/\text{SO}_3\text{CF}_3]^{-1}$ and $[\text{CF}_3\text{SO}_3/\text{H}^+/\text{H}_2\text{O}/\text{SO}_3\text{CF}_3]^{-1}$) using an ab initio density functional quantum calculation method.²⁴³ Curves for energy versus distance between H^+ and an oxygen atom on an adjacent SO_3^- group in a sulfonate–sulfonate pair, while the distance between the two S atoms was held constant, were generated. The value of the energy barrier in the presence of one water molecule, of 2.1 $\text{kcal}\cdot\text{mol}^{-1}$, is close to the experimental value of 2.3 $\text{kcal}\cdot\text{mol}^{-1}$ for an 1100 EW Nafion membrane in which there are 18.2 mol of water per mole of SO_3^- sites. Of course, these calculations involve very local proton hopping events in the absence of perturbations posed by other water molecules and the phase separated polymer structure as well as molecular dynamics.

At the time of this writing, it must be conceded that there have been no fundamental principles-based mathematical model for Nafion that has predicted significantly new phenomena or caused property improvements in a significant way. Models that capture the essence of percolation behavior ignore chemical identity. The more ab initio methods that do embrace chemical structure are limited by the number of molecular fragments that the computer can accommodate. Other models are semiempirical in nature, which limits their predictive flexibility. Nonetheless, the diversity of these interesting approaches offers structural perspectives that can serve as guides toward further experimental inquiry.

7. Conclusions

A comprehensive review of the state of understanding of the fundamental structure and properties of Nafion perfluorosulfonate materials, at the time of this writing, has been presented based on recent as well as historical literature that either survived the test of time or influenced further research trends. Since the greatest interest in Nafion in recent years derives from its consideration as a proton conducting membrane in fuel cells, research has been largely driven by this critical application. Through the collective information acquired from the detailed works of many research groups and institutions, a broader understanding of this technologically important material has emerged. Although many of these contributions have exposed a significant number of critical relationships between structure (both chemical and morphological) and the unique properties of Nafion, it is widely accepted that much more remains to be learned.

While most long-range structure interrogations via SAXS and SANS methods have had to assume

structure factor models, and microscopic methods have been limited by resolution limits, a theme that has persisted is that the morphology of Nafion is quite complex and at least of a three-phase nature. There is no long-range patterned organization of hydrophilic clusters in a hydrophobic and semi-crystalline perfluorocarbon phase. Hydrophilic–hydrophobic interfaces are not discrete phase discontinuities, but the evidence suggests them to be “rough” or “fuzzy”. The evolution of morphological models for this complex polymer has involved many distinct conceptual designs; however, the relevant aspects of structure in these models have shown several important unifying perspectives, depending on ion and water content and the specific range of dimensions probed by the varying methods of analysis. With the inevitable improvements in techniques and methods of morphological characterization, a much more detailed representation of the true structure of perfluorosulfonate ionomers will be realized.

Water in sufficiently hydrated samples is an extended phase, and the clusters can be anisotropic and are contiguous to form percolation pathways, although the exact nature of interdomain water structure remains under debate. The more local, that is, molecular, organization of water, cation–sulfonate interactions and associations, and cation hydration and mobility have been investigated using spectroscopic, thermal analyses, sorption isotherm, and electrical conductivity studies. Water has been classified in terms of freezing versus nonfreezing or tightly bound around ions versus free or liquidlike, and the degree of hydrogen bonding in water clusters has been well-characterized. This information has been, and will be, valuable in the interpretation of water, ion, and proton transport data issuing from diffusion and electrical conductivity studies.

The long- and short-ranged motions in the backbone and side chains in Nafion, that have appeared as variously assigned transitions in dynamic mechanical studies, have only recently been probed on a molecular level using methods of high resolution NMR spectroscopy. This valuable information concerning chain dynamics is only just now emerging to yield important insight into the origins of mechanical relaxations of perfluorosulfonate ionomers in a variety of physical states.

The static mechanical properties of Nafion, while not the primary concern, save for the requirement of membrane integrity in electrochemical cells, have been investigated as a function of equivalent weight, counterion type, and solvent uptake. Undoubtedly, these properties are also a function of morphology, yet little specific information on this topic exists to date. While the number of primary chemical structure variations of Nafion sulfonate materials is very limited, morphology and, therefore, properties can, however, be manipulated by sample prehistory variables such as temperature and temperature cycles, swelling in different solvents, orientation, and solution and melt preprocessing schemes. With new methods of membrane preparation and the drive toward thinner membranes for improved transport properties, the need for critical morphology-mechan-

ical property relationships will become an important future consideration.

As noted in the Molecular Simulation of Structure and Properties section, there have been no fundamental principle-based mathematical models for Nafion that have predicted new phenomena or caused property improvements in a significant way. This is due to a number of limitations inherent in one or the other of the various schemes. These shortcomings include an inability to sufficiently account for chemical identity, an inability to simulate and predict the long-range structure as would be probed by SAXS or TEM, and the failure to simulate structure over different hierarchy levels. Certainly, advances in this important research front will emerge and be combined with advances in experimentally derived information to yield a much deeper state of understanding of Nafion.

8. Acknowledgment

The authors wish to acknowledge support for this work provided by the MRSEC Program of the National Science Foundation under Award Number DMR-0213883. Original SAXS data presented in this article were obtained through research carried out at the National Synchrotron Light Source, Brookhaven National Laboratory, which is supported by the U.S. Department of Energy, Division of Materials Sciences and Division of Chemical Sciences, under Contract No. DE-AC02-98CH10886. Finally, the authors want to recognize the invaluable assistance of Laura Fosselman in the preparation of this document.

9. Literature References

- (1) Curtin, D. E.; Lousenberg, R. D.; Henry, T. J.; Tangeman, P. C.; Tisack, M. E. *J. Power Sources* **2004**, *131*, 41.
- (2) Hora, C. J.; Maloney, D. E. *Electrochem. Soc. Ext. Abstr.* **1977**, *77* (2), 1145.
- (3) Grot, W. G. U.S. Patents 3,969,285 (1976), 4,026,783 (1977), 4,030,988 (1977).
- (4) Burkhardt, S. K.; Maloney, D. E. U.S. Patent 4,168,216 (1979).
- (5) Covitch, M. J.; Lowry, S. R.; Gray, C. L.; Blackford, B. In *Polymeric Separation Media*; Cooper, A. R., Ed.; Plenum: New York, 1982; p 257.
- (6) Yeager, H. L.; Kipling, B.; Dotson, R. L. *J. Electrochem. Soc.* **1980**, *127* (2), 303.
- (7) Robertson, M. A. F. Ph.D. Thesis, University of Calgary, 1994.
- (8) Robertson, M. A. F.; Yeager, H. L. *Macromolecules* **1996**, *29*, 5166.
- (9) Seko, M.; Ogawa, S.; Kimoto, K. In *Perfluorinated Ionomer Membranes*; Eisenberg, A., Yeager, H. L., Eds.; ACS Symposium Series No. 180; American Chemical Society: Washington, DC, 1982; Chapter 15, p 365.
- (10) (a) Doyle, M.; Lewittes, M. E.; Roelofs, M. G.; Perusich, S. A. *J. Phys. Chem. B* **2001**, *105*, 9387. (b) Doyle, M. E.; Lewittes, M. E.; Roelofs, M. G.; Perusich, S. A.; Lowrey, R. E. *J. Membr. Sci.* **2001**, *184*, 257. (c) Perusich, S. A. *Macromolecules* **2000**, *33*, 3431. (d) Perusich, S. A.; McBrearty, M. *Polym. Eng. Sci.* **2000**, *40*, 214. (e) McBrearty, M.; Perusich, S. A. *Polym. Eng. Sci.* **2000**, *40*, 201. (f) Perusich, S. A.; Avakian, P.; Keating, M. Y. *Macromolecules* **1993**, *26*, 4756.
- (11) (a) Hashimoto, T.; Fujimura, M.; Kawai, H. p 217. (b) Seko, M.; Ogawa, S.; Kimoto, K. p 365. (c) Sata, T.; Onoue, Y. p 411. (d) Ukihashi, H.; Yamabe, M. p 427. In *Perfluorinated Ionomer Membranes*; Eisenberg, A., Yeager, H. L., Eds.; ACS Symposium Series No. 180; American Chemical Society: Washington, DC, 1982.
- (12) Doyle, M.; Rajendran, G. *Handbook of Fuel Cells Fundamentals, Technology and Applications*; John Wiley & Sons: Chichester, U.K., 2003; Vol. 3, Part 3, Chapter 30, p 351.
- (13) Tant, M. R.; Darst, K. P.; Lee, K. D.; Martin, C. W. In *Multiphase Polymers: Blends and Ionomers*; Utracki, L. A., Weiss, R. A., Eds.; ACS Symposium Series No. 395; American Chemical Society: Washington, DC, 1989; Chapter 15, p 370.

- (14) Xu, G. *Polymer* **1993**, *25*, 397.
- (15) Gierke, T. D.; Hsu, W. Y. In *Perfluorinated Ionomer Membranes*; Eisenberg, A., Yeager, H. L., Eds.; ACS Symposium Series No. 180; American Chemical Society: Washington, DC, 1982; Chapter 13, p 283.
- (16) Hsu, W. Y.; Gierke, T. D. *J. Membr. Sci.* **1983**, *13*, 307.
- (17) Gierke, T. D.; Munn, G. E.; Wilson, F. C. *J. Polym. Sci., Polym. Phys.* **1981**, *19*, 1687.
- (18) Yeager, H. L.; Steck, A. J. *Electrochem. Soc.* **1981**, *128*, 1880.
- (19) Eisenberg, A.; Yeager, H. L. *Perfluorinated Ionomer Membranes*; ACS Symposium Series 180; American Chemical Society: Washington, DC, 1982.
- (20) Heitner-Wirguin, C. *J. Membr. Sci.* **1996**, *120*, 1.
- (21) Holliday, L. *Ionic Polymer*; Applied Science Publishers: London, 1975.
- (22) Eisenberg, A.; King, M. *Ion Containing Polymers in Polymer Physics*; Academic: New York, 1977; Vol. 2.
- (23) MacKnight, W. J.; Taggart, W. P.; Stein, R. S. *J. Polym. Sci., Polym. Symp.* **1974**, *45*, 113.
- (24) Yarusso, D. J.; Cooper, S. L. *Macromolecules* **1983**, *16*, 1871.
- (25) Yarusso, D. J.; Cooper, S. L. *Polymer* **1985**, *26*, 371.
- (26) *Perfluorinated Ionomer Membranes*; Eisenberg, A., Yeager, H. L., Eds.; ACS Symposium Series No. 180; American Chemical Society: Washington, DC, 1982.
- (27) Gierke, T. D. *152nd Meeting of the Electrochemical Society, Ext. Abstr.*; **1977**, *124*, 319C.
- (28) Pineri, M.; Duplessix, R.; Gauthier, S.; Eisenberg, A. In *Ions in Polymers*; Eisenberg, A., Ed.; ACS Symposium Series No. 187; American Chemical Society: Washington, DC, 1980; p 283.
- (29) Duplessix, R.; Escoubes, M.; Rodmacq, B.; Volino, F.; Roche, E.; Eisenberg, A.; Pineri, M. In *Water in Polymers*; Rowland, S. P., Ed.; ACS Symposium Series No. 127; American Chemical Society: Washington, DC, 1980; p 469.
- (30) Rodmacq, B.; Coey, J. M.; Escoubes, M.; Roche, E.; Duplessix, R.; Eisenberg, A.; Pineri, M. In *Water in Polymers*; Rowland, S. P., Ed.; ACS Symposium Series No. 127; American Chemical Society: Washington, DC, 1980; p 487.
- (31) Hsu, W. Y.; Gierke, T. D. *Macromolecules* **1982**, *15*, 101.
- (32) Gierke, T. D.; Munn, G. E.; Wilson, F. C. In *Perfluorinated Ionomer Membranes*; Eisenberg, A., Yeager, H. L., Eds.; ACS Symposium Series No. 180; American Chemical Society: Washington, DC, 1982; p 195.
- (33) Eisenberg, A.; Hird, B.; Moore, R. B. *Macromolecules* **1990**, *23*, 4098.
- (34) Roche, E. J.; Pineri, M.; Duplessix, R.; Levelut, A. M. *J. Polym. Sci., Polym. Phys. Ed.* **1981**, *19*, 1.
- (35) Roche, E. J.; Pineri, M.; Duplessix, R. *J. Polym. Sci., Polym. Phys. Ed.* **1982**, *20*, 107.
- (36) Fujimura, M.; Hashimoto, T.; Kawai, H. *Macromolecules* **1981**, *14*, 1309.
- (37) Fujimura, M.; Hashimoto, R.; Kawai, H. *Macromolecules* **1982**, *15*, 136.
- (38) Roche, E. J.; Stein, R. S.; Russell, T. P.; MacKnight, W. J. *J. Polym. Sci., Polym. Phys. Ed.* **1980**, *18*, 1497.
- (39) Marx, C. L.; Caulfield, D. F.; Cooper, S. J. *Macromolecules* **2000**, *33*, 6541.
- (40) Miura, Y.; Yoshida, H. *Tokyo Metrop. Univ.* **1990**, *40*, 4349.
- (41) Starkweather, H. W., Jr. *Macromolecules* **1982**, *15*, 320.
- (42) Kumar, S.; Pineri, M. *J. Mol. Sci., Part B: Polym. Phys.* **1986**, *24*, 1767.
- (43) Manley, D. S.; Williamson, D. L.; Noble, R. D.; Koval, C. A. *Chem. Mater.* **1996**, *8*, 2595.
- (44) Dreyfus, B.; Gebel, G.; Aldebert, P.; Pineri, M.; Escoubes, M.; Thomas, M. *J. Phys. (Paris)* **1990**, *51*, 1341.
- (45) Lee, E. M.; Thomas, R. K.; Burgess, A. N.; Barnes, D. J.; Soper, A. K.; Rennie, A. R. *Macromolecules* **1992**, *25*, 3106.
- (46) Grot, W. G.; Chadds, F. European Patent 0,066,369, 1982.
- (47) Martin, C. R.; Rhoades, T. A.; Fergusson, J. A. *Anal. Chem.* **1982**, *54*, 1639.
- (48) Aldebert, P.; Dreyfus, B.; Pineri, M. *Macromolecules* **1986**, *19*, 2651.
- (49) Aldebert, P.; Dreyfus, B.; Gebel, G.; Nakamura, N.; Pineri, M.; Volino, F. *J. Phys. (Paris)* **1988**, *49*, 2101.
- (50) Rebrov, A. V.; Ozerin, A. N.; Svergun, D. I.; Bobrova, L. P.; Bakeyev, N. F. *Polym. Sci. U. S. S. R.* **1990**, *32*, 1515.
- (51) Loppinet, B.; Gebel, G.; Williams, C. E. *J. Phys. Chem. B* **1997**, *101*, 1884.
- (52) Loppinet, B.; Gebel, G. *Langmuir* **1998**, *14*, 1977.
- (53) Moore, R. B.; Martin, C. R. *Anal. Chem.* **1986**, *58*, 2569.
- (54) Moore, R. B.; Martin, C. R. *Macromolecules* **1988**, *21*, 1334.
- (55) Moore, R. B.; Martin, C. R. *Macromolecules* **1989**, *22*, 3594.
- (56) Gebel, G.; Aldebert, P.; Pineri, M. *Macromolecules* **1987**, *20*, 1425.
- (57) Halim, J.; Scherer, G. G.; Stamm, M. *Macromol. Chem. Phys.* **1994**, *195*, 3783.
- (58) Cable, K. M.; Mauritz, K. A.; Moore, R. B. *Polym. Prepr.* **1994**, *35* (1), 421.
- (59) Cable, K. M.; Mauritz, K. A.; Moore, R. B. *Polym. Prepr.* **1994**, *35* (2), 854.
- (60) Cable, K. M.; Mauritz, K. A.; Moore, R. B. *Chem. Mater.* **1995**, *7*, 1601.
- (61) Landis, F. A.; Moore, R. B.; Page, K. A.; Han, C. C. *Polym. Mater.: Sci. Eng.* **2002**, *87*, 121.
- (62) Elliott, J. A.; Hanna, S.; Elliott, A. M. S.; Cooley, G. E. *Polymer* **2001**, *42*, 2551.
- (63) Elliott, J. A.; Hanna, S.; Elliott, A. M. S.; Cooley, G. E. *Macromolecules* **2000**, *33*, 4161.
- (64) Londono, J. D.; Davidson, R. V.; Mazur, S. *Polym. Mater. Sci. Eng.* **2001**, *85*, 23.
- (65) Barbi, V.; Funari, S. S.; Gehrke, R.; Scharnagl, N.; Stribeck, N. *Polymer* **2003**, *44*, 4853.
- (66) Van der Heijden, P. C.; Rubatat, L.; Diat, O. *Macromolecules*, in press.
- (67) Gebel, G.; Lambard, J. *Macromolecules* **1997**, *30*, 7914.
- (68) Gebel, G.; Moore, R. B. *Macromolecules* **2000**, *33*, 4850.
- (69) Rollet, A.-L.; Gebel, G.; Simonin, J.-P.; Turq, P. *J. Polym. Sci., Part B: Polym. Phys.* **2001**, *39*, 548.
- (70) Litt, M. H. *Polym. Prepr.* **1997**, *38*, 80.
- (71) Haubold, H.-G.; Vad, T.; Jungbluth, H.; Hiller, P. *Electrochim. Acta* **2001**, *46*, 1559.
- (72) Rubatat, L.; Rollet, A.-L.; Gebel, G.; Diat, O. *Macromolecules* **2002**, *35*, 4050.
- (73) Szajdzinska-Pietek, E.; Schlick, S.; Plonka, A. *Langmuir* **1994**, *10*, 1101.
- (74) Orfino, F. P.; Holdcroft, S. *J. New Mater. Electrochem. Syst.* **2000**, *3*, 287.
- (75) Young, S. K.; Trevino, S. F.; Beck Tan, N. C. *J. Polym. Sci., Part B: Polym. Phys.* **2002**, *40*, 387.
- (76) Gebel, G. *Polymer* **2000**, *41*, 5829.
- (77) Rollet, A.-L.; Diat, O.; Gebel, G. *J. Phys. Chem. B* **2002**, *21*, 3033.
- (78) Ceynowa, J. *Polymer* **1978**, *19*, 73.
- (79) Xue, T.; Trent, J. S.; Osseo-Asare, K. *J. Membr. Sci.* **1989**, *45*, 261.
- (80) Rieberer, S.; Norian, K. H. *Ultramicroscopy* **1992**, *41*, 225.
- (81) Porat, Z.; Fryer, J. R.; Huxham, M.; Rubinstein, I. *J. Phys. Chem.* **1995**, *99*, 4667.
- (82) Lehmani, A.; Durand-Vidal, S.; Turq, P. *J. Appl. Polym. Sci.* **1998**, *68*, 503.
- (83) McLean, R. S.; Doyle, M.; Sauer, B. B. *Macromolecules* **2000**, *33*, 6541.
- (84) Zawodzinski, T. A.; Gottesfeld, S.; Shoichet, S.; McCarthy, T. J. *J. Appl. Electrochem.* **1993**, *23*, 86.
- (85) Schroeder, P. *Z. Phys. Chem. (Munich)* **1993**, *45*, 57.
- (86) Zawodzinski, T. A.; Derouin, C.; Radzinski, S.; Sherman, R. J.; Smith, V. T.; Springer, T. E.; Gottesfeld, S. *J. Electrochem. Soc.* **1993**, *140*, 1041.
- (87) Tovbin, Y. K. *Zh. Fiz. Khim.* **1988**, *72*, 55.
- (88) Ozerin, A. N.; Rebrov, A. V.; Yakunun, A. N.; Bessonova, N. P.; Dreiman, N. A.; Sokolov, N. F.; Bakeev, L. F. *Vysokomol. Soedin., Ser. A* **1986**, *28*, 2303.
- (89) Mauritz, K. A.; Rogers, C. E. *Macromolecules* **1985**, *18*, 483.
- (90) James, P. J.; McMaster, T. J.; Newton, J. M.; Miles, M. J. *Polymer* **2000**, *41*, 4223.
- (91) Kreuer, K. D. *Handbook of Fuel Cells—Fundamentals, Technology and Applications*; Vielstich, W., Lamm, A., Gasteiger, H. A., Eds.; John Wiley & Sons Ltd: Chichester, U.K., 2003; Vol. 3, Part 3.
- (92) Grot, W. G. F.; Munn, G. E.; Walmsley, P. N. Presented at the 141st National Meeting of the Electrochemical Society, Houston, TX, 1972.
- (93) Yeo, R. S. *Polymer* **1980**, *21*, 432.
- (94) Yeo, R. S. *J. Appl. Polym. Sci.* **1986**, *32*, 5733.
- (95) Gebel, G.; Aldebert, P.; Pineri, M. *Polymer* **1993**, *34*, 333.
- (96) Zawodzinski, T. A.; Neeman, M.; Sillerud, L. O.; Gottesfeld, S. *J. Phys. Chem.* **1991**, *95*, 6040.
- (97) Zawodzinski, T. A.; Derouin, C.; Radzinsky, S.; Sherman, R. J.; Smith, V. T.; Springer, T. E.; Gottesfeld, S. *J. Electrochem. Soc.* **1993**, *140*, 1041.
- (98) Hinatsu, J. T.; Mizuhata, M.; Takenaka, H. *J. Electrochem. Soc.* **1994**, *141* (6), 1493.
- (99) Yeo, S.; Eisenberg, A. *J. Appl. Polym. Sci.* **1977**, *21*, 875.
- (100) Zawodzinski, T. A.; Davey, J.; Springer, T.; Gottesfeld, S. *Electrochem. Soc. Ext. Abstr.* **1992**, *Vol. 92-2*, Abstract No. 94, p 149.
- (101) Futerko, P.; Hsing, I.-M. *J. Electrochem. Soc.* **1999**, *146* (6), 2049.
- (102) Flory, P. J. *Principles of Polymer Chemistry*; Cornell University Press: Ithaca, NY, 1953; pp 495–540.
- (103) Buzzoni, R.; Bordiga, G.; Ricchiardi, G.; Spoto, G.; Zecchina, A. *J. Phys. Chem.* **1995**, *99*, 11937.
- (104) Zecchina, A.; Geobaldo, G.; Spoto, G.; Bordiga, G.; Ricchiardi, G.; Buzzoni, R.; Patrini, G. *J. Phys. Chem.* **1996**, *100*, 16584.
- (105) Lowry, S. R.; Mauritz, K. A. *J. Am. Chem. Soc.* **1980**, *102*, 4665.
- (106) Komoroski, R. A.; Mauritz, K. A. *J. Am. Chem. Soc.* **1978**, *100*, 7487.
- (107) Komoroski, R. A.; Mauritz, K. A. In *Perfluorinated Ionomer Membranes*; Eisenberg, A., Yeager, H. L., Eds.; ACS Symposium Series 180; American Chemical Society: Washington, DC, 1982; p 113.

- (108) Robinson, R. A.; Stokes, R. H. *Electrolyte Solutions*, 2nd ed.; Dover: Mineola, NY, 2002; Chapter 14.
- (109) Diebler, H.; Eigen, M. *Z. Phys. Chem. (Muenchen)* **1959**, *20*, 299.
- (110) Eigen, M.; Tamm, K. *Z. Elektrochem.* **1962**, *66*, 93, 107.
- (111) Komoroski, R. A. *Adv. Chem. Ser.* **1980**, *187*, 155.
- (112) Heitner-Wirguin, C. *Polymer* **1979**, *20*, 371.
- (113) Falk, M. *Can. J. Chem.* **1980**, *58*, 1495.
- (114) Rollet, A.-L.; Gebel, G.; Simonin, J.-P.; Turq, P. *J. Polym. Sci., Part B: Polym. Phys.* **2001**, *39*, 548.
- (115) Kujawski, W.; Nguyen, Q. T.; Neel, J. *J. Appl. Polym. Sci.* **1992**, *44*, 951.
- (116) Quezado, S.; Kwak, J. C. T.; Falk, M. *Can. J. Chem.* **1984**, *62*, 958.
- (117) Cable, K. M.; Mauritz, K. A.; Moore, R. B. *J. Polym. Sci., Part B: Polym. Phys.* **1995**, *33*, 1065.
- (118) Falk, M. In *Perfluorinated Ionomer Membranes*; Eisenberg, A., Yeager, H. L., Eds.; ACS Symposium Series 180; American Chemical Society: Washington, DC, 1982; p 139.
- (119) Peluso, S. L.; Tsatsas, A. T.; Risen, W. M. *Spectral Studies of Ions in Perfluorocarbonsulfonate (Nafion) Ionomers*; Office of Naval Research Technical Report No. TR-79-01, 1971.
- (120) Yeager, H. L. In *Perfluorinated Ionomer Membranes*; Eisenberg, A., Yeager, H. L., Eds.; ACS Symposium Series 180; American Chemical Society: Washington, DC, 1982; p 25.
- (121) Barnes, D. J. In *Structure and Properties of Ionomers*; Pineri, M., Eisenberg, A., Eds.; D. Reidel Publ. Co.: Dordrecht, 1987; p 501.
- (122) Luck, W. A. P. In *Synthetic Membrane Processes*; Belfort, G., Ed.; Academic Press: New York, 1984; p 21.
- (123) Quezado, S.; Kwak, J. C. T.; Falk, M. *Can. J. Chem.* **1984**, *62*, 958.
- (124) Yeager, H. L.; Twardowski, Z.; Clarke, L. M. *J. Electrochem. Soc.* **1982**, *129* (2), 324.
- (125) Starkweather, H. W.; Chang, J. J. *Macromolecules* **1982**, *15*, 752.
- (126) Boyle, N. G.; McBrierty, V. J.; Douglass, D. C. *Macromolecules* **1983**, *16*, 75.
- (127) Bunce, N. J.; Sondheimer, S. J.; Fyfe, C. A. *Macromolecules* **1986**, *19*, 333.
- (128) Sivashinsky, N.; Tanny, G. B. *J. Appl. Polym. Sci.* **1981**, *26*, 2625.
- (129) Bloembergen, N.; Purcell, E. M.; Pound, R. V. *Phys. Rev.* **1948**, *73*, 679.
- (130) Resing, H. A. *Adv. Relaxation Proc.* **1967-8**, *1*, 109.
- (131) Boyle, N.; McBrierty, V. J.; Eisenberg, A. *Macromolecules* **1983**, *16*, 80.
- (132) Pineri, M.; Volino, F.; Escoubes, M. *J. Polym. Sci., Polym. Phys. Ed.* **1985**, *23*, 2009.
- (133) Yoshida, H.; Miura, Y. *J. Membr. Sci.* **1992**, *68*, 1.
- (134) Miura, Y.; Yoshida, H. *Mem. Fac. Technol., Tokyo Metropol. Univ.* **1990**, *40*, 4349.
- (135) Moore, R. B.; Cable, K. M. *Polym. Prepr. (Am. Chem. Soc., Div. Polym. Chem.)* **1997**, *38* (1), 272.
- (136) MacMillan, B.; Sharp, A. R.; Armstrong, R. L. *Polymer* **1999**, *40*, 2471.
- (137) Martin, C. R.; Rhoades, T. A.; Ferguson, J. A. *Anal. Chem.* **1982**, *54*, 1639.
- (138) Rieke, P. C.; Vanderborgh, N. E. *J. Membr. Sci.* **1987**, *32*, 313.
- (139) Escoubes, M.; Pineri, M. In *Perfluorinated Ionomer Membranes*; Eisenberg, A., Yeager, H. L., Eds.; ACS Symposium Series 180; American Chemical Society: Washington, DC, 1982; p 9.
- (140) MacMillan, B.; Sharp, A. R.; Armstrong, R. L. *Polymer* **1999**, *40*, 2481.
- (141) Angell, C. A. In *Water, a Comprehensive Treatise*; Franks, F., Ed.; Plenum: New York, 1982; Vol. 7.
- (142) Cahan, B. D.; Wainright, J. S. *J. Electrochem. Soc.* **1993**, *140*, L185.
- (143) Fontanella, J. J.; McLin, M. G.; Wintersgill, M. C.; Calame, J. P.; Greenbaum, S. G. *Solid State Ionics* **1993**, *66*, 1.
- (144) Gardner, C. L.; Anantaraman, A. V. *J. Electroanal. Chem.* **1998**, *449*, 209.
- (145) Gavach, C.; Pamboutzoglou, N.; Nedyalkov, N.; Pourcelly, G. *J. Membr. Sci.* **1989**, *45*, 37.
- (146) Pourcelly, G.; Oikonomou, A.; Gavach, C. *J. Electroanal. Chem.* **1990**, *287*, 43.
- (147) Lindheimer, A.; Molenat, J.; Gavach, C. *J. Electroanal. Chem.* **1987**, *216*, 71.
- (148) Eikerling, M.; Kornyshev, A. A.; Kuznetsov, A. M.; Ulstrup, J.; Walbran, S. *J. Phys. Chem. B* **2001**, *105*, 3636.
- (149) Zundel, G.; Metzger, H. *Z. Phys. Chem.* **1968**, *58*, 225.
- (150) Wicke, E.; Eigen, M.; Ackermann, T. *Z. Phys. Chem.* **1954**, *1*, 340.
- (151) Eikerling, M.; Kornyshev, A. A. *J. Electroanal. Chem.* **2001**, *502*, 1.
- (152) Aldebert, P.; Guglieme, M.; Pineri, M. *Polym. J.* **1991**, *23* (5), 399.
- (153) Helfferich, F. *Ion Exchange*; McGraw-Hill: New York, 1962; p 351.
- (154) Cappadonia, M.; Erning, J. W.; Stimming, U. *J. Electroanal. Chem.* **1994**, *376*, 189.
- (155) Cappadonia, M.; Erning, J. W.; Niake, S. M.; Stimming, U. *Solid State Ionics* **1995**, *77*, 65.
- (156) Chen, R. S.; Jayakody, S. G.; Greenbaum, S. G.; Pak, Y. S.; Xu, G.; McLin, M. G.; Fontanella, J. *J. Electrochem. Soc.* **1993**, *140*, 889.
- (157) Chen, R. S.; Stallworth, P. E.; Greenbaum, S. G.; Fontanella, J. J.; Wintersgill, M. C. *Electrochim. Acta* **1995**, *40* (3), 309.
- (158) Paddison, S. J.; Reagor, D. W.; Zawodzinski, T. A. *J. Electroanal. Chem.* **1998**, *459*, 91.
- (159) Ellison, W. J.; Lamkaouchi, K.; Moreau, J.-M. *J. Mol. Liq.* **1996**, *68*, 171.
- (160) Zawodzinski, T. A.; Neeman, M.; Sillerud, L. D.; Gottesfeld, S. *J. Phys. Chem.* **1991**, *95*, 6040.
- (161) Alberti, G.; Casciola, M.; Massinelli, L.; Bauer, B. *J. Membr. Sci.* **2001**, *185*, 73.
- (162) Glasstone, S.; Laidler, K. J.; Eyring, H. *The Theory of Rate Processes*; McGraw-Hill: New York, 1941; pp 550 and 573.
- (163) Mauritz, K. A. Morphological Theories. In *Ionomers: Synthesis, Structure, Properties and Applications*; Tant, M. R., Mauritz, K. A., Wilkes, G. L., Eds.; Blackie Academic & Professional: London, 1997.
- (164) Yeo, Y. S. In *Perfluorinated Ionomer Membranes*; Eisenberg, A., Yeager, H. L., Eds.; ACS Symposium Series No. 180; American Chemical Society: Washington, DC, 1982; p 453.
- (165) Kipling, B. In *Perfluorinated Ionomer Membranes*; Eisenberg, A., Yeager, H. L., Eds.; ACS Symposium Series No. 180; American Chemical Society: Washington, DC, 1982; p 475.
- (166) Yeager, H. L.; Gronowski, A. A. In *Ionomers: Synthesis, Structure, Properties and Applications*; Tant, M. R., Mauritz, K. A., Wilkes, G. L., Eds.; Blackie Academic & Professional: London, 1997; p 333.
- (167) Olah, G. A.; Dyer, P. S.; Prakash, G. K. S. *Synthesis* **1980**, *7*, 513.
- (168) Sondheimer, S. J.; Bunce, N. J.; Fyfe, C. A. *J. Macromol. Sci., Rev. Macromol. Chem. Phys.* **1986**, *C26* (3), 353.
- (169) Ferry, L. L. *J. Macromol. Sci., Chem.* **1990**, *A27* (8), 1095.
- (170) Zundel, G. *Hydration and Intermolecular Interaction*; Academic Press: New York, 1969.
- (171) Zundel, G. In *The Hydrogen Bond, Recent Developments in Theory and Experiments*; Schuster, P., Zundel, G., Sandorfy, C., Eds.; North Holland: Amsterdam, 1976; Vol. II, Chapter 15, p 683.
- (172) Eigen, M. *Angew. Chem.* **1963**, *75*, 489.
- (173) Zundel, G. *J. Membr. Sci.* **1982**, *11*, 249.
- (174) Interactions and Structures of Ionic Solvates—Infrared Results. Zundel, G.; Fritsch, J. In *Physics of Ionic Solvation*; Dogonadze, R. R., Kalman, E., Kornyshev, A. A., Ulstrup, J., Eds.; Elsevier: Amsterdam, 1984.
- (175) Leuchs, M.; Zundel, G. *J. Chem. Soc., Faraday Trans 2* **1978**, *74*, 2256.
- (176) Ostrowska, J.; Narebska, A. *Colloid Polym. Sci.* **1983**, *261*, 93.
- (177) Mauritz, K. A.; Gray, C. L. *Macromolecules* **1983**, *16*, 1279.
- (178) Kreuer, K. D. *Chem. Mater.* **1998**, *8*, 610.
- (179) Kreuer, K. D.; Rabenau, A.; Weppner, W. *Angew. Chem., Int. Ed. Engl.* **1982**, *21*, 208.
- (180) Kreuer, K. D. *J. Membr. Sci.* **2001**, *185*, 29.
- (181) Yeo, S. C.; Eisenberg, A. *J. Appl. Polym. Sci.* **1977**, *21*, 875.
- (182) Takamatsu, T.; Hashiyama, M.; Eisenberg, A. *J. Appl. Polym. Sci.* **1979**, *24*, 2199.
- (183) Yeager, H. L. In *Structure and Properties of Ionomers*; NATO ASI Series C; D. Reidel: Dordrecht, 1987; Vol. 198, p 377.
- (184) Yeager, H. L. In *Perfluorinated Ionomer Membranes*; Eisenberg, A., Yeager, H. L., Eds.; ACS Symposium Series No. 180; American Chemical Society: Washington, DC, 1982; p 42.
- (185) Millet, P. *J. Membr. Sci.* **1990**, *50*, 325.
- (186) Lopez, M.; Kipling, B.; Yeager, H. L. *Anal. Chem.* **1977**, *49*, 629.
- (187) Yeager, H. L.; Steck, A. *Anal. Chem.* **1979**, *51*, 862.
- (188) Yeager, H. L.; Kipling, B. *J. Phys. Chem.* **1979**, *83*, 1836.
- (189) Zawodzinski, T. A.; Neeman, M.; Sillerud, L. O.; Gottesfeld, S. *J. Phys. Chem.* **1991**, *95*, 6040.
- (190) Gong, X.; Bandis, A.; Tao, A.; Meresi, G.; Inglefield, P. T.; Jones, A. A.; Wen, W.-Y. *Polymer* **2001**, *42*, 6485.
- (191) Meresi, G.; Wang, Y.; Bandis, A.; Inglefield, P. T.; Jones, A. A.; Wen, W.-Y. *Polymer* **2001**, *42*, 6153.
- (192) Sodaye, H. S.; Pujari, P. K.; Goswami, A.; Manohar, S. B. *J. Polym. Sci., Part B: Polym. Phys.* **1997**, *35*, 771.
- (193) Plate, N. A.; Shibaev, V. P. *Brush-like Polymers and Liquid Crystals*; Khimija: Moscow, 1980; p 304 (Russ. transl.).
- (194) Timashev, S. F. *Physical Chemistry of Membrane Processes*; Khimija: Moscow, 1988; p 237 (Russ. transl.).
- (195) Rubatat, L.; Rollet, A. L.; Gebel, G.; Diat, O. *Macromolecules* **2002**, *35*, 4050.
- (196) Kalyanasundaram, K.; Thomas, J. K. *J. Am. Chem. Soc.* **1977**, *99* (7), 2039.
- (197) Lee, P. C.; Meisel, D. *Photochem. Photobiol.* **1985**, *41*, 21.
- (198) Szentirmay, M. N.; Prieto, N. E.; Martin, C. R. *J. Phys. Chem.* **1985**, *89*, 3017.
- (199) Robertson, M. A. F.; Yeager, H. L. *Macromolecules* **1996**, *29*, 5155.

- (200) Young, S. K.; Trevino, S. F.; Beck Tan, N. C.; Paul, R. L. Army Research Laboratory Report ARL-TR-2679, March 2002.
- (201) Twardowski, Z.; Yeager, H. L.; O'Dell, B. *J. Electrochem. Soc.* **1982**, *129* (2), 328.
- (202) Perusich, S. A. *Macromolecules* **2000**, *33*, 3431.
- (203) Grot, W. G. F.; Munn, G. E.; Walmsley, P. N. Presented at the Electrochemical Society Meeting, Houston, TX, May 7–11, 1972; paper no. 154.
- (204) Yeo, S. C.; Eisenberg, A. *J. Appl. Polym. Sci.* **1977**, *21*, 875.
- (205) Kyu, T.; Eisenberg, A. In *Perfluorinated Ionomer Membranes*; Eisenberg, A., Yeager, H. L., Eds.; American Chemical Society Symposium Series 180; American Chemical Society: Washington, DC, 1982; Chapter 6, p 79.
- (206) Tant, M. R.; Darst, K. P.; Lee, K. D.; Martin, C. W. In *Multiphase Polymers: Blends and Ionomers*; Utracki, L. A., Weiss, R. A., Eds.; American Chemical Society Symposium Series 395; American Chemical Society: Washington, DC, 1989; Chapter 15, p 370.
- (207) Miura, Y.; Yoshida, H. *Thermochim. Acta* **1990**, *163*, 161.
- (208) Cable, K. M. Tailoring Morphology-Property Relationships in Perfluorosulfonate Ionomers. Ph.D. Dissertation, University of Southern Mississippi, 1996.
- (209) Young, S. K.; Mauritz, K. A. *J. Polym. Sci., Part B: Polym. Phys.* **2001**, *39* (12), 1282.
- (210) Kyu, T.; Hashiyama, M.; Eisenberg, A. *Can. J. Chem.* **1983**, *61*, 680. Also cross reference #195 (version 7/6/04).
- (211) Moore, R. B.; Cable, K. M.; Croley, T. L. *J. Membr. Sci.* **1992**, *75*, 7.
- (212) Page, K. A.; Moore, R. B. *Polym. Prepr. (Am. Chem. Soc., Div. Polym. Chem.)* **2003**, *44* (1), 1144.
- (213) Landis, F. A.; Moore, R. B.; Page, K. A.; Han, C. C. *Polym. Mater. Sci. Eng. (Am. Chem. Soc., Div. Polym. Mater. Sci. Eng.)* **2002**, *87*, 121.
- (214) Page, K. A.; Cable, C. A.; Moore, R. B. Manuscript in preparation.
- (215) Mauritz, K. A. In *Ionomers: Synthesis, Structure, Properties and Applications*; Tant, M. R., Mauritz, K. A., Wilkes, G. L., Eds.; Blackie Academic & Professional: London, 1997; p 95.
- (216) Hsu, W. Y.; Barkley, J. R.; Meakin, P. *Macromolecules* **1980**, *13*, 198.
- (217) Cirkel, P. A.; Okada, T. *Macromolecules* **2000**, *33*, 4921.
- (218) Cirkel, P. A.; Okada, T.; Kinigasa, S. *Macromolecules* **1999**, *32*, 5321.
- (219) Hsu, W. Y.; Berzins, T. *J. Polym. Sci., Polym. Phys. Ed.* **1985**, *23*, 933.
- (220) Mauritz, K. A.; Rogers, C. E. *Macromolecules* **1985**, *18*, 483.
- (221) Verbrugge, M. W.; Hill, R. F. *J. Electrochem. Soc.* **1990**, *137*, 886.
- (222) Verbrugge, M. W.; Hill, R. F. *J. Electrochem. Soc.* **1990**, *137*, 893.
- (223) Pintauro, P. N.; Verbrugge, M. W. *J. Membr. Sci.* **1989**, *44*, 197.
- (224) Bontha, J. R.; Pintauro, P. N. *Chem. Eng. Sci.* **1994**, *49*, 3835.
- (225) Eikerling, M.; Kornyshev, A. A.; Stimming, U. *J. Phys. Chem. B* **1997**, *101*, 10807.
- (226) Paddison, S. J.; Zawodzinski, T. A. *Solid State Ionics* **1998**, *113–115*, 333.
- (227) Paddison, S. J. *Handb. Fuel Cells—Fundam., Technol. Appl.* **2003**, *3* (3), 396.
- (228) Kreuer, K. D. *J. Membr. Sci.* **2001**, *185*, 29.
- (229) Ise, M. Ph.D. Thesis, University of Stuttgart, 2000.
- (230) Paddison, S. J.; Paul, R.; Zawodzinski, T. A. In *Proton Conducting Membrane Fuel Cells II*; Gottesfeld, S., Fuller, T. F., Eds.; Electrochemical Society Proceedings Series; Electrochemical Society: Pennington, NJ, 1999; Vol. 98-27, p 106.
- (231) Paddison, S. J.; Paul, R.; Zawodzinski, T. A. *J. Electrochem. Soc.* **2000**, *147*, 617.
- (232) Paddison, S. J.; Paul, R.; Zawodzinski, T. A. *J. Chem. Phys.* **2001**, *115*, 7753.
- (233) Paul, R.; Paddison, S. J. *J. Chem. Phys.* **2001**, *115* (16), 7762.
- (234) Paul, R.; Paddison, S. J. *Solid State Ionics* **2004**, *168*, 245.
- (235) Vishnyakov, A.; Niemark, A. V. *J. Phys. Chem. B* **2000**, *104*, 4471.
- (236) Vishnyakov, A.; Niemark, A. V. U. S. Army NSC Report: Modeling of Microstructure and Water Vapor Sorption and Transfer in Permselective Membranes, 2000.
- (237) Khalatur, P. G.; Talitskikh, S. K.; Khokhlov, A. R. *Macromol. Theory Simulat.* **2002**, *11*, 566.
- (238) MacMillan, B.; Sharp, A. R.; Armstrong, R. L. *Polymer* **1999**, *40*, 2481.
- (239) Hsu, W. Y. *Macromolecules* **1983**, *16*, 745.
- (240) Matsushige, K.; Enoshita, R.; Ide, T.; Yamanchi, N.; Taki, S.; Takemura, T. *Jpn. J. Appl. Phys.* **1977**, *16*, 681.
- (241) Rosser, R. W.; Schrag, J. L.; Ferry, J. D.; Greaser, M. *Macromolecules* **1977**, *10*, 978.
- (242) Jang, S. S.; Molinero, V.; Cagin, T.; Goddard, W. A. *J. Phys. Chem. B* **2004**, *108*, 3149.
- (243) Tanimura, S.; Matsuoka, T. *J. Polym. Sci., Part B: Polym. Phys.* **2004**, *42*, 1905.

CR0207123

